UNIVERSIDAD AUTÓNOMA DE MADRID

Programa de Doctorado en Biociencias Moleculares

EVOLUTIONARY DIVERGENCE IN THE BIOACTIVE JASMONATE IN LAND PLANTS

Isabel Monte

PhD Thesis

Madrid, 2017

UNIVERSIDAD AUTÓNOMA DE MADRID

Programa de Doctorado en Biociencias Moleculares

Evolutionary divergence in the bioactive jasmonate in land plants

TESIS DOCTORAL

Isabel Monte Grondona

Madrid, 2017

UNIVERSIDAD AUTÓNOMA DE MADRID

Programa de Doctorado en Biociencias Moleculares

Evolutionary divergence in the bioactive jasmonate in land plants

TESIS DOCTORAL

Isabel Monte Grondona

Director

Roberto Solano Tavira

Madrid, 2017

UNIVERSIDAD AUTÓNOMA DE MADRID

Programa de Doctorado en Biociencias Moleculares

Facultad de Ciencias

Evolutionary divergence in the bioactive jasmonate in land plants

Dr. Roberto Solano Tavira

DIRECTOR

Dra. Marta Martín Basanta

TUTORA

Isabel Monte Grondona
Licenciada en Farmacia y Bioquímica

DOCTORANDA

Madrid, 2017

Acknowledgments

En estos años en Madrid he tenido la suerte de compartir muchas experiencias con muchas personas dentro y fuera del CNB. A todos vosotros me gustaría deciros:

¡GRACIAS!

Quiero aprovechar estas páginas para recordar a algunas de estas personas, empezando por Roberto Solano, mi director de tesis. Gracias por enseñarme tu forma de trabajar y de pensar; ahora me parece que no hay mejor opción que hacer lo que hacemos como lo hacemos. Gracias por dejar lo que estuvieras haciendo para ver cada resultado, por emocionarte tanto o más que yo con cada novedad, por arriesgar y tener ideas brillantes, por confiar en mí, por darme libertad para tomar decisiones, por pensar que tenemos el mejor trabajo del mundo y por defenderme en los momentos difíciles. Ha habido momentos duros y (muchos) cambios de prioridades, pero lo que mejor recordaré es que fue divertido.

Mats Hamberg, thank you for making our scientific dreams come true. Your expertise has been fundamental for our projects. You have allowed us to go further than we could have ever imagined and I feel grateful for that. This work is also yours.

Takayuki Kochi (Kohchi-sensei) and Ryuichi Nishihama, thank you for your help and your friendship. My stay in Kyoto in 2013 was one of the greatest experiences in my life! Thanks to you and your lab I learnt a lot about Marchantia and Japan. I also want to thank Sakiko Ishida for teaching me all the basic techniques to work with Marchantia: your skills are really impressive! I'm glad I learnt with the best! Thank you for trying the gene-targeting again and again. Okamoto-san, thank you for sharing with me (and Sakiko) so many good moments, especially the tea ceremony. You are the proof that words are not always needed to communicate, and despite the cultural differences, sometimes we just need a hug. All the lab members from Kohchi lab (Shohei, Akane, Take-san, Yokofuji, Manabe, Mika, Miya, Kata-san, Kato-san, Keitaro, Masaru, Kirita-san, Makoto...), thank you for making me so comfortable. I enjoyed every moment I spent with you: the trip to Osaka, the hiking, the dinners, the momiji, wearing kimono (thanks Aino!)... I have quite a lot of precious memories with you and a beautiful scrapbook!

To the organizers of the 2IMTC (Kohchi-sensei, Araki-sensei and Ryuichi), thank you for inviting me to the course. Thanks to all the 2IMTC teachers: Aino, Yoriko, Yoshihiro, Keisuke and Asuka. Thanks to the other trainees (Yen-Ting, Sean, Giulia and Anthony) for sharing the fascination about Marchantia and enjoying every second in Japan. As you, I am proud of being part of the Marchantia community and I hope we will maintain and spread the spirit of sharing and collaborating.

Liam Dolan, thanks for accepting me in your lab in Oxford. Thanks to Clement for teaching me how to do Marchantia screenings. Y gracias a Pablo, porque no sé qué habría hecho sin ti esos dos meses. Gracias a Javier Agustí por compartir impresiones después de los lab meeting.

Ángel, gracias por medir nuestras muestras, por las conversaciones por teléfono y por tu amabilidad.
Gracias a mis profesores de la Universidad de Salamanca, en especial a José Juan, a Mª Jesús y a Nines por ayudarme a dar mis primeros pasos en investigación. Thanks to Jos Vanderleyden and Stijn Spaepen for everything I learnt in your lab in KU Leuven. Thanks to Somya and Mayuko for your everlasting friendship and for all the great city trips.

Marta Martín, gracias por ser mi tutora. El papeleo siempre es más llevadero después de charlar un rato contigo.

Inés de Fotografía, gracias por tantísimas fotos chulas y por esforzarte por sacar el lado artístico de mis plantas. ¡Lo has conseguido! Gracias a todos los servicios del CNB por hacerme la vida más fácil. Gracias a Marina, por encontrar la solución cuando yo creía que estaba todo perdido.

Y volviendo al lab 317, gracias a Andrea por guiar mis primeros pasos en el mundo del jasmónico, por enseñarme a ser ordenada sin tener cuaderno, por ser metódico y a la vez flexible para cambiar (normalmente ampliar) los experimentos en el último minuto y sobre todo porque formábamos un buen equipo.

Gracias a todos los miembros del 317 pasados y presentes: a Alberto, por ser las dos manos que me faltan; a Andrés, por los planes de mejora del lab y por ser tan único; a Carlos, por enseñarme a no tener miedo de poner en marcha mis ideas; a Gemma, por ser mi amiga y mi apoyo en los momentos difíciles, aunque a veces nos merezcamos el "chaleco de pavas"; a Gloria, porque me gusta cómo piensas y algún día me gustaría ser

una madre como tú; a Guille, porque a pesar de los *facepalms* puedo hablar contigo de cualquier cosa (somos de la RAE) y gracias a ti recuperé mi lado friki; a Jose, por ser tan buen vecino; a María, por crear tan buen ambiente, por las risas y por ser mi compañera en el mundo de Marchantia; a Marta Boter, por tu entusiasmo; a Miki, por enseñarme otra realidad en la que pasan cosas inverosímiles, como cada vez que volvíamos juntos a Lavapiés; a Mónica, por tus abrazos espachurrantes y porque me habría encantado tenerte a mi lado siempre; a Piti, por tus consejos acertados sobre los riesgos de trabajar hasta tarde; a Sandra, por enseñarme la mejor técnica del mundo; a Selena, por saber disfrutar de cada momento (y cada recuerdo). ¡Somos 317 *power*! Gracias también a todos los que han estado de estancia en el 317: Laurens, Matt, Javier Pardal (alias Alonso), Chantal, Adrián... Me alegro de haber pasado tiempo con vosotros dentro y fuera del lab. Jorge, gracias por convertirte en colega, colaborador y amigo; espero que sigamos mucho tiempo trabajando con Marchantia y con muchas plantas raras más.

Gracias a la gente del Departamento de Genética Molecular de Plantas y en especial, gracias a los predocs GMP de mi quinta: han sido muchos buenos momentos juntos.

Gracias a la familia Chevalier por la etapa madrileña, por mantener el contacto y por todos los picnics que nos quedan en Francia. Gracias a Vicente por pasearnos por toda la Provenza.

Gracias a mi Laura, porque donde esperaba encontrar una compañera de piso, encontré una hermana. No importa lo lejos que estemos, porque cada vez que hablamos es como si no hubiera pasado el tiempo.
Gracias a Elisa y Stella (y Aitziber), por tantas cañas en Casa Patas y tantas tortas mexicanas, porque siempre lo paso genial con vosotras.

Fernando, gracias por hacer que los viajes en tren a Salamanca pasaran volando. Ahora que la tesis está acabada puedo saldar mi deuda de croquetas.

Gracias a Sofía por el reencuentro después de tantos años, por nuestras vidas paralelas y por entender tantas cosas dentro y fuera del laboratorio.

Rodrigo, Álvaro y Bregalad, gracias por ese gran primer año en Madrid; fue genial descubrirlo a vuestro lado.

Nacho, Isidro, Pilar y Javi, gracias por ser mis amigos, por las rutas, los viajes, las vacaciones, las cervezas y los quesos, porque me parece que el tiempo que paso con vosotros nunca es suficiente y porque me costaría mucho cortar la cuerda si sois vosotros los que estáis en el otro extremo.

Neil, Nicole, Bambos and Siya, thanks for showing me that the best way to celebrate a PhD is a *barbacoa*.

Mic, gracias por escucharme, cuidarme y protegerme, por darme la tranquilidad que necesito y ayudarme en todo, porque intentas que se me pegue un poco de *anticipation* y porque sé que no importa si en nuestro próximo destino hay nieve o un jardín de cactus, porque seguiremos siendo felices.

Raquel, gracias por estar ahí desde el principio, por estar orgullosa de mí y por alegrarte de cada uno de mis logros. Tu amistad es un auténtico tesoro.

Gracias a Carmen, por vivirlo todo tan de cerca. Gracias a Gulli, por interesarte siempre por mí y mis plantas.

Gracias a mi tía María por ser mi ancla en Madrid, por tu disposición y tu cariño, por tu generosidad. Te voy a echar de menos, pero ya iré a verte a tu casita de Sevilla y a la del Puerto. Gracias a mi tía Cova, por ser mi hada madrina. Gracias a mis tíos y mis primos, porque las vacaciones en Sevilla no habrían sido lo mismo sin vosotros. Gracias a mis abuelos, porque sé que se habrían sentido muy orgullosos.

Gracias a mi hermano Quique. Me encanta tenerte cerca y que nos riamos de las mismas cosas. ¡Quién lo iba a decir hace unos años!

Gracias a mi madre por todo el apoyo, por las horas y horas de teléfono, por entenderme como nadie y por todo lo que me has enseñado. Gracias a mi padre, porque sabes cómo funciona esto, porque sé que sólo quieres lo mejor para mí y aunque a veces parece que no nos entendemos lo que ocurre es que nos parecemos demasiado. Soy como soy gracias a vosotros y nunca podré agradeceros lo suficiente todo lo que habéis hecho por mí. Os quiero muchísimo.

Table of contents

Summary

Jasmonates are phytohormones involved in defence and developmental processes such as fertility. In eudicots, the active hormone JA-Ile induces the interaction between the two members of the co-receptor: the F-box COI1 and one of the JAZ repressors. The jasmonate signalling pathway has been mainly studied in the model plant *Arabidopsis thaliana*, but little is known about this pathway in other plant lineages. Sequence analyses of available algae and land plants genomes showed that all the signalling components of the JA-Ile pathway might have been already present in the common ancestor of all land plants. Extant bryophytes are the most basal group of land plants, and among them, liverworts are considered the sister lineage to all other land plants. In this work, we have used the model liverwort *Marchantia polymorpha* to study the evolution and functional conservation of the jasmonate pathway. Besides its key evolutionary position, *M. polymorpha* shows an extraordinary low gene redundancy that facilitates the study of large gene families. Our results demonstrate that the jasmonate perception and signalling machinery are conserved in land plants but the hormone is different in bryophytes and vascular plants. We have identified dinor-OPDA as the active hormone in bryophytes as well as the residue that determines the ligand specificity in COI1. Taken together our results explain the evolutionary events that lead to the appearance of JA-Ile and COI1 in vascular plants from their ancestral counterparts. In addition, the characterization of the COI1/JAZ co-receptor in land plants has allowed us to develop a specific antagonist of JA-Ile perception with biotechnological potential.

Resumen

Los jasmonatos son fitohormonas implicadas en activación de defensas y en procesos de desarrollo. En eudicotiledóneas la hormona activa, JA-Ile, induce la interacción entre los dos componentes del co-receptor: la F-box COI1 y uno de los represores JAZ. La ruta de señalización del jasmonato se ha estudiado fundamentalmente en la planta modelo *Arabidopsis thaliana*, pero apenas se ha caracterizado en otros grupos de plantas. El análisis de genomas disponibles de diversos linajes vegetales sugiere que todos los componentes de la ruta de señalización de jasmonatos ya estaban presentes en el ancestro común de las plantas terrestres. Los briófitos actuales son el grupo más primitivo de este tipo de plantas, y dentro de ellos, las hepáticas se consideran el linaje hermano al resto de plantas terrestres. En este trabajo hemos utilizado como planta modelo la hepática *Marchantia polymorpha* para estudiar la evolución y la conservación funcional de la ruta del jasmonato. Además de su posición evolutiva privilegiada, *M. polymorpha* tiene una redundancia génica extraordinariamente baja, lo que facilita el análisis funcional de familias multigénicas en plantas superiores. Nuestros resultados demuestran que la percepción de jasmonatos y su maquinaria de señalización están conservados en plantas terrestres, pero la hormona es diferente en briófitos y plantas vasculares. Hemos identificado el dinor-OPDA como la hormona activa en briófitos y hemos demostrado que un solo aminoácido en el receptor COI1 determina la especificidad de ligando. En conjunto, nuestros resultados explican los acontecimientos evolutivos que condujeron a la aparición del JA-Ile y COI1 en plantas vasculares a partir de sus ortólogos ancestrales. Además, la caracterización del co-receptor COI1/JAZ en plantas terrestres nos ha permitido desarrollar un antagonista específico de la percepción de JA-Ile con potencial biotecnológico

Abbreviations

10,11-EHT	10,11(*S*)-epoxy-hexadecatrienoic acid
11-HPHT	11(*S*)-hydroperoxy-hexadecatrienoic acid
12,13-EOT	12,13(*S*)-epoxy-octadecatrienoic acid
13-HPOT	13(*S*)-hydroperoxy-octadecatrienoic acid
16:3	Hexadecatrienoic acid
18:3	α-Linolenic acid
3,7-ddh-JA	3,7-didehydro-jasmonic acid
3,7-ddh-JA-Ile-Me	3,7-didehydro-jasmonoyl-isoleucine methylated
4,5-ddh-JA	4,5-didehydro-jasmonic acid
4,5-ddh-JA-Ile	4,5-didehydro-jasmonoyl-isoleucine
ABA	Abscisic acid
ACX	AcylCoA oxidase
AD	Activation Domain
AmTr	*Amborella trichopoda*
AOC	Allene Oxide Cyclase
AOS	Allene Oxide Synthase
ARF	Auxin Response Factor
At	*Arabidopsis thaliana*
ATP	Adenosine triphosphate
BAR	Bio-Analytic Resource for Plant Biology
BD	Binding Domain
bHLH	basic Helix-Loop-Helix
bp	base pair
Bradi	*Brachypodium distachyon*
BRs	Brassinosteroids
CaMV	Cauliflower Mosaic Virus
CBB	Coomassie Brilliant Blue
CFU	Colony-forming units
CHL	Chlorophyllase
CKs	Cytokinins
CMID	Cryptic MYC Interaction Domain
CMT	Comatose
Co	*Coleochaete orbicularis*
COI1	Coronatine Insensitive 1
Col	Columbia
COR	Coronatine
COR-MO	COR-methyloxime
CRISPR	Clustered Regularly Interspaced Short Palindromic Repeats
CYP	Cytochrome P450
d	days
d5	Deuterated in five positions
d6	Deuterated in six positions
dn-*iso*-OPDA	2,3-dinor-12-oxo-9(13),15(Z)-phytodienoic acid
dn-OPDA	2,3-dinor-OPDA
DNA	Deoxyribonucleic acid
EAR	Ethylene Responsive Factor-associated amphiphilic repression
EF1	Elongation Factor 1
EGL3	Enhancer of GL3
EIL1	EIN3-like 1
EIN3	Ethylene Insensitive 3
ET	Ethylene
FDR	False Discovery Rate
FL	Full-length
FR	Far-red

GA	Gibberellin
gDNA	Genomic DNA
GEO	Gene Expression Omnibus
GFP	Green Fluorescent Protein
GH3	Gretchen Hagen 3
GL	Glabra
GO	Gene Ontology
GST	Glutathione S-Transferase
GUS	β-glucuronidase
HDA	Histone Deacetylases
HRP	Horseradish peroxidase
IAA	3-indole-acetic Acid
IC_{50}	Half-maximum inhibitory concentration
ICE	Inducer of CBF Expression
iso-OPDA	iso-12-oxo-phytodienoic acid
JA	Jasmonic acid
JA-Ile	Jasmonoyl-isoleucine
JA-Ile-MO	JA-Ile-methyloxime
JA-MO	JA-methyloxime
JA-Trp	Jasmonoyl-tryptophan
JAM	JA-Associated MYC2-like
JAR1	Jasmonate Resistant 1
JAs	Jasmonates
JAT	Jasmonate Transporter
JGI	Joint Genome Institute
JID	JAZ Interaction Domain
JMT	JA Methyl Transferase
KAT	3-ketoacyl-CoA thiolase
KEG	Keep On Going
Kfl	*Klebsormidium flaccidum* (now correctly annotated as *K. nitens*)
LC-MS	Liquid Chromatography-Mass Spectrometry
LOX	Lipoxygenase
Mapoly	*Marchantia polymorpha*
Mb	Megabase pairs
MBP	Maltose Binding Protein
MED25	Mediator 25
MeJA	Methyl-jasmonate
MFP	Multifunctional protein
MiSSP7	Mycorrhizal induced small secreted protein 7
Mp	*Marchantia polymorpha*
MS	Murashige and Skoog
MSA	Multiple Sequence Alignment
Mv	*Mesostigma viridae*
NINJA	Novel Interactor of JAZ
Nm	*Nitella mirabilis*
Nt	*Nicotiana tabacum*
OD	Optical Density
OH	Hydroxy
OPC-4	3-oxo-2-(2-pentenyl)-cyclopentane-1-butyric acid
OPC-6	3-oxo-2-(2-pentenyl)-cyclopentane-1-hexanoic acid
OPC-8	3-oxo-2-(2-pentenyl)-cyclopentane-1-octanoic acid
OPCL1	OPC-8:0 CoA Ligase 1
OPDA	12-oxo-phytodienoic acid

OPDA-Ile	OPDA-isoleucine
OPR	OPDA reductase
Os	*Oryza sativa*
PAM	Protospacer Adjacent Motif
PAP1	Production of Anthocyanin Pigment 1
Phpat	*Physcomitrella patens*
PI	Protease inhibitor
Pp	*Physcomitrella patens*
pro	Promoter
Pst	*Pseudomonas syringae* pv. *tomato*
Q-PCR	Quantitative Real-Time PCR
RES	Reactive Electrophile Species
RNA	Ribonucleic acid
RT	Room Temperature
SA	Salicylic acid
SCF	Skip-Cullin-F-box
S.D.	Standard Deviation
SD	Synthetic Defined yeast medium
sgRNA	Short guide RNA
Sl	*Solanum lycopersicum*
Sm	*Selaginella moellendrofii*
Sp	*Spirogyra pratensis*
SSITL	Sclerotinia sclerotiorum integrin-like
T-DNA	Transferred DNA
TAD	Transactivation Domain
TF	Transcription Factor
tn-*iso*-OPDA	2,3,4,5-tetranor-*iso*-OPDA
tn-OPDA	2,3,4,5-tetranor-OPDA
TPL	TOPLESS
TPR	TPL-related proteins
TSS	Transcription Start Site
TT8	Transparent Testa 8
UTR	Untranslated region
vs	versus
WT	Wild-type

Introduction

Plants colonized land around 470 million years ago. In this new habitat, plants had to face new biotic and abiotic stresses that shaped the development of a wide range of defence mechanisms. They evolved physical barriers as cuticles, and specialized structures such as trichomes, stings, thorns and silica or crystal deposition (Farmer, 2014). Plants also developed inducible defences including toxic chemicals, antinutritional proteins and proteinase inhibitors (PI) to damage insect digestion, and volatile compounds to attract predators. Plant chemicals involved in defence are secondary metabolites like glucosinolates, alkaloids, terpenoids or phenolic compounds (Farmer, 2014). Among them there are molecules with important therapeutical applications such as vinblastine, artemisin or taxol, and other compounds with interesting properties for different industries such as latex, tannins or capsaicin (Farmer, 2014; Wasternack and Hause, 2013).

Many of these defence responses are orchestrated by a group of plant hormones called jasmonates (JAs). Mutants affected in the biosynthesis or perception of JAs are more susceptible than the wild-type plants to invertebrate herbivores (Howe and Jander, 2008; Howe et al., 1996) and even vertebrates such as tortoises (Mafli et al., 2012). JAs were first identified in the essential oil of *Jasminum grandiflorum* (Demole et al., 1962). They are products of lipid peroxidation derived from the 13-lipoxygenase pathway and their chemical structure is similar to that of prostaglandins (Hamberg and Gardner, 1992).

JAs regulate plant responses to herbivory, wounding and necrotroph pathogens (Browse and Howe, 2008; Farmer et al., 2003; Wasternack and Hause, 2013). They are elicitors of secondary metabolism including for instance the biosynthesis of glucosinolates and taxol (Schweizer et al., 2013; Yukimune et al., 1996). They are involved in anthocyanin accumulation and trichome formation, laticifer differentiation in rubber plants and production of extrafloral nectaries (Feys et al., 1994; Hao and Wu, 2000; Heil et al., 2001; Li et al., 2004). In carnivorous plants, JAs are responsible for the switch from defensive to "attacking" molecules that help digesting the prey (Böhm et al., 2016). Noteworthy, JAs also regulate developmental traits such as fertility, where they are involved in filament elongation, pollen maturation and anther dehiscence (Wasternack and Hause, 2013). In Arabidopsis, mutants affected in the biosynthesis of JAs (*aos* and *opr3*) or perception of JA-Ile (*coi1*) are male sterile, whereas the analogous perception mutant in tomato (*jai1*) is female sterile (Li et al., 2004; Park et al., 2002; Stintzi and Browse, 2000; Turner et al., 2002; Xie et al., 1998). Root growth, fruit ripening, senescence, cell cycle and response to abiotic stresses such as cold and salt are also modulated by JAs (Dathe et al., 1981; Fan et al., 1998; Hu et al., 2013; Pauwels et al., 2008; Staswick et al., 1992; Toda et al., 2013; Ueda and Kato, 1980). Thus, JAs are important regulators of the allocation of plant resources towards growth or defence.

JA BIOSYNTHESIS

JA biosynthesis has been mainly studied in the model plant *Arabidopsis thaliana* and in tomato. Jasmonates originate from the fatty acid precursors linolenic acid (18:3) and hexadecatrienoic acid (16:3; Figure 1). These two fatty acids are released by phospholipases from the chloroplast membranes where they form phospholipids and galactolipids. Then, the concerted action of 13-lipoxygenases (13-LOX), allene oxide synthase (AOS) and allene oxide cyclase (AOC) transforms linolenic acid into OPDA (12-oxo-phytodienoic acid; (Wasternack, 2007). Alternatively, hexadecatrienoic acid can be transformed into dinor-OPDA (dn-OPDA) by the same enzymes (Weber et al., 1997). OPDA is synthesized in the chloroplast and the subsequent steps of JA biosynthesis take place in the peroxisome. It has been proposed that the transport of OPDA into the peroxisome requires the ATP Binding Cassette (ABC) transporter COMATOSE (CMT; Theodoulou et al., 2005) although this is not the sole import mechanism. In the peroxisome the double bond of the cyclopentenone ring of OPDA is reduced by OPDA reductase 3 (OPR3; Schaller et al., 2000) to produce OPC-8 [3-oxo-2-(2-pentenyl)-cyclopentane-1-octanoic acid].

The transformation of OPC-8 into JA occurs through the β-oxidation (Figure 1). β-oxidation is a common process to all living organisms and it is used to generate energy from the catabolism of fatty acids. Every cycle of β-oxidation shortens the carboxylic acid side chain of the substrates in two carbons. In order to enter the β-oxidation the substrates need to form esters with CoA. The enzymes that catalyse this step are the fatty acids CoA synthetases and 4-coumarate:CoA ligases. The reduced form of OPDA, OPC-8, is conjugated to acyl-CoA by the OPDA-Co-Ligase OPCL1 (Kienow et al., 2008). Other acyl-CoA synthases also show a wide specificity towards different substrates, including OPDA, dinor-OPDA and OPCs (Kienow et al., 2008). Hence, OPC-8 is converted into OPC-6 in the first cycle of β-oxidation, into OPC-4 in the second cycle and finally into jasmonic acid (JA). Interestingly, the first enzyme of the β-oxidation in tomato, the acyl-CoA oxidase ACX1A, can accept OPDA-CoA as a substrate *in vitro*, suggesting that OPDA could undergo the β-oxidation without prior reduction by OPR3 (Li et al., 2005).

JA is transported to the cytoplasm where the Jasmonoyl amino acid conjugate synthetase enzyme JAR1 (Jasmonate Resistant 1) conjugates it to Ile (Figure 1) to form (+)-7-*iso*-jasmonoyl-isoleucine, the active hormone (Fonseca et al., 2009; Katsir et al., 2008; Staswick and Tiryaki, 2004; Staswick et al., 2002; Thines et al., 2007). JAR1 belongs to the Gretchen Hagen 3 (GH3) family and is also named GH3.11. Most GH3 enzymes have poor substrate specificity and some of them (GH3.3, GH3.5 and GH3.6) can conjugate JA to aspartate, methionine and tryptophan *in vitro*. The role of these conjugates has not been well characterized, with the exception of JA-Trp, that acts as an auxin transport inhibitor (Staswick, 2009; Staswick et al., 2017). Most members of the GH3 family are mainly involved in auxin deactivation. JA-Ile is synthesized in the cytoplasm but it is imported into the nucleus by the JA/JA-Ile transporters JATs (Li et al., 2017), and perceived by COI1 (see below). JA-

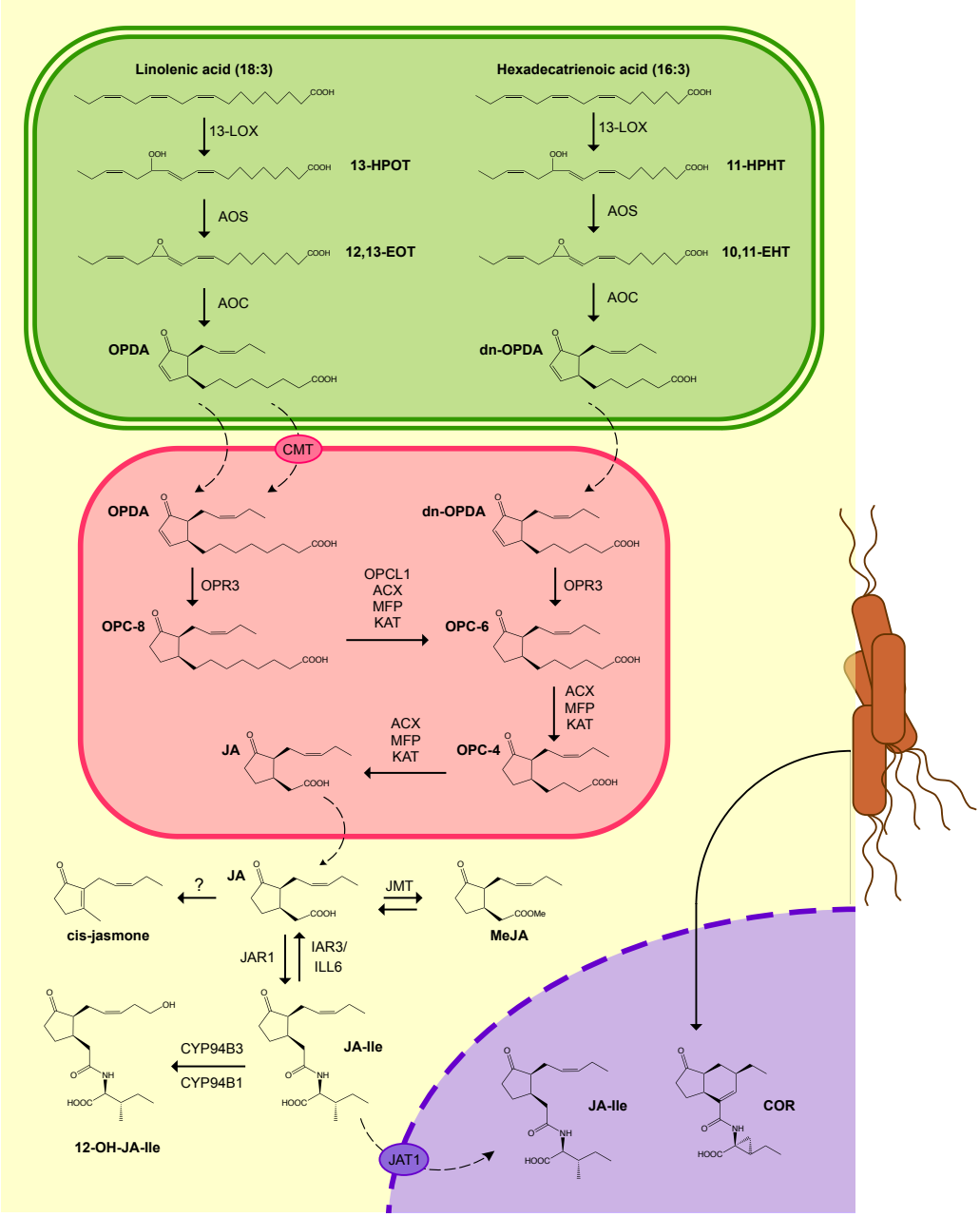

Figure 1: Biosynthetic pathway of JA-Ile. JA-Ile biosynthesis occurs in the chloroplast (green), the peroxisome (pink) and the cytoplasm (yellow). *Pseudomonas syringae* (brown) synthesizes the JA-Ile mimic coronatine (COR). Both JA-Ile and COR are perceived in the nucleus (purple) by the COI1/JAZ co-receptor complex.

Ile biosynthesis is regulated by a positive feedback loop, substrate availability and tissue specificity (Wasternack and Hause, 2013).

CATABOLISM/MODIFICATIONS OF JASMONATES

The over-activation of the JA pathway could be harmful for the plant so JA-Ile levels need to be tightly regulated. The inactivation of JA-Ile occurs by deconjugation or hydroxylation (Figure 1). The amidohydrolases IAR3/ILL6 cleave the isoleucine from JA-Ile (Widemann et al., 2013). The

hydroxylation and subsequent carboxylation of JA-Ile is catalysed by the cytochrome P450 CYP94B3 and CYP94C1 (Heitz et al., 2012; Koo et al., 2011). After hydroxylation JA-Ile can undergo sulfatation and glycosylation (Wasternack and Hause, 2013).

The JA precursors OPDA and dn-OPDA can be esterified with mono- and digalactosyl-diglycerides to form arabidopsides. These molecules are specific of *A. thaliana* and might act as storage forms of OPDA/dn-OPDA as they rapidly release these oxylipins upon wounding (Göbel and Feussner, 2009; Stelmach et al., 2001). Recently it was reported that OPDA can be conjugated to isoleucine to form OPDA-Ile (Floková et al., 2016). JA can be methylated by JA methyl transferase (JMT) to form the volatile compound MeJA (Figure 1; Seo et al., 2001), that was considered the active jasmonate for many years. As a volatile molecule, MeJA was proposed to have a role in interplant communication (Farmer and Ryan, 1990). Methyl-esterification of JA is a reversible process mediated by JMT and esterases. JA can be decarboxylated to form another volatile odorant compound: cis-jasmone (Figure 1), which attracts insects for pollination (Koch et al., 1997). Cis-jasmone has been considered both a catabolic product and a signalling molecule regulating COI1-independent genes (Matthes et al., 2010). OPDA has also been proposed to exhibit COI1-independent responses (Taki et al., 2005). The chemical structure of OPDA and cis-jasmone contains an α,β-unsaturated carbonyl group, characteristic of reactive electrophile species (RES). The presence of this group might at least partially account for these COI1-independent effects (Farmer and Mueller, 2013; Matthes et al., 2010). For instance, OPDA is known to upregulate the expression of genes related to detoxification as well as heat shock proteins, being this transcriptional response common to other RES (Farmer and Mueller, 2013).

Different JAs have been identified in non-model plant species such as 4,5-didehydro-JA in *Equisetum* and *Jasminum grandiflorum*, or dicranenones in the moss *Dicranum* (Dathe et al., 1989; Ichikawa et al., 1984; Kaiser and Lamparsky, 1974). One of the dicranenones, also known as 9,13-didehydro-12-oxo-phytodienoic acid or *iso*-OPDA, was also detected in stressed barley leaves and the lycophyte *Selaginella martensii* (Kramell et al., 2000; Ogorodnikova et al., 2015). Interestingly, there is one enzyme in the insect gut that can catalyse the isomerization of OPDA to *iso*-OPDA (Dabrowska et al., 2009) although it is not known if a similar enzyme exists in plants.

PERCEPTION

Once released upon a specific stimulus JA-Ile is perceived in the nucleus by its co-receptor integrated by COI1 (Coronatine Insensitive 1), the F-box component of the SCF^{COI1} (Skip-Cullin-F-box) E3 ubiquitin-ligase, and one of the JAZ repressors (Figure 2; Chini et al., 2007; Fonseca et al., 2009; Katsir et al., 2008; Sheard et al., 2010; Thines et al., 2007; Xie et al., 1998). Similar to the case of auxins (Tan et al., 2007), JA-Ile acts as a molecular glue that induces the interaction between the SCF^{COI1} complex and its substrates, the JAZ repressors, which are ubiquitinated and targeted to the

26S proteasome for degradation (Figure 2; Chini et al., 2007; Maor et al., 2007; Saracco et al., 2009; Thines et al., 2007; Yan et al., 2007). As a consequence the transcription factors (TFs) targeted by JAZs are de-repressed and activate transcriptional reprogramming in response to JA-Ile (Chini et al., 2007; Dombrecht et al., 2007; Fernández-Calvo et al., 2011; Lorenzo et al., 2004; Niu et al., 2011; Reymond et al., 2000).

Besides JA-Ile, the only known ligand of COI1-JAZ co-receptor is coronatine (COR), a bacterial mimic of JA-Ile synthesized by some *Pseudomonas syringae* strains (Bender et al., 1999; Brooks et al., 2004; Fonseca et al., 2009). COR shows higher affinity for COI1 than JA-Ile and can even bind directly to COI1 in the absence of JAZ (Sheard et al., 2010). Its high activity is due to the cyclohexene ring, that provides a stronger interaction surface compared to the corresponding pentenyl side chain in JA-Ile (Sheard e al., 2010).

Structural studies of the co-receptor complexes revealed that binding of COR or JA-Ile requires also the cofactor inositol pentakisphosphate (Sheard et al., 2010). Most of the bioactive hormone or its mimic remain buried inside the binding pocket of COI1 while the keto and carboxyl residues of both ligands are exposed and available for further interactions with JAZ (Sheard et al., 2010). The modification of these two residues would result in the interference with JAZ proteins interaction and, therefore, could attenuate JA responsiveness of the plant. An approach to rationally design a hormone-based specific antagonist has been successfully carried out to synthesize auxinole, a potent auxin antagonist (Hayashi et al., 2012). Engineering of COI1 amino acid sequence in specific residues involved in hormone binding was a different strategy to modulate perception (Zhang et al., 2015b). The point mutation A384V in AtCOI1 resulted in uncoupling JA-Ile and COR perception. The introduction of a residue with an increased side chain size allowed the accommodation of the flexible JA-Ile but not of COR, which is more rigid than JA-Ile (Zhang et al., 2015b).

JAZ

JAZ repressors belong to the TIFY superfamily, which also contains ZIMs, PPDs and TIFY8, all of them sharing the TIF[F/Y]XG motif (Vanholme et al., 2007). In *A.*

thaliana the JAZ family traditionally encompasses 12 members (Chini et al., 2007; Thines et al., 2007). Canonical JAZ proteins share two conserved regions: the Jas motif in the C-terminus and the ZIM domain containing the TIF[F/Y]XG motif (Figure 2; Chini et al., 2007; Thines et al., 2007; Vanholme et al., 2007; Yan et al., 2007). Recently, a 13th member with divergent ZIM and Jas domains was added to the JAZ family (Thireault et al., 2015). The Jas motif is necessary for the interaction with several TFs in basal conditions and with COI1 in a JA-Ile-dependent manner (Chini et al., 2007; Katsir et al., 2008). The ZIM domain mediates homo- and hetero-dimerization of JAZ (Chini et al., 2009; Chung and Howe, 2009; Chung et al., 2009) and is responsible for the interaction with the adaptor protein Novel Interactor of JAZ (NINJA; Figure 2; Pauwels et al., 2010). Other members of the TIFY

superfamily, namely PPD and TIFY8, also interact with NINJA through their ZIM domain (Pauwels et al., 2010). NINJA contains the EAR domain (Ethylene Responsive Factor-associated amphiphilic repression; Figure 2) that enables its interaction with the general co-repressor TOPLESS (TPL) and TPL-related proteins (TPR; Kagale et al., 2010; Pauwels et al., 2010). The EAR domain is present in four JAZ proteins: JAZ5, JAZ6, JAZ7 and JAZ8, which can bind directly to TPL (Causier et al., 2012; Pauwels et al., 2010; Shyu et al., 2012). TPL genetically interacts with the histone deacetylases 6 and 19 (HDA6 and HDA19; Figure 2) and histone-deacetylation is probably the mechanism behind the repression of transcription exerted by TPL, that cannot bind directly to DNA (Wu et al., 2008; Zhou et al., 2005).

The presence of 13 genes encoding JAZ proteins in the Arabidopsis genome raises the question about their redundancy or specificity (Chini et al., 2016). Several *jaz* single loss-of-function mutants have been isolated but only *jaz10-1* mutant shows hypersensitivity to JA (Demianski et al., 2012; Sehr et al., 2010). Multiple *jaz* mutants enhance the hypersensitive phenotype of *jaz10-1*, which argues for JAZ redundancy (Campos et al., 2016; Chini et al., 2016; Thireault et al., 2015; de Torres Zabala et al., 2016). Conversely, JAZ show different transcriptional expression patterns and different affinities for the COI1 F-box depending on the hormone threshold (Demianski et al., 2012; Melotto et al., 2008) pointing out that they might regulate different responses. Recently the specific role of one JAZ protein was uncovered: JAZ2 modulates stomatal dynamics during infection by the pathogen *P. syringae* (Gimenez-Ibanez et al., 2016a).

Several alternative repression mechanisms of JAZ repressors have been described, highlighting the need for a tight repression of the transcription factors in basal conditions. For instance, the Jas domain of JAZ7 and JAZ8 lack certain residues required for interaction with COI1. These two proteins are unable to bind to COI1 and are not degraded by the proteasome in response to JA-Ile (Shyu et al., 2012). However, their Jas domain still interact with the MYC TFs and therefore these two JAZ act as constitutive repressors upon induction. Most *JAZ* genes can produce alternative splicing transcripts mainly by retention of the Jas intron (Chung et al., 2010). Some of these alternative JAZ lacking at least partially the Jas domain resulted in dominant JAZ repressors, as it is the case of the splice variant JAZ10.4 (Moreno et al., 2013). These splicing variants were instrumental for the identification of a Cryptic MYC-Interaction Domain (CMID) located in the N-terminal of JAZ1 and JAZ10 (Moreno et al., 2013; Zhang et al., 2017). The lack of Jas domain results in resistance to JA-Ile-mediated degradation through COI1 and the proteasome, but the presence of the CMID enables the binding and constitutive repression of MYC2, MYC3 and MYC4 (Moreno et al., 2013). The interaction with MYC2 is also required for the nuclear import of JAZ (Withers et al., 2012). In the case of full-length JAZ this interaction is mediated by the Jas domain, but the interaction through the CMID could be a plausible explanation for the localization of JAZΔJas in the nucleus. Alternatively, homo- and hetero-dimerization of JAZ could also play a role in nuclear localization.

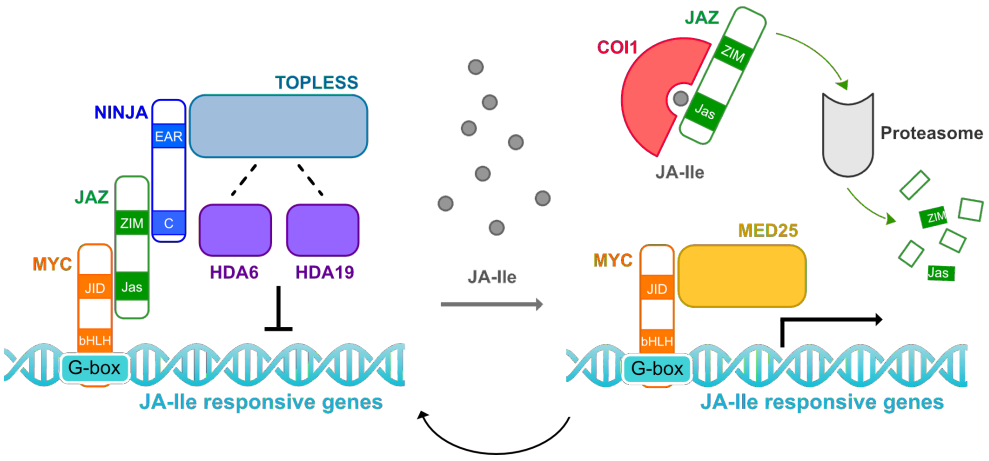

Figure 2: Repression and activation of JA-Ile signalling pathway. In the absence of the hormone, JA-Ile, MYC transcription factors are repressed by a complex formed by JAZ, NINJA and TOPLESS, that recruits the Histone Deacetylases HDA6 or HDA19 to prevent the expression of JA-Ile responsive genes. JA-Ile release triggers the interaction between JAZ and the F-box COI1, which induces the proteasome-dependent JAZ degradation. Once released from the repression, MYCs bind MED25, that together with the other components of the mediator complex (not shown) activates JA-Ile responsive genes transcription, which contain the G-box. *JAZ* are JA-Ile responsive genes and therefore their hormone-dependent expression is a feedback loop that restores the basal situation. Domains of MYC (bHLH and JID), JAZ (ZIM and Jas) and NINJA (EAR and C) are depicted in the figure.

TRANSCRIPTION FACTORS

JAZ proteins bind and repress transcription factors from different families. The best characterized are those belonging to the bHLH (basic Helix-Loop-Helix) superfamily, but other JAZ targets are MYBs, YABBY, EIN3/EIL1, TOE and WRKY (Chini et al., 2016). The clade IIIe of the bHLH family includes MYC2, the most prominent transcription factor regulating JA responses (Boter et al., 2004; Lorenzo et al., 2004) and MYC3, MYC4 and MYC5, that act synergistically with MYC2 to regulate JA responses (Cheng et al., 2011; Fernández-Calvo et al., 2011; Figueroa and Browse, 2015; Niu et al., 2011; Qi et al., 2015). MYC2 controls predominantly (but not exclusively) root responses to JA, whereas MYC3 and MYC4 regulate mostly the JA-responses in the aerial part, which correlates with their differential expression patterns (Cheng et al., 2011; Fernández-Calvo et al., 2011; Niu et al., 2011). MYC5 controls stamen development and pollen viability together with the other MYCs but it does not play a role in defence (Figueroa and Browse, 2015; Qi et al., 2015). All MYCs show the same DNA binding specificity for the G-box and related elements in the promoters of their target genes (Fernández-Calvo et al., 2011; Figueroa and Browse, 2015; Godoy et al., 2011). Among those targets we can find JAZ genes, which are transcribed in response to JA-Ile to shut down the activation of the pathway through a negative feedback loop (Figure 2).

Both JAZs and MYCs are regulated by environmental cues. Shade from dense canopies is enriched in far-red light reflected from other plants. In this situation, it is well known that plants tend to grow to

reach sunlight and this resource allocation towards growth diminishes their ability to defend themselves. Shade promotes MYC destabilization and JAZ accumulation which results in a strong repression of the JA pathway to facilitate growth (Chico et al., 2014).

MYC proteins contain a bHLH domain for DNA binding, the JID (JAZ Interaction Domain) for JAZ interaction and the transactivation domain (TAD) responsible for their activity as transcriptional activators (Fernández-Calvo et al., 2011). The crystal structure of the complex MYC3-JAZ9 revealed that the interaction between the Jas from JAZ9 and MYC3 requires not only the JID domain but also the TAD helix (Zhang et al., 2015a). JAZ9 binding to MYC3 generates conformational changes in MYC3 that results in competitive binding between JAZ9 and MED25 (Mediator 25; Figure 2), one of the subunits of the mediator complex and part of the general transcriptional activation machinery (Zhang et al., 2015a). This mechanism explains that JAZ-mediated repression takes place through the recruitment of the NINJA-TPL complex and the competition with MED25 for MYC binding.

The clade IIId of bHLH is formed by bHLH003/JAM3 (JA Associated MYC2-like 3), bHLH013/JAM2, bHLH014 and bHLH017/JAM1, which are also direct targets of JAZ. The sequence of these bHLH is very similar to MYCs, although they act as repressors of the JA pathway because they lack the activation domain (Fonseca et al., 2014a; Nakata et al., 2013; Sasaki-Sekimoto et al., 2013; Song et al., 2013). These TFs are considered to fine-tune JA-responses through competition with MYCs for the G-box and direct repression by JAZ/NINJA/TPL complexes (Fonseca et al., 2014a).

JA is a positive regulator of freeze tolerance. This response is regulated by the clade IIIb of bHLH ICE1 and ICE2 (Inducer of CBF Expression), which can also bind to certain JAZ repressors (Hu et al., 2013).

Other bHLH closely related to MYCs and JAMs are GL3 (Glabra 3), EGL3 (Enhancer of Glabra 3) and TT8 (Transparent Testa 8), which belong to the clade IIIf. They bear the JID domain and are targets of JAZ proteins. They form complexes with WD40 and MYB75/PAP1 (Production of Anthocyanin Pigment 1) and GL1 (Glabra 1) to regulate anthocyanin accumulation and trichome initiation. MYB75 and GL1 are also direct targets of several JAZ proteins (Qi et al., 2011). Anthocyanin accumulation is also mediated by the interaction of JAZ3 through its ZIM domain with YAB1 and YAB3, members of the YABBY family. YAB1 binds to the promoter of *MYB75*,

controlling its expression, so this is an indirect mechanism of JAZ to regulate anthocyanin biosynthesis (Boter et al., 2015).

In addition to anthocyanin accumulation and trichome formation, MYBs control other JA-dependent processes. MYB21, MYB24 and MYB108 can be also repressed by JAZ proteins and control stamen development (Mandaokar et al., 2006; Qi et al., 2015; Song et al., 2011) while other MYBs, namely MYB28, MYB29, MYB34, MYB51, MYB76 and MYB121, interact with MYCs to control glucosinolate synthesis (Frerigmann et al., 2014; Schweizer et al., 2013).

CROSSTALK WITH OTHER HORMONES

JAs are known to interact with different hormones in a positive and negative way. This is the case of the ethylene (ET) signalling pathway, which acts in a synergistic and antagonistic manner with JAs, depending on the situation. For instance, JA-Ile and ET cooperate against necrotroph pathogens but have different roles in apical hook formation and defence against insects (Broekaert et al., 2006; Song et al., 2014). JAZ directly interact with Ethylene Insensitive 3 (EIN3) and EIN3-Like 1 (EIL1), therefore repressing the ET signalling pathway (Zhu et al., 2011). JA-Ile-dependent degradation of JAZ releases EIN3 and EIL1, which require ethylene for stabilization. This mechanism explains how both hormones are necessary to activate gene expression in response to nectrotroph pathogens. Additionally, the interaction between MYC2 and EIN3 diminishes the activity of either TF and this mechanism could be responsible for the opposite effects of JA/ET pathway in other circumstances (Song et al., 2014).

The JA pathway interacts with the gibberellin (GA) pathway to regulate the balance between growth and defence. The interaction between JAZ and DELLAs, the repressors of the GA pathway, reduces the available pool of repressors that interact with their corresponding TFs. When GA degrades DELLAs, there is more repression of MYCs by JAZ and *vice versa* (Hou et al., 2010; Yang et al., 2012).

The cross-talk between JA and abscisic acid (ABA) occurs at least at the level of JAZ12, which is regulated by the E3-ligase Keep On Going (KEG). This protein acts as a negative regulator of ABA signalling. It seems that this interaction is specific for JAZ12, since none of the other JAZ could interact with KEG (Pauwels et al., 2015).

MANIPULATION OF JA/SA PATHWAY DURING DEFENCE

JA and salicylic acid (SA) play a central role in plant immunity and exhibit a reciprocal antagonism. In a simplistic way, JA controls defence against herbivores and nectrotroph pathogens and SA against biotrophs. Because of the negative cross-talk, the resistance to necrotroph pathogens increases the susceptibility to biotroph pathogens, and *vice versa* (Glazebrook, 2005). The tight regulation between these two pathways enables the plant to mount effective defences against the different pathogens.

Pathogens have evolved several strategies to turn the JA-SA cross-talk towards their own benefit. One of the finest examples of this manipulation is the production of COR by certain strains of *P. syringae* (Bender et al., 1999; Brooks et al., 2004). COR suppresses host defences by activating the JA pathway which has an inhibitory effect on SA-mediated defences against the bacteria (Feys et al., 1994; Fonseca et al., 2009; Laurie-Berry et al., 2006; Spoel et al., 2003; Thilmony et al., 2006; Uppalapati et al., 2005, 2007; Zhao et al., 2003). As a result, production of COR allows *P. syringae* to manipulate the interactions between these hormonal pathways to open stomata, grow in the apoplast and induce disease symptoms in plants (Brooks et al., 2004; Kloek et al., 2001; Melotto et al., 2006, 2008; Uppalapati et al., 2007). Some pathogenic fungi such as *Fusarium oxysporum* or *Lasiodiplodia theobromae* can synthesize JA and JA-Ile to activate the JA pathway (Aldridge et al., 1971; Brodhun et

al., 2013; Cole et al., 2014; Miersch et al., 1989, 1999). In other cases, the strategy to infect the plants consists of inactivating JA, as it occurs with the fungal monooxygenase produced by *Magnaporthe oryzae* to hydroxylate JA in the terminal carbon (Patkar et al., 2015).

In order to evade host defences, many pathogens deliver effector proteins into the plant cells. Most of the targets and mechanism of action of these effectors is unknown, but some of them target the JA pathway (Gimenez-Ibanez et al., 2016b). The bacterial effectors HopX1 and HopZ1a from *P. syringae* are proteases that degrade the JAZ repressors in a COI1-independent and dependent manner, respectively (Gimenez-Ibanez et al., 2014; Jiang et al., 2013). One of the first characterized *Pseudomonas* effectors, AvrB, targets the plasma membrane H+-ATPase AHA1 to open the stomata and increase the COI1/JAZ binding by a yet unknown mechanism (Zhou et al., 2015). The effector RxL44 from the pathogen *Hyalopernospora arabidopsidis* targets one component of the mediator complex to attenuate the SA pathway (Caillaud et al., 2013). Either by activating the JA pathway or attenuating the SA pathway, the goal of these strategies is rendering the plants more susceptible to biotroph pathogens.

Other effectors have evolved to suppress JA-dependent defences. The necrotrophic fungi *Sclerotinia sclerotiorum* secretes an effector-like protein called SSITL (sclerotinia sclerotiorum integrin-like) to inhibit the JA pathway, whereas the exopolysaccharide from *Botrytis cinerea* activates the SA pathway to dampen the JA-mediated defences (El Oirdi et al., 2011; Zhu et al., 2013). The ectomycorrhizal fungus *Laccaria bicolor* uses the effector MiSSP7 (mycorrhizal induced small secreted protein 7) to stabilize JAZ from poplar and establish a successful symbiosis with the plant root (Plett et al., 2014). Virus can also deliver effectors into the plant, as it is the case of the Tomato yellow leaf curl virus, inoculated into Arabidopsis by the whitefly. The virus releases an effector called bC1 that targets MYC2 and reduces the production of terpenoids, making the plant more susceptible to the whitefly (Li et al., 2014).

Previous examples show that COI1/JAZs are signalling hubs targeted by many different pathogens to unbalance the JA/SA cross-talk and overcome plant defences. Therefore, the repression of the JA signalling pathway is an interesting biotechnological strategy to enhance defences against biotroph pathogens. Two examples of this strategy are the JAR1-antagonist jarin-1 and the engineered COI1 A384V protein which is COR-insensitive but retains response to JA-Ile (Meesters et al., 2014; Zhang et al., 2015b).

EVOLUTION

The limited availability of divergent plant models in the past years has restricted our knowledge about the JA pathway to a handful of angiosperms. The current plant models, namely Arabidopsis or tomato, show a high gene redundancy that also hampers the study of this pathway. Recent research has focused on the sequence conservation of the JA signalling machinery in both algae and land plants

(Bowman et al., 2017). Such analyses revealed that the JA signalling pathway was already present in the common ancestor of land plants. However, the lack of a key enzyme for JA-Ile biosynthesis (OPR3) in bryophytes, the most basal lineage of land plants, suggests that the hormone activating this pathway might be different from JA-Ile. Complementary hormone measurements in bryophytes failed to detect JA-Ile, supporting the idea that the hormone might be other than JA-Ile. These preliminary results pose a fascinating question about the conservation and evolution of this pathway in early land plants: if there is no JA-Ile, which is the hormone? To answer this, we have chosen the model plant *Marchantia polymorpha*, since this liverwort shows a key evolutionary position, extraordinary low gene redundancy and a haploid-dominant life cycle.

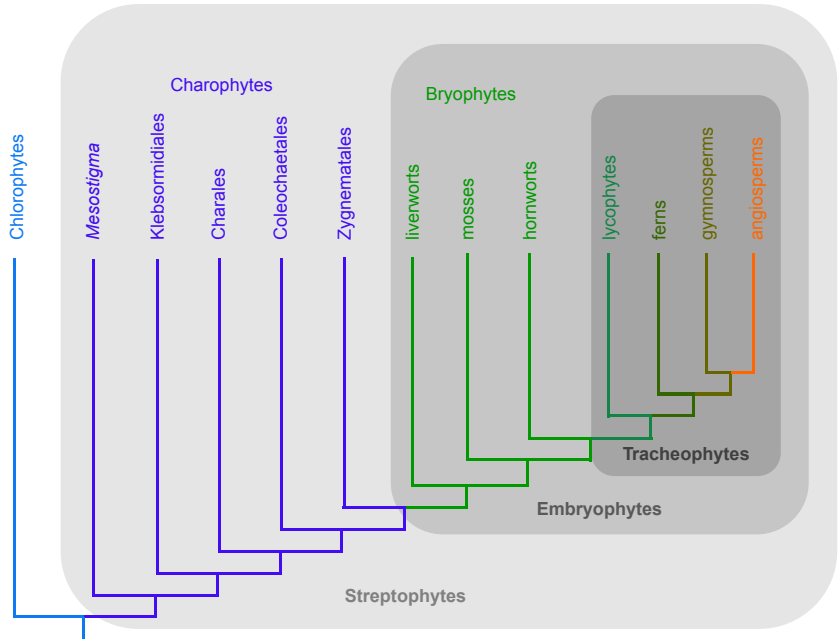

Figure 3: Phylogenetic relationships among the green plants. Chlorophytes and charophytes are green algae. Streptophytes (light grey) comprise charophytes and land plants (embryophytes; grey). Vascular plants or tracheophytes (dark grey) include lycophytes, ferns, gymnosperms and angiosperms.

Colonization of land by green plants is one of the most important events in the history of Earth. It is considered that land plants, or Embryophyta, evolved from freshwater green algae (Figure 3). Interestingly, terrestrialization was not a unique event during evolution and terrestrial algae can be found among chlorophytes and charophytes, the two main lineages of green algae (Harholt et al., 2016). Although terrestrial algae spend most of their life out of water, their life cycle cannot be completed without it (Lewis and McCourt, 2004). Hence, it seems that the adaptation to terrestrial environments started in green algae (Harholt et al., 2016). Subsequent innovations such as alternation of generations and evolution of multicellular sporophyte likely appeared first in the common ancestor of land plants and these traits were retained in the extant bryophytes, the most basal group of land plants (Bowman et al., 2007).

The oldest fossil records of land plants date back to the middle Ordovician, around 470 million years ago, and consist of cryptospores strikingly similar to modern liverworts (Wellman et al., 2003). Macrofossils from the Devonian period support the idea that the thalloid gametophyte of the ancient land plants was similar to liverworts (Guo et al., 2012). Liverworts, together with mosses and hornworts are the three lineages that are collectively named bryophytes (Figure 3). Bryophytes are considered a sister lineage to the rest of land plants (Tracheophyta or vascular plants), but the specific order in which each bryophyte lineage appeared is still controversial. Based on morphology and fossil records, liverworts arise as the oldest lineage among bryophytes. However, recent genomic comparisons propose a different model where hornworts are sister to all land plants and liverworts and mosses form a clade sister to vascular plants (Wickett et al., 2014). Comparative genomics of a sufficient number of diverse bryophytes are required to clarify this issue. The key evolutionary position of bryophytes as extant members of the plant lineage that colonized land makes them attractive models for evolutionary studies. However, only one moss, *Physcomitrella patens*, and one liverwort, *Marchantia polymorpha*, reunite the basic characteristics to be considered model plants: their genome is sequenced and they are amenable for reverse and forward genetic studies. *P. patens* has been an established model plant for the past decades, but one feature of *M. polymorpha* that makes it even more interesting than *P. patens* is its low gene redundancy (Bowman et al., 2017).

MARCHANTIA POLYMORPHA

Ancient Greek philosophers such as Dioscorides and Theophrastus already acknowledged *M. polymorpha*. They described thalloid plants that grew on the bark of trees and they referred to them as lichen, a term that probably included liverworts (Bowman, 2016). In the 18th century, the genus *Marchantia* received its name after the French botanist Nicolas Marchant (Bowman, 2016).

A. thaliana has been the dominant model for plant biology research since 1960s (Provart et al., 2016). Unfortunately, the use of other model plants such as *M. polymorpha* has lagged behind mainly due to the lack of genetic tools and a sequenced genome (Chang et al., 2016). This problem has been solved in the beginning of 21st century thanks to the JGI initiative to sequence the *M. polymorpha* genome (Bowman et al., 2017) and the development of transformation techniques (Ishizaki et al., 2008, 2015; Kubota et al., 2013) and gene-targeting (Ishizaki et al., 2013; Sugano et al., 2014).

M. polymorpha is a dioic plant. As other early divergent land plants, its life cycle shows a dominant haploid gametophyte and a diploid sporophyte that nutritionally depends on the gametophyte. Its genome is about 230 Mb packed in eight chromosomes plus one sex-chromosome namely X or Y. *M. polymorpha* shows a complex thallus with specialized structures and marked dorsiventrality. The upper layer of the thallus forms the air chambers and gemma cups. The air chambers contain assimilatory filaments to perform the photosynthesis and air pores to facilitate gas exchange in the absence of stomata. In the middle, the storage region is formed by parenchymatous and oil body

cells, which are specialized cells that accumulate secondary metabolites and probably play a role in plant defence (Tanaka et al., 2016). The ventral part of the thallus develops three rows of scales and two types of rhizoids, mainly for anchoring, water uptake and fungal symbiosis (Shimamura, 2016).

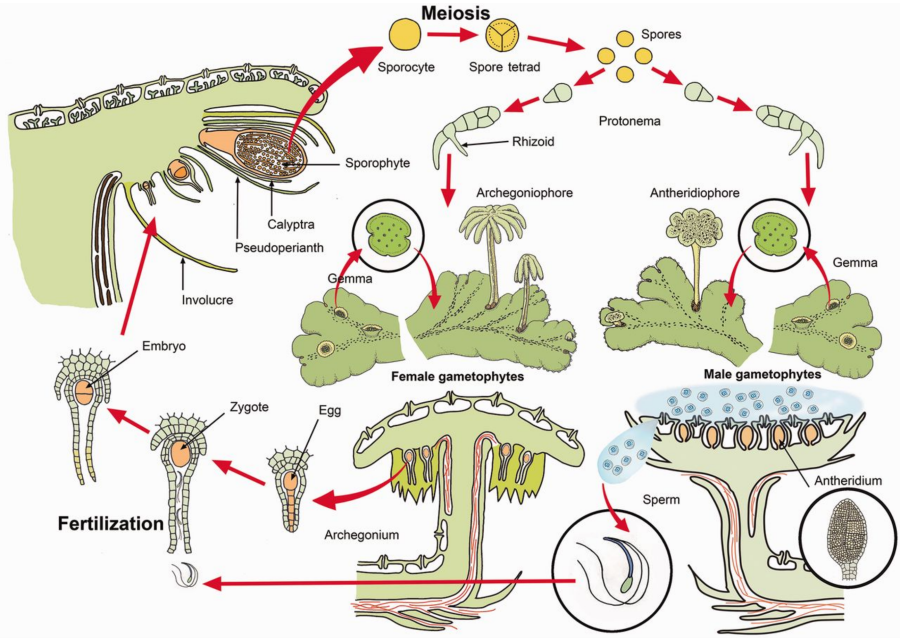

Figure 4: *Marchantia polymorpha* life cycle. (Shimamura, 2016)

M. polymorpha can reproduce both sexually and asexually. The propagation by asexual reproduction consists of the formation of clones (gemmae) in the gemma cups (Figure 4). Gemma cups are formed on the dorsal side of the thallus and appear at regular intervals. Sucrose and short-day photoperiod enhance the formation of gemma cups (Terui, 1981). During the first stages of development gemmae are attached through a stalk cell to the bottom of the gemma cup and remain dormant until they are liberated from the cup. Gemmae show a discoidal shape and two apical notches containing the meristem in opposites sides of the disc. Gemmae lack dorsiventrality but once it is established gemmalings develop air chambers on the dorsal side and rhizoids and scales on the ventral side. The growth of *M. polymorpha* follows a dicotomous branching where two apical notches from the same meristem diverge and lead the bifurcated growth of the thallus (Solly et al., 2017). In about three weeks gemmae can grow to form a thallus with gemma cups, thus completing the cycle in a short time.

Alternatively *M. polymorpha* can reproduce sexually and form unicellular spores. Every spore generates a young protonema with a rhizoid that will grow into a thallus after a few days (Figure 4). Male and female thalli grown under long-day conditions or irradiated with far-red light can develop gametangiophores (Chiyoda et al., 2008; Kubota et al., 2014). Male gametangiophores are called antheridiophores and female gametangiophores are the archegoniophores (Figure 4). During the first

steps of the development of both structures they are just a portion of thallus elevated on a stalk, keeping the same features of the regular thallus, such as rhizoids and air pores. Antheridial receptacle typically shows eight lobes and antheridial chambers that contain the antheridia, where the spermatogenesis and spermiogenesis take place (Higo et al., 2016). When a drop of water splashes onto the antheridiophore, motile sperm cells are released to the surface through a pore and swim towards the archegoniophore (Figure 4). Interestingly sperm cells can climb the stalks of archegoniophores through capillarity of the rhizoids of the stalk. The upper part of the archegoniophore shows nine to eleven digitate rays in a radial disposition. The archegonia are located between the bases of the rays. Unlike antheridia, they are not exposed to the external surface of the plant but face the stalk of the archegoniophore. Upon fertilization the diploid zygote is formed and undergoes several mitotic cell divisions to form many sporocytes within the sporophyte (Figure 4). The sporophyte remains attached to the gametophyte through the seta for nutrient transfer. Finally, every sporocyte undergoes meiosis and gives rise to four haploid unicellular spores. The spores are enclosed in a sporangium surrounded by a capsule and when it dries, the helicoidal cells called elaters contribute to the massive spore dispersal (Shimamura, 2016).

The recent use of *M. polymorpha* as a model plant has proved the conservation of diverse pathways between the different lineages of land plants (Flores-Sandoval et al., 2015; Inoue et al., 2016; Kato et al., 2015; Kubota et al., 2014; Proust et al., 2016). Moreover, there are several examples of mechanisms operating in the gametophyte of bryophytes that were likely recruited to increasingly complex sporophytes in vascular plants (Kubota et al., 2014; Proust et al., 2016).

The conservation of hormone signalling pathways in bryophytes has been mainly studied through homologue sequence analyses and hormone profiling (Bowman et al., 2017; Sabovljević et al., 2014; Wang et al., 2015; Záveská Drábková et al., 2015). ABA, auxins, cytokinins (CKs), ET, SA and strigolactones have been detected in bryophytes but only the precursors of GA and BRs (ent-kaurene and castasterone) have been detected (Sabovljević et al., 2014; Záveská Drábková et al., 2015). The signalling pathways of CKs and ET already existed in algae, while the signalling pathways of the other hormones probably evolved in the common ancestor of land plants, recruiting pre-existing algal components (Bowman et al., 2017). For instance the transcription factors that mediate auxin responses are the ARFs (Auxin Response Factors) and appeared in algae. However, the perception machinery involving the F-box TIR1, the Aux/IAA repressors and the hormone was an innovation of the ancestral land plant (Bowman et al., 2017). Interestingly, charophytes have F-box orthologues to both TIR1 and COI1, the most closely related protein to TIR1. Careful examination of the sequences of these F-box revealed that they lack the key residues for ligand interaction, suggesting that COI1 and TIR1 evolved in the ancestral land plant by gene duplication from an algal F-box (Bowman et al., 2017). Besides COI1, sequences for all the signalling components of the JA pathway (JAZ, MYC,

NINJA and TPL) are present in bryophytes. MYC and TPL could be also identified in algae and were likely recruited during terrestrialization (Bowman et al., 2017).

Jasmonate biosynthesis has been studied in early divergent plants with opposite results. The characterization of the biosynthetic enzymes AOS and AOC in *K. flaccidum*, *M. polymorpha*, *P. patens* and *Selaginella moellendorfii* have demonstrated that the synthesis of OPDA is conserved among these organisms (Koeduka et al., 2015; Ponce de León et al., 2015; Pratiwi et al., 2017; Scholz et al., 2012; Stumpe et al., 2010; Yamamoto et al., 2015). Moreover, these studies provide evidence that JA and JA-Ile biosynthesis do not occur in bryophytes but is conserved in lycophytes (early tracheophytes; Pratiwi et al., 2017). Other studies provide alternative scenarios where bryophytes accumulate JA or JA-Ile (Záveská Drábková et al., 2015) and the lycophyte *Selaginella martensii* is unable to produce jasmonates (Ogorodnikova et al., 2015). The presence of JA or JA-Ile does not necessarily mean that these are signalling molecules. Indeed, OPDA but not JA can inhibit growth in *P. patens* and *M. polymorpha* (Ponce de León et al., 2015; Yamamoto et al., 2015). In *P. patens*, it has been proposed that OPDA regulates fertility and defence responses against *B. cinerea* (Ponce De León et al., 2012; Stumpe et al., 2010). The controversy about the presence of an active jasmonate in early divergent plants is intriguing. The conservation of the signalling pathway with a minimal set of components in *M. polymorpha* suggests that there should be a jasmonate-like ligand. In addition, the study of this signalling pathway in *M. polymorpha* could be useful to unravel possible new regulatory mechanisms conserved or not in other lineages.

Objectives

Arabidopsis thaliana has been an instrumental model system to identify the bioactive jasmonate and elucidate its signal transduction pathway in eudicots. However, the existence of a similar functional pathway in other plant lineages remains unexplored. Sequence analyses of bryophytes, the most basal lineage of extant land plants, have revealed that the JA signalling pathway might have been present in the common ancestor of land plants. However, bryophytes lack two key enzymes for JA-Ile biosynthesis (OPR3 and JAR1) and, therefore, the existence of the vascular plants hormone is unlikely. The main objective of this thesis is to study the functional conservation and evolution of the JA signalling pathway and to identify the hormone that activates it. For this, we have chosen the model plant *Marchantia polymorpha*. This liverwort shows a key evolutionary position, extraordinary low gene redundancy and a haploid-dominant life cycle. Its genome has been recently sequenced and many tools are available for genetic and biochemical studies.

The specific objectives addressed in this work are:

- The study of the conservation of the COI1/JAZ co-receptor complex in *Marchantia polymorpha*

- The identification of the active hormone binding to MpCOI1/MpJAZ

- The application of the knowledge about the co-receptor COI1/JAZ to design a specific antagonist with biotechnological potential

Material and Methods

Plant material and growth conditions

Marchantia polymorpha accession Takaragaike-1 (Tak-1; male) and Takaragaike-2 (Tak-2; female) were used as wild-type. Lines generated in this study are listed in Supplementary Table S2. *M. polymorpha* plants were grown on half strength Gamborg's B5 medium containing 1% agar under continuous light (50-60 µmol m^{-2} s^{-1}) and 22°C. Plants were subcultivated by cutting pieces of thalli including the notch (meristem) or by sowing gemmae from the gemma cups. Gemmae were stored in vials containing 0.5 Gamborg's B5 1% agar 1% sucrose at 4ºC and darkness for several years.

Gemmae used for confocal microscope observation were grown on liquid half strength Gamborg's B5 liquid medium. Plants used for RNA extraction were grown on 0.5 Gamborg's B5 medium containing 0.5% agar to facilitate removal from the agar plate when transferring the plants to 0.5 Gamborg's B5 liquid medium for hormone treatments. For transformation assays (Ishizaki et al., 2008; Kubota et al., 2013), F1 spores (Tak-1 x Tak-2), BC4 spores (F1 plants back-crossed with Tak-1 four times) or cut-thalli (Tak-1) were grown in liquid 0M51C medium. Transformed plants were plated on 0.5 Gamborg's B5 1% agar medium plus hygromycin and/or chlorosulfuron. Cefotaxime sodium salt (also known as Claforan, Duchefa) was included in all the plates to prevent *Agrobacterium tumefaciens* growth. *M. polymorpha* plants used for crossing were grown on soil under continuous white light and covered with a lid to maintain humidity. Gametangiophores were induced under white light supplemented with far-red. Alternatively, Tak-1 and Mp*jaz-1* were grown on jars containing 0.5 Gamborg's B5 1% agar under white light supplemented with far-red to induce antheridiophore formation. Spores were sterilized with 0.25% sodium hypochlorite (Sigma) and 0.05% Triton X-100 and sown on 0.5 Gamborg's B5. Individual thalli were used for DNA extraction and genotyped with specific primers (see Supplementary Table S3).

Physcomitrella patens (kindly provided by Dr. Begoña Benito, CBGP-UPM-INIA, Madrid) was grown on BCDAT medium under 16-h light/8-h dark cycle at 21 °C.

Plant material was grinded at room temperature with mortar and pestle in a small volume of sterile water and drops of similar size were plated on BCDAT supplemented with different molecules. *Anthoceros agrestis* was kindly provided by Professor Jane Langdale (Dept. of Plant Sciences, University of Oxford, Oxford). Fragments of 3 mm x 3 mm of *A. agrestis* were grown on 0.5 Gamborg's B5 supplemented with the indicated hormones under continuous light (50-60 µmol m^{-2} s^{-1}) and 22ºC for 39 days.

Arabidopsis thaliana Columbia (Col-0) is the genetic background of WT and transgenic *A. thaliana* lines used throughout the work (Supplementary Table S2). Seeds were surface-sterilized by the chlorine gas method (50 ml bleach and 3 ml HCl 37% for 3 h) and stratified for 2–3 d at 4 °C. All seedlings were grown under a 16-h light/8-h dark cycle at 21 °C (except for DR5:GUS, which was grown under continuous light at 25 °C). WT and 35S:At*COI1*-Flag seedlings were grown in Johnson medium and 35S:Mp*COI1*-flag was grown on MS medium. 35S:At*JAZ1*-GUS, 35S:At*JAZ9*-GUS and

35S:At*JAZ10*-GUS seedlings were grown vertically on MS plates, whereas 35S:Mp*JAZ*-GFP, 35S:Mp*JAZΔJas*-GFP, DR5:GUS, Dexp:At*TIR1*-myc/tir1-1 (kindly provided by Professor M. Estelle, University of California-San Diego) and $_{prom}$At*JAZ2*:GUS were grown in liquid MS. *A. thaliana* and *Nicotiana benthamiana* grew on soil in the greenhouse under a photoperiod of 16-h light/8-h dark at 21ºC for transformation experiments and seed propagation (*A. thaliana*) and infection with *Pseudomonas syringae* (*N. benthamiana*). *A. thaliana* plants used for bioassays with *P. syringae* and *Botrytis cinerea* were grown under short-day conditions and 21ºC for four weeks before infection.

Half strength Gamborg's B5, MS, Johnson and BCDAT media were supplemented with the following molecules when indicated: jasmonic acid (JA), methyl-jasmonate (MeJA) and coronatine (COR) from Sigma; OPDA and OPDA-Ile synthesized by Dr. Kosaku Takahashi (Agricultural University of Hokkaido); dn-*cis*-OPDA, dn-*trans*-OPDA, dn-*iso*-OPDA, tn-*iso*-OPDA, 3,7-ddh-JA, 3,7-ddh-JA-Ile-Me, (+)-7-*iso*-JA-Ile, 4,5-ddh-JA, (+)-4,5-ddh-JA-Ile, JA-MO, JA-Ile-MO, COR-MO and methyl esters of JA-Ile and COR synthesized by Dr. Mats Hamberg (Karolinska Institutet).

Gene identification and phylogenetic analyses

M. polymorpha sequences were obtained from the *M. polymorpha* JGI database now available through Phytozome. Sequences from *A. thaliana*, *P. patens*, *Selaginella moellendorfii*, *Oryza sativa*, *Brachypodium distachyon*, *Picea abies*, *Amborella trichopoda*, *Solanum lycopersicum* and algae were retrieved either from Phytozome or from the Marchantia community website (http://marchantia.info). NtCOI1 sequence was obtained from NCBI. Bryophyte sequences were obtained through OneKP database (Matasci et al., 2014). All sequences were aligned with either MUSCLE or DiAlign and trees were built with PhyML or BioNJ using 100 bootstraps.

In silico analysis

The structural data of COI1/JAZ/COR complex was obtained from the Protein Data Bank (PDB code 3OGM). Edition and visualization of COR-MO was performed with PyMOL (http://www.pymol.org/).

Cloning

Full-length Mp*COI1*, Mp*JAZ*, Mp*JAZΔJas*, At*JAZ9* and At*JAZ10* coding sequences were amplified with Expand High Fidelity polymerase (Roche) using Gateway-compatible primers (Supplementary Table S3) and cloned into pDONR207 through BP reaction (Invitrogen). Plasmids pDONR207 At*JAZ3* and pDONR207 At*COI1* were already available in the lab (Chini et al., 2007; Fonseca et al., 2009). The chimeras Mp*COI1*$^{1\text{-}187}$-At*COI1*$^{189\text{-}592}$ and At*COI1*$^{1\text{-}188}$-Mp*COI1*$^{188\text{-}581}$, the point mutation Mp*COI1*^{V377A} and the Cas9-resistant version of Mp*JAZ* were amplified with Expand High Fidelity (Roche) with specific primers for the mutations (Supplementary Table S3) and cloned also into pDONR207 through BP reaction (Invitrogen). Numbers correspond to the amino acids from the

original MpCOI1 and AtCOI1 maintained in the chimeric proteins. The 2 kb promoter region of AtJAZ2 was PCR amplified with Expand High Fidelity polymerase (Roche) and the PCR product was cloned into pENTR/D-TOPO (Invitrogen). *Escherichia coli* DH5α was used for transformation of both entry and destination vectors. The sequences cloned into either pDONR207 or pENTR/D-TOPO were transferred to different destination vectors by recombination reaction using Gateway LR II Clonase kit (Invitrogen). Y2H constructs for At*JAZ*, At*COI1* and At*NINJA* were kindly provided by Alain Goossens (VIB Ghent, Belgium). Vectors pMpGWB, pEG103, pGWB3 and pMDC140 carrying the different inserts were transferred into *Agrobacterium tumefaciens* strains GV3101 or GV6620 for plant transformation.

Plant transformation

M. polymorpha was transformed following either the sporeling transformation method for F1 or BC4 sporelings (Ishizaki et al., 2008) or the cut-thalli transformation method (Kubota et al., 2013). *A. thaliana* was transformed by floral dipping (Clough and Bent, 1998). T3 homozygous plants were selected in the appropriate antibiotics and these plants were used for further experiments. Specific details for every line are listed in Supplementary Table S2.

Gene-targeting homologous recombination to obtain Mp*coi1-1* mutant

As previously described (Ishizaki et al., 2013), two fragments of 3.5 kb were amplified from Tak-1 genomic DNA using primers listed in Supplementary Table S2. Both fragments were cloned into the PacI and AscI sites of pJHY-TMp1 vector using In-Fusion cloning kit (Clontech). This vectors was transferred to *A. tumefaciens* GV6620 and used for F1 sporeling transformation (Supplementary Table S2). The Mp*coi1-1* mutant line carrying the T-DNA insertion in the first exon was identified by PCR using primers listed in Supplementary Table S3 and KODFx Neo Polymerase to check that the insertion disrupted the MpCOI1 locus.

CRISPR/Cas9-mediated mutagenesis to obtain Mp*jaz-1* and Mp*jaz-2* mutants

One sgRNA was designed in the first exon of Mp*JAZ* (Supplementary Table S3) and cloned into pMpGE_En03 vector carrying the Cas9. This vector was incorporated into *A. tumefaciens* GV3101, used to transform Tak-1 plants (Supplementary Table S2). Transformants were genotyped and sequenced to identify the indels.

CRISPR/Cas9^{D10A} nickase-mediated mutagenesis to obtain Mp*coi1-2* and Mp*coi1-3* mutants

Two sgRNAs were designed ~700 bp upstream the ATG of Mp*COI1* and two gRNAs ~250 bp downstream the stop codon of Mp*COI1* (Supplementary Table S2). The four sgRNAs were cloned into the pMpGE_En04 vector carrying the Cas9^{D10A} (nickase) and then transformed into *A. tumefaciens*

GV6620. *Marchantia polymorpha* F1 spores and cut-thalli (Tak-1) were transformed (Supplementary Table S2). Transformants were selected on hygromycin, genotyped and sequenced to assess the size of the deletion.

Measurements of root length and thallus surface

For root growth inhibition assays, root length of 35 to 45 seedlings was measured 10 d after germination in Johnson medium in presence or absence of JA or COR plus COR-MO or JA-Ile-MO when indicated. *M. polymorpha* WT plants were grown on either OPDA, dinor-*cis*-OPDA, dinor-*trans*-OPDA or dinor-*iso*-OPDA. Pictures were taken with a NIKON D1-x digital camera, and root length or area was measured using ImageJ software.

Anthocyanin quantification

A. thaliana seedlings were grown for 10 d in Johnson medium, in the presence of the indicated compounds. In the case of JA-Ile-MO, seeds were also germinated in Johnson medium, and 8 d after germination, seedlings were treated for 48 h with different combinations of JA and JA-Ile-MO. Eight to ten seedlings were weighed and pooled for each replicate. Four independent replicates (seedling pools) were measured for each sample. For every replicate, seedlings were soaked overnight in 1.2 ml of hydrochloric acid in aqueous methanol (HCl 0.5 N; methanol 80% (v/v)). Then, the solution was divided into two tubes. The solution of the first tube (sample) was diluted with one volume of methanolic hydrochloric acid (5:1 v/v, 3N). One volume of the peroxide reagent (1 part of 30% hydrogen peroxide in 9 parts of methanolic hydrochloric acid [5:1 v/v, 3N]) was added to the second tube (blank). Absorbance was measured at 530 nm, and anthocyanin content was expressed as A_{530} sample – A_{530} blank per g fresh weight. Values represent mean ± S.D.

Confocal microscopy

Gemmae of transgenic plants expressing either MpJAZ-Citrine or MpJAZΔJas-Citrine were grown on liquid 0.5 Gamborg's B5 for two days and then visualized in a Leica TCS SP5 laser scanning confocal microscope. Citrine signal was detected using an excitation beam splitter TD 488/561/633 (20% power) and emission bandwith between 661 and 747 nm. A 20X objective was used to acquire Z-series section images (1024 x 1024 resolution). Images were acquired and processed using Leica Application Suite (LAS-AF, v.2.7.3) and merged pictures were obtained by Z projection using ImageJ.

Yeast two-hybrid

Yeast two-hybrid assay was performed as indicated in (Cuéllar et al., 2013), using the LexA system and the Gateway-compatible vectors pB42AD (bearing the activation domain, AD) and pGILDA (for fusions to the binding domain, BD). Yeast strain was EGY48 (p8opLacZ).

Protein extraction and pull-down assays

Protein extraction and subsequent pull-down assays between COI1 and JAZ were performed as previously described (Fonseca and Solano, 2013; Fonseca et al., 2009). Briefly, *A. thaliana* extracts over-expressing either MpCOI1-flag or AtCOI1-flag were incubated with recombinant MBP-fused proteins (expressed in *E. coli* BL21) for 1 h at 4ºC in a daisy-wheel rotator. When indicated, hormones were added for the pull-down reaction. Samples were washed with 500 µl pull-down buffer for 3 min twice. Then samples were resuspended in 35 µl pull-down buffer and incubated with Factor Xa (NEB) for 2 h at RT for cleavage of MBP. Then, one fraction was used for immunodetection with anti-flag antibody (Sigma) and anti-mouse-HRP (GE Healthcare). Another fraction was used for Coomassie Blue Staining as loading control. Protein bands were quantified using ImageJ software.

Pull-down assays with AtTIR1-myc, obtained from transgenic *Arabidopsis* plants, and AtIAA7-GST, expressed in BL21 *E. coli* cells, were performed similarly. Dexp:At*TIR1*-myc/tir1-1 *Arabidopsis* seeds and the AtIAA7-GST clone were kindly provided by Professor M. Estelle (University of California-San Diego). The extraction buffer contained 200 mM NaCl, 100 mM Tris-HCl, pH 7.4, 5 mM $MgCl_2$, 0.5% Igepal, 10% glycerol, 1 mM PMSF, 10 µM MG132, 10 µM DTT and Complete EDTA-free protease inhibitor cocktail (Roche). Samples were incubated with IAA 0.5 µM with or without COR-MO 30 µM for 30 min at 4 °C under rotation. Samples were washed three times with 500 µl of extraction buffer for 3 min. AtTIR1-myc protein was immunodetected with anti-myc-HRP antibody (Santa Cruz).

Degradation assays of GFP/Citrine-fusions

A. thaliana transgenic plants overexpressing either MpJAZ-GFP or MpJAZΔJas-GFP were grown on liquid MS for 7 days and treated with different compounds (JA-Ile, COR and MG132) for 3 hours. *M. polymorpha* gemmae were grown on 0.5 Gamborg's B5 for 5 days and then transferred to liquid medium in a 12-well-plate, where OPDA was added for 6 hours. Plates were incubated under white light with shaking and then collected in liquid nitrogen. Both GFP and Citrine fusions were immunodetected with anti-GFP-HRP antibody (MACS).

GUS staining and quantification

35S:At*JAZ1*-GUS vertically grown seedlings were incubated in liquid MS containing COR-MO 5 µM or JA-Ile-MO 100 µM for 1 h and then JA 1 µM or COR 50 nM was added for another hour. Seedlings were then submerged in GUS staining buffer (50 mM phosphate buffer, pH 7; 0.5 mM $K_4Fe(CN)_6$; 0.5 mM $K_3Fe(CN)_6$; 0.2% Triton X-100; 0.7 mg/ml 5-bromo-4-chloro-3-indolyl β-D-glucuronic acid (X-Gluc) and incubated at 37 °C overnight. Alternatively, 20–25 35S:At*JAZ1*-GUS, 35S:At*JAZ9*-GUS or 35S:At*JAZ10*-GUS seedlings were treated as described above, and roots were collected and frozen in liquid nitrogen. Roots were homogenized in extraction buffer containing 50 mM phosphate buffer, pH 7, 10 mM β-mercaptoethanol, 10 mM EDTA , 0.1% sarcosyl (*N*-lauroylsarcosine sodium salt) and

0.1% Triton X-100. Total protein content was quantified by the Bradford method (Bio Rad Protein Assay). Then, 30 µl extract were incubated with 70 µl protein extraction buffer containing 1 mM MUG (methylumbelliferyl-β-D-glucuronide hydrate) for 1 h at 37 °C. 10-µl samples were taken at t = 0 and t = 1 h, and 90 µl 0.2 M Na_2CO_3 was used to stop the reaction. Fluorescence was measured at Ex/Em 365/460 nm with the spectrophotometer SpectraMax M2 (Molecular Devices). Seven independent replicates were measured, and values represent mean ± S.D.

$_{prom}$At*JAZ2*:GUS, seedlings were treated with JA 5 µM, COR 100 nM and COR-MO 5 µM or JA-Ile-MO 100 µM when indicated and incubated for 1 h prior to GUS staining. For DR5:GUS assay, seedlings were treated with or without COR-MO 10 µM for 1 h. Then, IAA 5 µM (3-indole-acetic acid, Duchefa) was added when indicated for 80 min prior GUS staining.

Analysis of gene expression using microarrays, qPCR and bioinformatic analysis

A custom microarray for analysis of gene expression in Marchantia was designed using Agilent's eArray tool (https://earray.chem.agilent.com/earray/). Fasta files for target transcripts (Mpolymorpha_320_v3.1.transcript_primaryTranscript.fa and Mpolymorpha_320_v3.1.transcript.fa) were obtained from Phytozome v12.0 web portal (https://phytozome.jgi.doe.gov), and contained 19,287 and 24,674 transcripts, respectively, corresponding to 19,287 loci. Two probes per primary transcript were designed, following eArray's recommendations for eukaryotic transcriptomes (60 nucleotides long, with base composition and best probe methodologies in sense orientation). This step yielded two probe groups of 19,216 probes each that passed quality filters. In a second step, we selected different splicing isoforms as target transcripts to design specific probes, applying the same parameters as above. After filtering new probes not included in previous batches, this analysis generated a third probes group with 1,990 probes. Finally, an Agilent microarray in 8x60k format was designed (ID 084032) that included two copies of one of the probe groups obtained during first step (that corresponded to the most 3'-end matching probes), and one copy of the second and third groups, making in total 60,103 probes with at least 3 probes per gene.

Total RNA from Marchantia was extracted with either RNeasy Plant Mini Kit (Qiagen) or Favorgen Plant RNA Extraction and DNase on-column digestion (Qiagen) was performed to remove genomic DNA contamination. Quality was assessed in a Bionalyzer 2100 (Agilent), according to the manufacturers' instructions. Two hundred nanograms were amplified and Cyanine 3- (Cy3-) and Cy5-labeled using Two-Color Low Input Quick Amp Labeling Kit (Agilent Technologies) following the manufacturer's recommendations. Labeled cRNAs were purified with RNeasy columns (Qiagen) and RNA yield and Cy3/Cy5 incorporation measured in a Nanodrop spectrophotometer (Nanodrop Technologies). Preparation of probes, hybridization and washes were performed as described for Agilent's 8x60k microarrays (Two-Color Microarray-Based Gene Expression Analysis, Agilent Technologies). Alternatively, total RNA from Arabidopsis was extracted using Trizol reagent

(Invitrogen) and further purified with High Pure RNA isolation Kit (Roche). The Two-Color Microarray-Based GeneExpression Analysis Protocol (Agilent Technologies) was used to amplify and label RNA. 825 ng of Cy3 and Cy5 probes were mixed and hybridized to an *Arabidopsis* Oligo Microarray 4x44K (021169, Agilent Technologies). Images for Cy3 and Cy5 channels were captured in an Agilent DNA Microarray Scanner at a resolution of 2 µm, and spots quantified using Agilent Feature Extraction Software.

Background correction and normalization of expression data were performed using the methods "normexp" and loess in LIMMA, respectively (Smyth, 2004). Differentially expressed genes were evaluated by the non-parametric algorithm 'Rank Products' available as RankProd package at Bioconductor (Hong et al., 2006). We considered as differentially expressed those genes with LogRatio greater than 1 or lower than -1 and the expected false discovery rate (FDR) less than 5%. Given that every gene was represented by at least three oligonucleotide probes, we obtained a table of gene expression values across all the experiments, and simplified it by selecting just one probe per gene showing the lowest FDR value. Clustering of genes was performed using K-Means with euclidean distance (Figure 7; Soukas et al., 2000) or Pearson correlation with absolute distance (Figure 16) in Multi Experiment Viewer (http://mev.tm4.org/), and Venn diagrams obtained with BioVenn (Hulsen et al., 2008). Promoter regions (1 kb upstream the annotated transcription start site) were obtained using BEDTOOLS (Quinlan and Hall, 2010) from the Marchantia genome sequence (Mpolymorpha_320_v3.0.fa) and the annotation file (Mpolymorpha_320_v3.1.gene.gff3), both downloaded from Phytozome. Sequence scan for the perfect G-box (CACGTG) was performed with the 'dna-pattern' tool in RSAT (Medina-Rivera et al., 2015).

Data from microarrays were deposited in the National Center for Biotechnology Information (NCBI) Gene Expression Omnibus (GEO) (http://www.ncbi.nlm.nih.gov/geo; accession nº: GSE56027 for Arabidopsis data and GSE99727 for Marchantia data).

For quantitative PCR experiments, total RNA was extracted with Trizol reagent (Invitrogen) and cleaned with RNA purification Kit (Roche) including DNAse treatment. cDNA was synthesized from 1 µg of total RNA using the High Capacity cDNA reverse transcription kit (Applied Biosystems). Diluted cDNA was used as template of the Power SYBR Green (Applied Biosystems) mix and the expression of Mp*COI1*, Mp*JAZ*, Mp*JAZ* FL, Mp*JAZΔJas*, Mp*AOS2* (Mapoly0185s0014), Mp*AOC* (Mapoly0057s0049) and Mp*CHL* (Mapoly0008s0176) was analysed using Mp*ACT* as housekeeping gene (primer sequence in Supplementary Table S3).

Herbivory assays

Marchantia polymorpha gemmae were grown on half Gamborg's medium (Duchefa) containing 1% agar in continuous light (20°C, 120 µmol m^{-2} s^{-1}) for seven days before being transferred to soil (three per pot). Thalli were then grown for five weeks in a growth chamber (21°C, 10/14 h light/dark cycle,

100 µmol m^{-2} s^{-1}) using a lid to cover the tray and maintain high humidity. For insect assays, experiments were performed with 6-week-old *M. polymorpha* thalli in transparent plastic boxes. For each biological replicate, a total of 60 neonate *Spodoptera littoralis* larvae (eggs obtained from Syngenta) were placed on eighteen thalli. After 9 to 10 days of feeding, larvae were collected and weighed using a precision balance (Mettler-Toledo XP205).

Bacterial assays

Pseudomonas syringae pv. *tomato* (Pst) DC3000 and DC3118 (COR–) bacterial assays in *Arabidopsis* and *N. benthamiana* were performed by infiltration and spray inoculation. Briefly, bacterial cultures were incubated at 28 °C for 3-4 h until OD_{600} = 0.6. Then cells were pelleted and resuspended in sterile 10 mM $MgCl_2$. Four week-old plants, grown directly in soil under short-day conditions and at 21 °C, were infiltrated with COR-MO diluted in 10 mM $MgCl_2$ to a final concentration of 10 µM, and 24 h after infiltration, plants were sprayed with a bacterial suspension containing 10^8 CFU/ml bacteria (OD_{600} = 0.2) with 0.04% Silwet L-77. Leaf discs were harvested 3 d after infection and grounded in 10 mM $MgCl_2$. Serial dilutions of leaf extracts were plated on LB agar with the appropriate antibiotics. Each data point represents the average of eight replicates, each containing two leaf discs from different plants. Error bars indicate S.E.M.

For the infiltration assay, COR-MO was infiltrated together with a bacterial suspension containing 5 × 10^5 CFU/ml bacteria (OD_{600} = 0.001). Symptoms were recorded 5 d after infection.

***Botrytis cinerea* bioassays**

B. cinerea strain was kindly provided by my father, Professor E. Monte (CIALE, University of Salamanca, Salamanca). Plugs containing mycelium were grown in PDA (OXOID) and V8 8% (Campbell's Soup Company). Spores were collected, resuspended in 15% glycerol and stored at -80 °C. Four-week-old *Arabidopsis* plants, grown directly in soil under short-day conditions and at 21 °C, were inoculated with 10 µl of a suspension of 5 ×10^5 spores/ml PDB (Difco). COR-MO 10 µM or the equivalent volume of ethanol was included in the spores suspension. 15 plants (3 leaves per plant) were inoculated per treatment. Disease symptoms were scored 4 d after inoculation. ImageJ software was used to measure the area of the necrotic lesion. Then symptoms were categorized in three stages depending on the size of the necrotic lesions (1: <10 mm^2, 2: 10–20 mm^2 or 3: >20 mm^2). Spores were quantified in a hemocytometer with a light microscope (Leica DMR UV/VIS). Three inoculated leaves of five plants (15 leaves in total) were pooled for every replicate. Three independent replicates were measured for each treatment. This experiment was repeated twice with similar results.

Statistical analysis

Statistical significance based on Student's *t*-test analysis was calculated using Excel (Microsoft). ANOVA was performed with R commander.

Hormone measurements

Mechanical wounding was performed with tweezers all over the 21-day-old thalli of Tak-1. Alternatively, plants were transferred to a 6-well plate containing liquid 0.5 Gamborg's B5 and deuterated compounds (d5-18:3, d6-16:3 or d5-OPDA) for the indicated times. Plants were then grinded in liquid nitrogen prior hormone measurements. (-)-Jasmonic acid (JA), cis-12-oxo-phytodienoic acid (OPDA) and N-(-)-jasmonoyl isoleucine (JA-Ile) were purchased from OlChemim Ltd (Olomouc, Czech Republic), dinor-12-oxo-phytodienoic acid (dn-OPDA) from Cayman Chemical Company (Ann Arbor, MI, USA) and 4,5-ddh-JA, 4,5-ddh-JA-Ile, OPDA-Ile, dn-*iso*-OPDA, tn-*iso*-OPDA, 3,7-ddh-JA and 3,7-ddh-JA-Ile-Me were synthesized (see below). OPC-6 was already available in our lab. The deuterium-labeled internal standards $^{2}H_{2}$-N-(-)-jasmonoyl isoleucine (d2-JA-Ile) and $^{2}H_{5}$-cis-12-oxo-phytodienoic acid (d5-OPDA) were obtained from OlChemim Ltd., $^{2}H_{5}$-jasmonic acid (d5-JA) from CDN Isotopes (Pointe-Claire, Quebec, Canada) and $^{2}H_{5}$-dinor-12-oxo-phytodienoic acid (d5-dnOPDA) from Cayman Chemical Co.

Endogenous JA, JA-Ile, OPDA, dn-OPDA, dn-*iso*-OPDA, OPC-6, 4,5-ddh-JA and 4,5-ddh-JA-Ile and the corresponding $^{2}H_{5}$-phytohormones in plants were analyzed using high performance liquid chromatography-electrospray-high-resolution accurate mass spectrometry (HPLC-ESI-HRMS). The hormones were extracted and purified as follows: 0.25 g frozen plant tissue (ground to a powder in a mortar with liquid N_2) was homogenized with 2.5 ml precooled (-20ºC) methanol:water:HCOOH (90:9:1, v/v/v with 2.5 mM Na-diethyldithiocarbamate) and 25 µl of a stock solution of 1000 ng ml^{-1} deuterium-labeled internal standards d5-JA and d5-dn-OPDA, 200 ng ml^{-1} d2-JA-Ile and 400 ng ml^{-1} d5-OPDA in methanol. Samples were extracted by shaking in a Multi Reax shaker (Heidolph Instruments) (60 min, 2000 rpm, room temperature). After extraction, solids were separated by centrifugation (10 min, 20,000 G, 4ºC) in a Sigma 4-16K Centrifuge (Sigma Laborzentrifugen), and re-extracted with an additional 1.25 ml extraction mixture, followed by shaking (20 min) and centrifugation.

Pooled supernatants (2 ml) were separated and evaporated at 40ºC in a RapidVap Evaporator (Labconco Co., Kansas City, MO). The residue was redissolved in 500 µl methanol/0.133% acetic acid (40:60, v/v) and centrifuged (10 min, 20,000 RCF, 4ºC) before injection into the HPLC-ESI-HRMS system.

Hormones were quantified using a Dionex Ultimate 3000 UHPLC device coupled to a Q Exactive Focus Mass Spectrometer (Thermo Fisher Scientific) equipped with an HESI(II) source, a quadrupole mass filter, a C-trap, a HCD collision cell and an Orbitrap mass analyzer, using a reverse-phase

column (Synergi 4 mm Hydro-RP 80A, 150 x 2 mm; Phenomenex, Torrance, CA). A linear gradient of methanol (A), water (B) and 2% acetic acid in water (C) was used: 38% A for 3 min, 38% to 96% A in 12 min, 96% A for 2 min and 96% to 38% A in 1 min, followed by stabilization for 4 min. The percentage of C remained constant at 4%. Flow rate was 0.30 ml min^{-1}, injection volume 40 µl, and column and sample temperatures were 35 and 15ºC, respectively. Ionization source working parameters were optimized (see Supplementary Table S4).

For phytohormone detection and quantification, we used a full MS experiment with MS/MS confirmation in the negative-ion mode, using multilevel calibration curves with the internal standards. MS^1 extracted from the full MS spectrum was used for quantitative analysis, and MS^2 for confirmation of target identity. For full MS, a m/z scan range from 62 to 550 was selected, resolution set at 70,000 full width at half maximum (FWHM), automatic gain control (AGC) target at $1e^6$ and maximum injection time (IT) at 250 ms. A mass tolerance of 5 ppm was accepted. The MS/MS confirmation parameters were resolution of 17,500 FWHM, isolation window of 3.0 m/z, AGC target of $2e^5$, maximum IT of 60 ms, loop count of 1 and minimum AGC target of $3e^3$. Instrument control and data processing were carried out with TraceFinder 3.3 EFS software. Accurate masses of phytohormones and internal standard and their principal fragments are shown in Supplementary Table S5, with the exception of $^2H_5$-JA-Ile, $^2H_5$-4,5-ddh-JA, $^2H_5$-ddh-JA-Ile, $^2H_5$-OPC-4, $^2H_5$-OPC-6 and [$^2H_5$]-tn-OPDA.

Chemical synthesis

Analytical and chromatographic methods. Gas chromatography-mass spectrometry (GC-MS) was carried out on an Agilent mass selective detector 5977E connected to an Agilent 7820A gas chromatograph, with a capillary column of 5% phenylmethylsiloxane (12 m, 0.33 µm film thickness), with helium as the carrier gas. Temperature was raised from 80ºC to 320ºC at a rate of 10ºC/min. Reversed-phase HPLC (RP-HPLC) was carried out using a 250 x 10 mm Nucleosil 100-7 C_{18} column eluted with methanol-water-acetic acid (55:45:0.02, v/v/v) at a 4 ml/min flow rate. Straight-phase HPLC (SP-HPLC) was performed with a Nucleosil 50-7 (250 x 10 mm) column using the same solvent systems and flow rate.

Chemicals. 11(*S*)-Hydroperoxy-7(*Z*),9(*E*),13(*Z*)-hexadecatrienoic acid (11-HPHT) was obtained from Larodan AB (Stockholm, Sweden) whereas methyl (±)-jasmonate, L-isoleucine and all other chemicals used were purchased from Sigma-Aldrich.

Methyl (±)-4,5-didehydrojasmonate. This compound was prepared by modification of reported protocols (Dang et al., 2012). Methyl (±)-jasmonate (1 mmol, 224 mg) was added to dry *N,N*-dimethylformamide (3 ml) containing diethyl allyl phosphate (2 mmol, 388 mg), Na_2CO_3 (2.4 mmol, 254 mg) and palladium(II) acetate (0.12 mmol, 27 mg). The solution was purged with argon and stirred (24 h, 80ºC). Water was added and the mixture extracted with diethyl ether; after drying over $MgSO_4$ the solvents were evaporated, leaving a 250 mg residue, subsequently purified on a silica gel

column (5 g) eluted with diethyl ether/hexane (1:9, v/v), in 15 fractions of 15 ml. Unreacted methyl jasmonate was recovered in fractions 5-7 and methyl 4,5-ddh-JA was present in fractions 9-14. The latter were combined and evaporated, leaving 76 mg of compound (34% yield), accompanied by 4 mg of an unknown allyl adduct of methyl 3,7-ddh-JA and traces of methyl 7,8-ddh-JA and methyl methyl 3,7-ddh-JA. Preparative SP-HPLC using a 2-propanol-hexane (1:99, v/v) solvent system yielded a pure compound as a colorless oil. The mass spectrum showed prominent ions at *m/z* 222 (30%, M +), 193 (15, M+ - C_2H_5), 167 (13), 154 (70, rearrangement with loss of the C-8 to C-12 side chain), 133 (30), 107 (25), and 95 (100). The UV spectrum (EtOH) showed λ_{max} 217 nm and the ^{1}H NMR spectrum recorded with a Bruker 400 MHz instrument of a solution in $CDCl_3$ showed signals at 0.97 (t, ^{3}H, H-12), 2.05-2.12 (m, ^{3}H), 2.32 (m, 1H), 2.47 (dd, ^{1}H), 2.51-2.57 (m, ^{1}H), 2.61 (dd, ^{1}H), 3.02 (m, ^{1}H), 3.72 (s, ^{3}H, OCH_3), 5.28 (m, *J* = 10.7, ^{1}H, H-9), 5.47 (m, *J* = 10.7, ^{1}H, H-10), 6.19 (dd, ^{1}H, H-5), and 7.64 (dd, ^{1}H, H-4), in full agreement with published values (Dang et al., 2012; Kiyota et al., 1997).

Methyl (+)-4,5-didehydrojasmonate. The (+)-rotatory form of the side chain *trans* isomer of methyl 4,5-didehydrojasmonate is the 3S,7R enantiomer (Asamitsu et al., 2006), the form that is stereochemically related to natural methyl (-)-jasmonate (3R,7R). Introduction of the ring double bond reverses the sign of optical rotation, and the change in configurational assignment at C-3 is a result of the Cahn-Ingold-Prelog rules. Here, methyl (+)-4,5-ddh-JA was prepared by palladium-catalyzed dehydrogenation of the methyl ester of (-)-JA (22 mg), previously prepared (Suza et al., 2010). The material obtained (9 mg) showed λ_{max} (EtOH) 217 nm and the mass spectrum was identical to that for the (±) form.

(±)-4,5-didehydrojasmonic acid. Methyl (±)-4,5-didehydrojasmonate (100 mg, 0.45 mmol) was added to a solution of 24 mg LiOH (1 mmol) in 6 ml water and 24 mL tetrahydrofuran, and stirred (18 h, 23ºC). After extraction with diethyl ether, the product was purified by preparative SP-HPLC using a 2-propanol-hexane-acetic acid (4:96:0.02, v/v) solvent system, which yielded the pure compound as a colorless oil (59 mg) showing λ_{max} 217 nm. The mass spectrum of a methyl-esterified sample was identical to that of methyl 4,5-ddh-JA, and the mass spectrum of the trimethylsilyl (Me_3Si) ester derivative showed prominent ions at *m/z* 280 (22%, M^+), 251 (7, M^+ - C_2H_5), 212 (18, rearrangement with loss of the C-8 to C-12 side chain), 148 (21), 117 (15, O=C=O+$SiMe_3$) and 73 (100, Me_3Si+).

(+)-4,5-didehydrojasmonic acid. Methyl (+)-4,5-didehydrojasmonate (9 mg, 0.04 mmol) was treated with LiOH (2.4 mg, 0.1 mmol) using the above protocol. The pure compound was obtained by SP-HPLC as above. Its properties, including the UV and mass spectra, were identical to those for the racemic compound.

Coupling of (±)-4,5-didehydrojasmonic acid to (S)-isoleucine. (±)-4,5-Didehydrojasmonic acid (90 mg, 433 µmol) was dissolved in 18 ml redistilled ethyl acetate containing 9.8 mg (97 µmol) triethylamine. *O*-(benzotriazol-1-yl)-*N,N,N´,N´*-tetramethyluronium tetrafluoroborate (TBTU, 161 mg,

501 µmol) was added and the solution stirred (30 min, 23ºC). (*S*)-Isoleucine (171 mg, 1303 µmol) suspended in 9 mL of dry *N,N*-dimethylformamide was added and the mixture stirred (18 h, 23ºC); ethyl acetate extraction (pH 2) yielded a product that was purified on a silica gel column (5 g). Elution with ethyl acetate/chloroform/acetic acid (4:6:0.05, v/v/v) yielded a diasteromeric mixture of comparable amounts of (*S*)-isoleucine conjugates of (+)- and (-)-4,5-ddh-JA, which were resolved by preparative RP-HPLC and yielded an early- and a late-eluting conjugate (retention volumes, 86 and 104 mL, respectively). The methyl esters of these diastereomers showed minimal separation in GC-MS analysis in which, in the conditions used, the early- and late-eluting conjugates had retention times of 16.68 and 16.74 min, respectively.

In view of previous data for the (+)- and (-) (*S*)-isoleucine conjugates of (±)-JA (Fonseca et al., 2009) the results suggested that the early- and late-eluting 4,5-ddh-JA conjugates obtained above were the (-)- and (+)-isomers, respectively. To confirm these data, a separate experiment was conducted in which (+)-4,5-ddh-JA (5 mg) was coupled to (*S*)-isoleucine. RP-HPLC analysis of the product showed a single peak that matched that ascribed to the (+) conjugate obtained from (±)-4,5-ddh-JA, and showed unequivocally that the diastereomer that eluted more rapidly on RP-HPLC was the (-)- or (3R, 7S) isomer, whereas the slower-eluting diastereomer was the (+)- or (3S,7R) isomer.

N-[(+)-4,5-didehydrojasmonoyl]-(S)-isoleucine. The late-eluting (*S*)-isoleucine conjugate (16 mg) was a colorless semisolid whose UV spectrum (EtOH) showed

λ_{max} 217 nm (ε 10,800). An aliquot was dissolved in 50 µl methanol, treated with diazomethane, and dried after ~5 s (longer treatment led to formation of byproducts). GC-MS analysis showed a single peak and the mass spectrum showed prominent ions at *m/z* 335 (27%, M^+), 306 (16, M^+ - C_2H_5), 276 (22, M^+ - CH_3COO), 190 (11, M^+ - [NH-CH($OOCCH_3$)-C4H9 + H]), 146 (44, [NH-CH($OOCCH_3$)-C4H9 + 2 H]), 128 (34, [CH($OOCCH_3$)-C4H9 - H]), and 86 (100, 146 - CH_3COOH). The NMR spectrum showed a single peak and the mass spectrum showed prominent ions at *m/z* 335 (27%, M^+), 306 (16, M^+ - C_2H_5), 276 (22, M^+ - CH_3COO), 190 (11, M^+ - [NH-CH($OOCCH_3$)-C_4H_9 + H]), 146 (44, [NH-CH($OOCCH_3$)-C_4H_9 + 2 H]), 128 (34, [CH($OOCCH_3$)-C_4H_9 - H]), and 86 (100, 146 - CH_3COOH).

N-[(-)-4,5-didehydrojasmonoyl]-(S)-isoleucine. The early-eluting (*S*)-isoleucine conjugate (15 mg) showed λ_{max} 217. An aliquot treated with diazomethane (5-10 s) gave a single peak on GC-MS. The mass spectrum was virtually identical to that of the (+)-conjugate.

3,7-Didehydrojasmonic acid (3,7-ddh-JA). Methyl (±)-4,5-didehydrojasmonate (60 mg) was dissolved in 0.3 mL of ethanol and added to 15 mL of 0.5% aqueous KOH. The solution was refluxed for 1 h and then acidified and extracted with diethyl ether. Analysis of an aliquot as the methyl ester by GC-MS revealed the disappearance of the 4,5-ddH-JA and the presence of 3,7-ddh-JA accompanied by about 20% jasmone. Purification by RP-HPLC using a solvent system of acetonitrile-water-acetic acid (30:70:0.02, v/v/v) afforded pure 3,7-ddh-JA as a colorless oil (34 mg). The UV spectrum (EtOH)

showed λ_{max} 234 nm (ε 12,800) and the mass spectrum of the methyl ester derivative showed prominent ions at *m/z* 222 (28%, M^+), 193 (100, $M^+ - C_2H_5$), 191 (8, $M^+ - OCH_3$), 149 (78, CH_2-$COOCH_3$), 133 (52). 105 (46), and 91 (70) in agreement with the spectrum previously published (Chapuis et al., 2005). As expected, 3,7-ddh-JA was easily decarboxylated upon heating. For example, when injected on the gas chromatograph as the free carboxylic acid the only observable peak was that of jasmone.

N-(3,7-didehydrojasmonoyl)-(S)-isoleucine methyl ester. Coupling of 3,7-ddh-JA to (*S*)-isoleucine using various standard methods was met with problems of decarboxylative esterification, however, a slightly modified protocol (Nakamura et al., 2014) using the methyl ester of (*S*)-isoleucine proved successful. Thus, 3,7-ddh-JA (0.41 mmol, 85 mg), 2,4,6-trimethylpyridine (1.2 mmol, 145 mg) and (*S*)-isoleucine methyl ester hydrochloride (0.6 mmol, 109 mg) were dissolved in 8 mL of dry *N,N*-dimethylformamide and stirred for 3 min at 23°C. COMU, *i.e.* (1-cyano-2-ethoxy-2-oxoethylidenaminooxy)dimethylamino-morpholino-carbenium hexafluorophosphate (0.47 mmol, 201 mg), was added and the mixture stirred at 23°C for 2.5 h. The product obtained after extraction with diethyl ether was subjected to silica gel chromatography (elution with ethyl acetate-chloroform 2:8, v/v) affording a faintly colored oil (93 mg). Further purification by RP-HPLC (solvent system, methanol-water 6:4, v/v) afforded the pure title compound as a colorless oil (74 mg). Its UV spectrum (EtOH) showed λ_{max} 235 nm (ε 12,400) and the mass spectrum showed prominent ions at *m/z* 335 (39%, M^+), 306 (100, $M^+ - C_2H_5$), 276 (14, $M^+ - COOCH_3$), 246 (12), 220 (14), 146 (29, [NH-CH($OOCCH_3$)-C_4H_9 + 2 H]), 133 (51), and 86 (65, 146 - CH_3COOH). An aliquot of the material was saponified in order to obtain the free carboxylic acid, however, this appeared to be chemically unstable and no attempts at its purification were made.

2,3-dinor-12-Oxo-9(13),15(Z)-phytodienoic acid (dinor-iso-OPDA). The title compound was prepared by four-carbon chain elongation of JA followed by dehydrogenation of the cyclopentanone and alkali-promoted isomerization of the ring double bond into the more stable tetrasubstituted position. Thus, (±)-JA (7.2 mmol, 1.51 g) and methyl hydrogen adipate (21.9 mmol, 3.5 g) were dissolved in 100 mL of methanol containing sodium methoxide (1.65 mmol). The solution was placed in a water-cooled electrolytic cell equipped with platinum electrodes, and a current of 1 A was passed through for 1.5 h at which time the solution was

slightly alkaline. Extractive isolation afforded a residue (3.1 g) which was subjected to silica gel chromatography. Elution with diethyl ether-hexane 1:9, v/v, afforded about 90% pure 2,3-dinor-10,11-dihydro-OPDA methyl ester (0.76 g, yield, 34%). The sample was dissolved in 9 mL of dry *N,N*-dimethylformamide and dehydrogenated by treatment with diethyl allyl phosphate (5.55 mmol, 1077 mg), Na_2CO_3 (6.66 mmol, 705 mg) and palladium(II) acetate (0.35 mmol, 78 mg) at 80°C for 20 h. Extraction with diethyl ether followed by silica gel chromatography and elution with diethyl ether-hexane 12:88, v/v, afforded 2,3-dinor-OPDA methyl ester (200 mg). Further elution with diethyl ether-

hexane 25:75, v/v, afforded 2,3-dinor-iso-OPDA methyl ester (90 mg), apparently formed from the dinor-OPDA during the heating period (Vick et al., 1979). The materials were combined, dissolved in 12 mL of ethanol and treated with 4 mL of 2 M NaOH at 70°C for 75 min. Extractive isolation followed by RP-HPLC using a solvent system of acetonitrile-water-acetic acid (45:55:0.01, v/v/v) afforded nearly pure dinor-iso-OPDA (137 mg). Part of this material was subjected to a final purification using SP-HPLC (solvent system, 2-propanol-hexane-acetic acid 3:97:0.01, v/v/v) affording >98% pure dinor-iso-OPDA as a colorless viscous oil. UV spectrometry showed λ_{max} 236 nm (ε 13,600) and the mass spectrum of a methyl-esterified sample showed prominent ions at *m/z* 278 (43%, M^+), 249 (14, $M^+ - C_2H_5$), 247 (10, $M^+ - OCH_3$), 177 (100, $M^+ - (CH_2)_3\text{-}COOCH_3$), 149 (76, $M^+ - (CH_2)_5\text{-}COOCH_3$), 135 (37), 105 (29), and 91 (50). The fragmentation pattern was in full agreement with that expected on the basis of previously published mass spectra of the methyl ester of iso-OPDA (Vick et al., 1979) and other tetrasubstituted cyclopentenones (Samuelsson and Ställberg, 1963).

Alternatively dinor-iso-OPDA could be obtained by alkali-promoted double bond isomerization of dinor-cis-OPDA prepared enzymatically as described below.

2,3,4,5-tetranor-12-Oxo-9(13),15(Z)-phytodienoic acid (tetranor-iso-OPDA). tetranor-iso-OPDA was prepared as described for the corresponding dinor compound but using methyl hydrogen succinate in the anodic coupling step. Palladium-catalyzed dehydrogenation afforded 2,3,4,5-tetranor-10,11-dihydro-OPDA methyl ester (250 mg), which was subjected to alkali-promoted double bond isomerization. The product was purified by RP-HPLC to provide nearly pure tetranor-iso-OPDA (108 mg). Final purification by SP-HPLC (solvent system, 2-propanol-hexane-acetic acid 4:96:0.01, v/v/v) afforded >98% pure tetranor-iso-OPDA (75 mg) as an almost colorless viscous oil. The UV spectrum (EtOH) showed λ_{max} 235 nm and the mass spectrum of a methyl-esterified aliquot showed prominent ions at *m/z* 250 (64%, M^+), 221 (91, $M^+ - C_2H_5$), 219 (22, $M^+ - OCH_3$), 177 (87, $M^+ - CH_2\text{-}COOCH_3$), 149 (100, $M^+ - (CH_2)_3\text{-}COOCH_3$), 135 (73), 105 (60), and 91 (96).

2,3-dinor-12-Oxo-10,15(Z)-phytodienoic acid side chain cis isomer (dinor-cis-OPDA). The title compound was prepared from 11-HPHT by incubation with allene oxide synthase (AOS) from flaxseed (Zimmerman and Vick, 1970) in the presence of allene oxide cyclase (AOC) from potato (Hamberg and Fahlstadius, 1990). Potato tubers (350 g) were minced, added to 300 mL of 0.1 M potassium phosphate buffer pH 7.4, and homogenized at 0°C using a Polytron. The supernatant collected after centrifugation at 47,000 g for 30 min (source of AOC) was supplemented with of 6 g of hexane-defatted powder of flaxseed (source of AOS). To the preparation (250 mL) was added 11-HPHT (28 mg; final concentration, 400 µM) and the mixture was stirred at 22°C for 20 min. Extractive isolation afforded a product (132 mg) that was subjected to RP-HPLC using a solvent system of acetonitrile-water-acetic acid 45:55:0.01, v/v/v. Effluent containing dinor-cis-OPDA was collected and the material subjected to a final purification using SP-HPLC (solvent system, 2-propanol-hexane-acetic acid 1:99:0.01, v/v/v). Pure dinor-cis-OPDA was obtained as a colorless oil (7 mg). Its UV

spectrum (EtOH) showed λ_{max} 219 nm, and the mass spectrum of a methyl-esterified sample showed prominent ions at m/z 278 (31%, M^+), 249 (15, M^+ - C_2H_5), 247 (10, M^+ - OCH_3), 210 (26, rearrangement and loss of C_5H_8), 177 (24, M^+ - $(CH_2)_3$-$COOCH_3$), 163 (37, M^+ - $(CH_2)_4$-$COOCH_3$), 109 (50), 107 (53), and 96 (100). This spectrum was in agreement with that previously published for the methyl ester of dinor-OPDA (Weber et al., 1997). A further aliquot was methyl- esterified and subjected to chiral-phase HPLC (Hamberg, 1998), demonstrating an optical purity of 93%, *i.e.* 93% of the 9(*S*),13(*S*) (natural) enantiomer and 7% of the 9(*R*),13(*R*) (unnatural) enantiomer.

2,3-dinor-12-Oxo-10,15(Z)-phytodienoic acid side chain trans isomer (dinor-trans-OPDA). A sample of dinor-cis-OPDA (2 mg) was dissolved in 3 mL of methanol and 0.3 mL of 2 M aqueous NaOH was added. The solution was kept at 23°C for 30 min and then extracted with diethyl ether. The product was purified by SP-HPLC using a solvent system of 2-propanol-hexane-acetic acid 1:99:0.01, v/v/v, to provide the pure side chain-isomerized derivative, *i.e.* dinor-trans-OPDA (1.5 mg). The UV spectrum showed λ_{max} 220 nm and the mass spectrum of a methyl-esterified aliquot was virtually identical to that of the corresponding *cis* isomer. On the other hand, the retention times of the methyl esters of dinor-cis- and dinor-trans-OPDA differed: under the conditions used for GC-MS the former isomer eluted at 13.6 min and the latter at 13.1 min.

[7,8,10,11,13,14-$^2H_6$]7(Z),10(Z),13(Z)-Hexadecatrienoic acid (d6-16:3). The title compound was prepared by catalytic deuteration of 7,10,13-hexadecatriynoic acid followed by purification by RP-HPLC. The specimen had a chemcical purity of >98% and consisted of >99.5% deuterated molecules.

Coronatine O-methyloxime (COR-MO, **3***)*. Coronatine (about 10 mg, >95%, Sigma-Aldrich) was dissolved in dry pyridine (3 ml) and treated at 23°C for 18 h with *O*-methylhydroxylamine hydrochloride (81 mg, 98%, Sigma-Aldrich). Water was added, and the product was extracted with redistilled ethyl acetate. The organic phase was washed with water and taken to dryness. If needed, further purification can be achieved by preparative reverse-phase HPLC using methanol/water/acetic acid (60:40:0.01, v/v/v) as the mobile phase. An aliquot was methyl-esterified (described below) and analyzed by GC/MS using a Hewlett-Packard model 5970B mass selective detector connected to a Hewlett-Packard model 5890 gas chromatograph equipped with a 12-m phenylmethylsilicone capillary column. The chromatogram demonstrated a complete conversion of COR into COR-MO, which appeared as two peaks (ratio 7:1) because of *syn-anti* isomerism of the methyloxime functional group. By selected monitoring of mass-spectral ions typical for COR methyl ester (*m/z* 333, *m/z* 301 and *m/z* 191), the absence of unreacted COR could be further verified. The mass spectrum of COR-MO methyl ester showed the following prominent ions: *m/z* 362 (35%; M+), 331 (8; M+ – OCH_3), 299 (4; M+ – (OCH_3 + CH_3OH)), 271 (3), 220 (100; cleavage of the amide bond and charge retention on the coronafacic moiety), 192 (7; 220 – 28, loss of CO from the coronafacic fragment), 188 (7), 145 (14), 142 (19; cleavage of the amide bond and charge retention on the coronamic moiety) and 91

(13). COR-MO, prepared as described above, was stored under a high vacuum for 2 h and obtained as a colorless viscous oil, weight 10 mg. Confirmation of the structure was provided by ^{1}H and ^{13}C NMR spectroscopy (Supplementary Table S6) using the earlier published spectra of coronatine (Okada et al., 2009) as references. The nitrogen-bonded OCH_3 group generated ^{1}H signals at δ3.79–3.80 and ^{13}C signals at δ61.5–61.7 p.p.m.

(±)-Jasmonic acid O-*methyloxime (JA-MO,* **1***)*. (±)-Jasmonic acid methyl ester (100 mg, ≥ 95%, Sigma-Aldrich) was dissolved in dry pyridine and treated with *O*-methylhydroxylamine hydrochloride as described above. The extracted product was saponified by treatment with 0.4 M NaOH in 80% aqueous ethanol at 23 °C for 18 h. Purification by normal-phase HPLC using a mobile phase of 2-propanol/hexane/acetic acid (1:99:0.01, v/v/v) afforded pure JA-MO (84 mg) as a colorless oil. An aliquot was methyl-esterified and analyzed by GC/MS, which showed two peaks (ratio 6:1) owing to *syn-anti* isomerism of the methyloxime group. The mass spectrum recorded on the major isomer showed the following prominent ions: *m/z* 253 (8%; M+), 224 (15; M+ - C_2H_5), 222 (39; M+ – OCH_3), 180 (100; M+ – CH_2-$COOCH_3$), 148 (40; 180 – 32, loss of CH_3OH) and 112 (68). ^{1}H and ^{13}C NMR spectroscopy confirmed the structure (Supplementary Table S7). In addition to signals expected on the basis of NMR data recorded for (–)-JA (Okada et al., 2009), the methoxime OCH_3 gave signals at δ3.78–3.80 and δ61.7 p.p.m.

N-((–)-Jasmonoyl)-L-*isoleucine* O-*methyloxime (JA-Ile-MO,* **2***)*. *N*-((–)-Jasmonoyl)-L-isoleucine (95 mg, prepared as described in (Fonseca et al., 2009) was treated with 200 ml of a 30-mM solution of *O*-methylhydroxylamine hydrochloride in methanol/water (95:5, v/v) at 23°C for 18 h. The product obtained by extraction with ethyl acetate was subjected to reverse-phase HPLC using methanol/water/acetic acid (60:40:0.01, v/v/v) as the mobile phase. This afforded pure JA-Ile-MO (75 mg) as a white solid. Analysis of the methyl- esterified compound by GC/MS showed two peaks (ratio 6:1) owing to the methyloxime *syn-anti* isomers. The mass spectrum recorded on the major peak showed the following ions: *m/z* 366 (0.1%; M+), 335 (100; M+ – OCH_3), 305 (53; tentatively M+ – (C_2H_5 + CH_3OH)), 267 (12; 335 – 68, loss of pentenyl side chain – ^{1}H), 190 (16), 180 (23; cleavage at C2/C3 with charge retention at the five-membered ring fragment), 148 (64; 180 – 32, loss of CH_3OH) and 86 (23). A trace (0.4–0.8%) of (+)-7-*iso*-JA-Ile-MO was present in the preparation. The structure was confirmed by ^{1}H and ^{13}C NMR spectroscopy (Supplementary Table S8) using the previously recorded spectra of (–)-JA-Ile (Fonseca et al., 2009) as references. In addition to signals at 3.79 p.p.m. and 61.7 p.p.m. from to the N-bonded methoxy group, $^{1}H,^{15}N$ HMBC showed ^{15}N chemical shifts at δ360.4 and δ355.5, respectively owing to the nitrogen of the major and minor methoxime *syn/anti* isomers.

Preparation of methyl esters. Methyl esters of the abovementioned compounds and other jasmonates were prepared in connection with analyses by GC/MS and to generate compounds for biological testing. Samples in amounts ranging from a few µg to several mg were dissolved in methanol (0.–1

ml) and treated for 1 min with an excess of ethereal diazomethane. The solvents and the diazomethane reagent (a gas) were removed *in vacuo*.

NMR spectroscopy

Proton and ^{13}C NMR spectra were recorded at 600 MHz (reference, tetramethylsilane at 0 p.p.m.) and 151 MHz (reference, CD3OD at 49.0 p.p.m.), respectively, in CD3OD using an Agilent (former Varian) VNMRS 600 spectrometer. In case of (–)-JA-Ile-MO, the ^{15}N chemical shifts were derived from an $^{1}H,^{15}N$ HMBC NMR spectrum (^{15}N: 61 MHz; reference, [^{15}N] NH_3 at 0 p.p.m.).

Experimental contributions

I, Isabel Monte, performed all the experiments except the chemical syntheses (Mats Hamberg, Karolinska Institutet, Stockholm and Kosaku Takahashi, Agricultural University of Hokkaido, Hokkaido), NMR (Andrea Porzel, Leibniz Institute of Plant Biochemistry, Halle), hormones measurements (Ángel M. Zamarreño and José M. García-Mina, University of Navarra, Pamplona), insect bioassays (Caroline Gouhier-Darimont and Philippe Reymond, UNIL, Lausanne), microarray design, hybridization and transcriptomic data analyses (Gloria García-Casado and José Manuel Franco, Genomics Unit, CNB-CSIC, Madrid), generation of $_{prom}$At*JAZ2*:GUS line (Marta Boter, Roberto Solano's lab, CNB-CSIC, Madrid), generation of 35S:At*JAZ9*-GUS and 35S:At*JAZ10*-GUS plants and fluorometric assays (Andrea Chini, Roberto Solano's lab, CNB-CSIC, Madrid) and modelling of COR-MO binding to AtCOI1 (Florencio Pazos, CNB-CSIC, Madrid).

Sakiko Ishida (Kohchi lab, Graduate School of Biostudies, Kyoto) helped me with gene-targeting for Mp*coi1-1* and taught me all the basic techniques to work with Marchantia under the supervision of Ryuichi Nishihama and Takayuki Kohchi. Keisuke Inoue (Kohchi lab, Graduate School of Biostudies, Kyoto) helped me with the cloning of the Cas9 nickase constructs. Sylvia Gutiérrez Erlandsson (Confocal Microscopy Service, CNB-CSIC, Madrid) helped with confocal imaging and Selena Gimenez-Ibanez (Roberto Solano's lab, CNB-CSIC, Madrid) with *N. benthamiana* infection assays.

Results

Chapter 1:
Functional conservation of MpCOI1 and identification of the bioactive jasmonate in bryophytes

Bryophytes neither synthesize nor perceive JA-Ile

The reported accumulation of OPDA in *M. polymorpha* is very late (8 hours post-stimulation), which questions its function as a signalling molecule (Yamamoto et al., 2015). To test wether *M. polymorpha* can produce JA-Ile and to characterize OPDA accumulation kinetics, we measured OPDA, JA and JA-Ile levels in WT male (Tak-1) plants after stimulation by wounding (Supplementary Figure S1A). As in vascular plants, wounding induced rapid (5 min), transient OPDA accumulation, which decreased 1 h post-stimulation. JA-Ile was not detected in these plants, and only residual amounts of JA, near the detection limit, were measured (Supplementary Figure S1B). This is consistent with the fact that the two GH3-like enzymes in *M. polymorpha* are less related phylogenetically to JAR1 than those in *P. patens,* which are involved in auxin conjugation (Supplementary Figure S1C; Ludwig-Müller et al., 2009). It is also consistent with the phylogenetic proximity of the two *M. polymorpha* OPR-like enzymes to OPR1 and OPR2, rather than to OPR3 (Supplementary Figure S1C). These results indicate that, if the pathway is functionally conserved, the hormone that activates it in bryophytes must differ from JA-Ile.

In vascular plants, JA-Ile and its precursors JA and OPDA inhibit growth. Exogenous treatment of *M. polymorpha* Tak-1 plants with OPDA also inhibited growth (Supplementary Figure S1D), whereas these plants were completely insensitive to JA and JA-Ile, which indicated that JA-Ile is neither produced nor perceived in *M. polymorpha*. Similar growth-inhibitory effects of OPDA, but not of JA or JA-Ile, were observed in the moss *P. patens* and the hornwort *Anthoceros agrestis* (Supplementary Figure S1D). These results show that in bryophytes the hormone that activates this pathway is potentially related to OPDA but not to JA or JA-Ile, as bryophytes do not synthesize nor perceive JA or JA-Ile.

Identification of the Marchantia orthologue of the JA-Ile receptor AtCOI1

The finding of COI1- and JAZ-related sequences in the *M. polymorpha* genome suggests that bryophytes conserve the hormone perception machinery (Bowman et al., 2017). To confirm functional conservation of the signalling pathway in a plant that lacks the hormone of vascular plants, we generated knock-out mutant alleles for the Marchantia genome sequence closest to At*COI1*, Mapoly0025s0025 (Mp*COI1*), using homologous recombination-mediated gene targeting (Mp*coi1-1*; Ishizaki et al., 2013) and CRISPR/Cas9^{D10A} technology (Mp*coi1-2* and Mp*coi1-3*; Ran et al., 2013; Supplementary Figure S2). All three Mp*coi1* alleles were insensitive to OPDA-triggered growth inhibition (Figure 5A) and this phenotype could be reversed by complementation with the WT *MpCOI1* gene (Figure 5B). These data indicate that MpCOI1 is the orthologue of the AtCOI1 receptor in *M. polymorpha* and that, similar to angiosperms, the MpCOI1-dependent pathway controls growth in response to OPDA.

Besides growth, the COI1 pathway regulates jasmonate biosynthesis, plant defence and fertility in Arabidopsis (Wasternack and Hause, 2013). Liquid chromatography-mass spectrometry (LC-MS) quantification of OPDA levels showed that the Mp*coi1-1* mutant has approximately one third of the OPDA produced by Tak-1 in basal conditions (Figure 5C), which suggests that the positive feedback that regulates this biosynthetic pathway in Arabidopsis is also found in Marchantia (Wasternack and Hause, 2013).

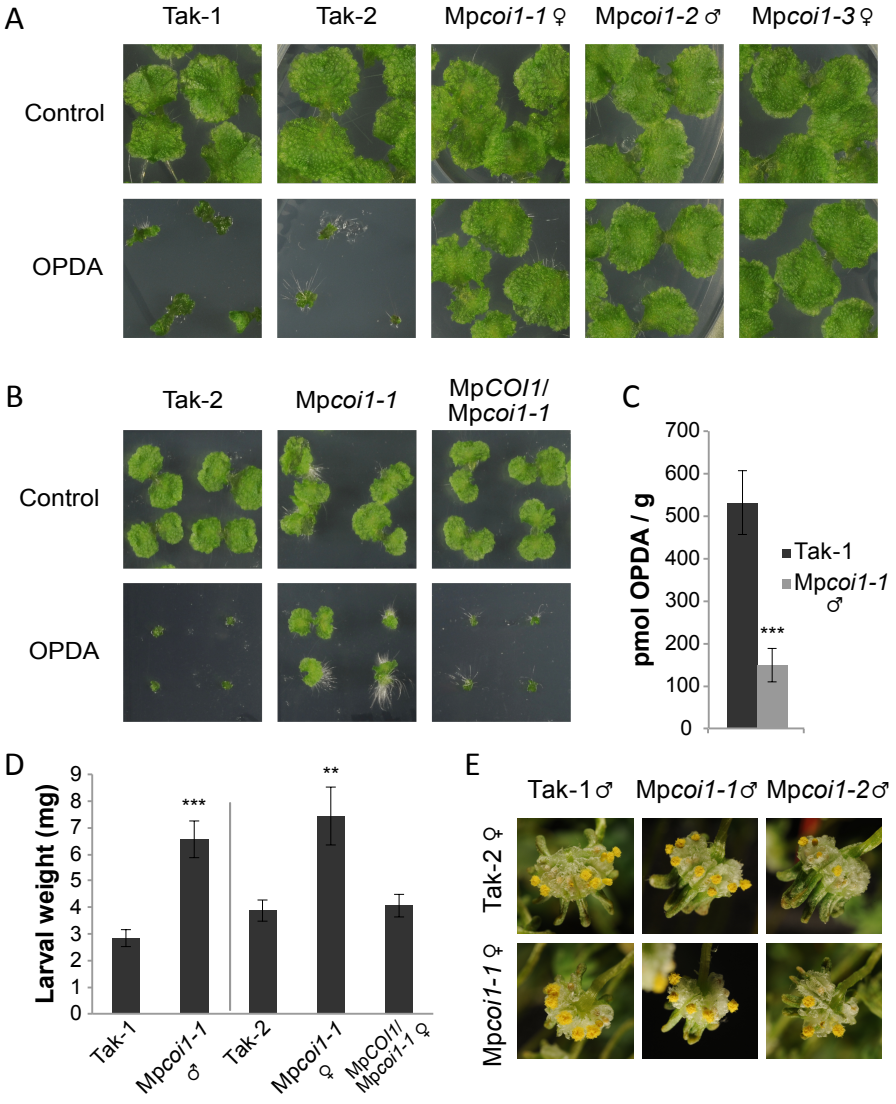

Figure 5: MpCOI1 regulates responses to OPDA. A) Growth inhibitory effect of OPDA (50 µM) on 14-day-old *Marchantia polymorpha* gemmalings of WT plants (Tak-1 and Tak-2) or *Mpcoi1-1*, Mp*coi1-2* and Mp*coi1-3* mutants B) Mp*COI1* complements the Mp*coi1-1* mutant. Effect of OPDA (50 µM) on WT Tak-2, Mp*coi1-1* and 35S:Mp*COI1*/Mp*coi1-1* gemmalings grown for 11 days. C) OPDA accumulation in Tak-1 and Mp*coi1-1* male plants (Mp*coi1-1* female backcrossed once with Tak-1). D) *Spodoptera littoralis* larval weight after 9 days feeding on *M. polymorpha* thalli of Tak-1, Tak-2, Mp*coi1-1* and 35S:Mp*COI1*/Mp*coi1-1*. ** p<0.01; *** p<0.001. E) Mature sporangia from crossing parental lines Tak-1 ♂ x Tak-2 ♀, Tak-1 ♂ x Mp*coi1-1* ♀, Mp*coi1-1* ♂ x Tak-2 ♀ and Mp*coi1-1* ♂ x Mp*coi1-1* ♀. 15 archegoniophores were used per cross. C-D, data shown as mean ± S.D.

To determine whether this pathway regulates defence responses in *M. polymorpha* as it does in eudicots, we challenged Mp*coi1-1* and wild-type thalli with larvae from the generalist herbivore *Spodoptera littoralis*. Larvae fed on the Mp*coi1-1* mutant weighed twice as much as those that fed on wild-type Tak-1 or Tak-2 (Figure 5D), indicating that MpCOI1 is necessary for insect defence in *M. polymorpha*, and that the role of this signalling pathway in plant defence is thus also conserved in land plants.

Fertility is compromised in Arabidopsis mutants with altered JA-Ile biosynthesis, such as *aos1* (Park et al., 2002) or perception, such as *coi1* (Feys et al., 1994; Xie et al., 1998). OPDA biosynthetic *P. patens* mutants also show reduced fertility (Stumpe et al., 2010). In contrast, Mp*coi1* female and male mutants were crossed successfully and backcrossed to wild-type. The sporangia showed no developmental defects and the mutation segregated as expected (1:1; Figure 5E; Supplementary Figure S2C). Fertility is therefore not an ancient character regulated by the COI1 pathway, which was likely co-opted more recently in evolution.

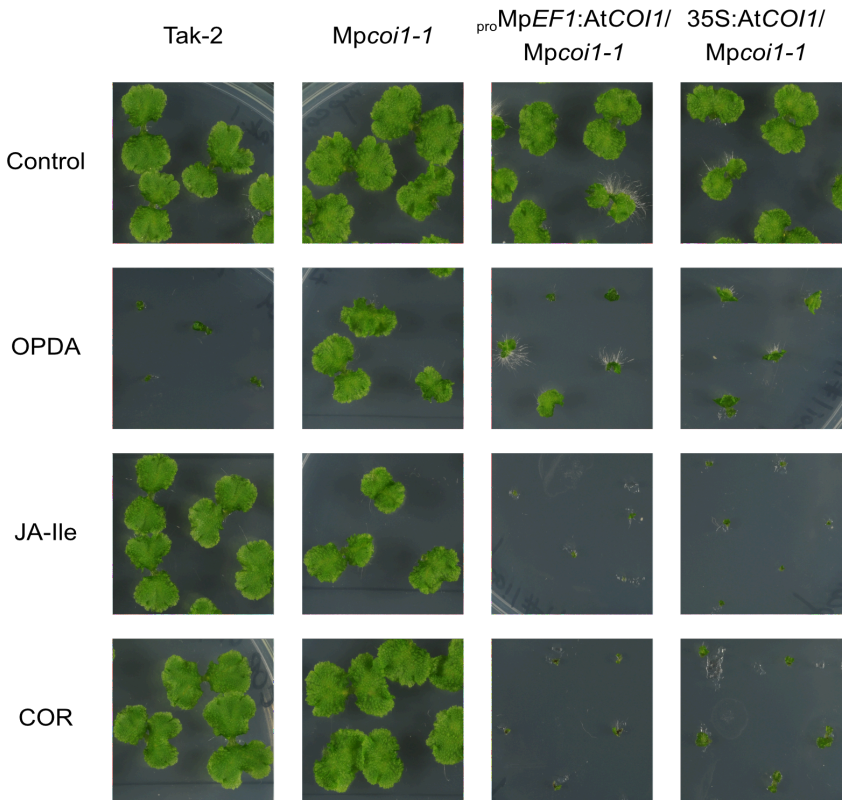

Figure 6: At*COI1* complements the Mp*coi1-1* mutant and confers JA-Ile/COR responsiveness to *M. polymorpha*. Growth inhibitory effect of OPDA (50 µM), JA-Ile (50 µM) and COR (0.5 µM) on 15-day-old *M. polymorpha* gemmalings of WT Tak-2, Mp*coi1-1* mutant and the $_{pro}$Mp*EF1*:At*COI1*/ Mp*coi1-1* and 35S:At*COI1*/Mp*coi1-1* complemented lines.

To confirm the evolutionary conservation of COI1 function, we attempted to complement the Mp*coi1-1* mutant by expressing the Arabidopsis At*COI1* receptor in transgenic Marchantia plants. Expression of At*COI1* using two distinct constitutive promoters (Mp*EF1* and CaMV 35S) restored

partial OPDA responsiveness (Figure 6). This suggests that AtCOI1 remains able to perceive the bryophyte hormone, although with lower affinity than MpCOI1. In contrast to WT plants, transgenic Mp*coi1* mutants expressing AtCOI1 (*pro*Mp*EF1*:At*COI1*/Mp*coi1-1* and 35S:At*COI1*/Mp*coi1-1*) remarkably perceived JA-Ile and its mimic coronatine (COR, a bacterially-produced ligand of COI1; Katsir et al., 2008; Figure 6). These data confirm functional conservation between MpCOI1 and AtCOI1, albeit with differences in ligand specificity. In addition, the results indicate conservation of the entire signalling pathway, since AtCOI1 recapitulates all events that lead to growth inhibition in response to molecules that do not act on WT Marchantia.

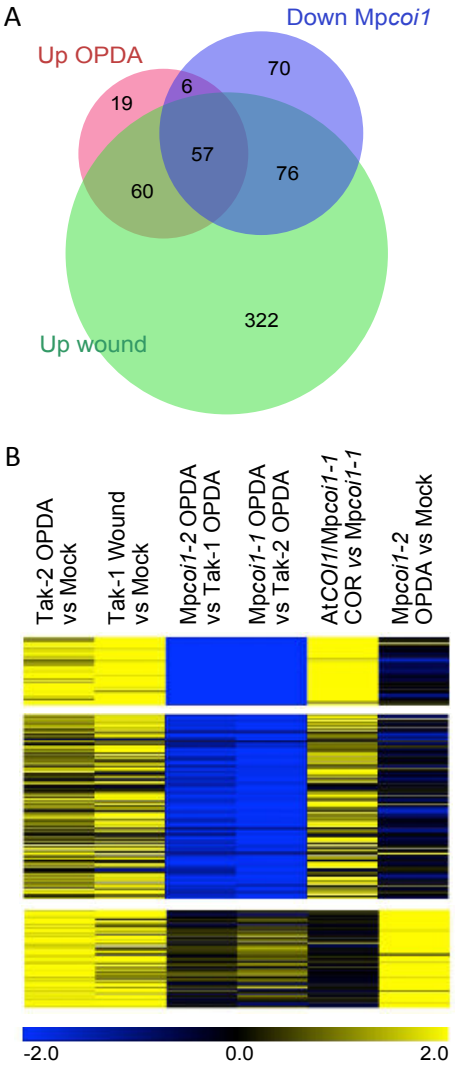

Figure 7: At*COI1* complements Mp*coi1* insensitivity to OPDA-induced gene expression. A) Overlapping sets of genes upregulated (Log-ratio >1; FDR <0.05) by OPDA (Up OPDA) or post-wounding (Up wound) and genes downregulated (Log-ratio <-1; FDR <0.05) in two independent Mp*coi1-1* and Mp*coi1-2* alleles after OPDA treatment (Down Mp*coi1*). B) Clustering analysis of genes upregulated (Tak-2 OPDA vs Mock) and/or genes downregulated by OPDA in the two Mp*coi1* alleles compared to WT (Mp*coi1-1* OPDA vs Tak-2 OPDA and Mp*coi1-2* OPDA vs Tak-1 OPDA). Clustering includes Log-ratio values of selected genes in three additional experiments: Mp*coi1-1* mutant complemented with At*COI1* in response to COR (At*COI1*/Mp*coi1-1* COR vs Mp*coi1-1*), Mp*coi1-2* response to OPDA (Mp*coi1-2* OPDA vs Mock), and Tak-2 response to wounding (Wound vs Mock). Analysis was set to three clusters, in which clusters 1 (top) and 2 (centre) correspond to genes upregulated in response to OPDA and/or wound and downregulated in both Mp*coi1* alleles, and cluster 3 (bottom) o genes OPDA-induced, MpCOI1-independent genes. Total number of genes = 282.

For molecular confirmation of this phenotypic complementation, we designed a microarray of the Marchantia genome (see Methods). Transcriptomic analyses showed that most genes upregulated by OPDA treatment were also upregulated by wounding (Figure 7A,B), which indicated that as in the JA-Ile pathway in vascular plants (Wasternack and Hause, 2013), OPDA regulates wounding responses in *M. polymorpha*. In Mp*coi1*, OPDA did not induce expression of most OPDA-upregulated genes in the WT (Figure 7B). COR treatment mimicked OPDA responsiveness in complemented Mp*coi1*

mutants that expressed At*COI1* ($_{pro}$Mp*EF1*:At*COI1*/Mp*coi1-1*), which further confirmed functional conservation of COI1 (Figure 7B). Gene ontology (GO) analysis of the MpCOI1-dependent clusters using Arabidopsis annotation indicated enrichment of jasmonate-, wounding-, defence and lipid metabolism-related processes, further substantiating functional conservation (Supplementary Table S1).

The G-box (CACGTG) is the target of AtCOI1-regulated AtMYC transcription factors (Chini et al., 2007; Godoy et al., 2011). We detected significant enrichment of this box in the proximal promoter region of OPDA- or wounding-upregulated genes compared to its presence in the Marchantia genome. This suggests that MYC function is also conserved downstream of hormone perception (Supplementary Figure S3).

A single amino acid in MpCOI1 determines ligand specificity

To identify the COI1 protein residues that determine ligand specificity, we examined the *in vivo* function of chimaeric proteins that combine the N-terminal half of AtCOI1 and C-terminal half of MpCOI1 (At*COI1*-Mp*COI1*) or *vice versa* (Mp*COI1*-At*COI1*). Both chimaera types complemented the Mp*coi1* response to OPDA (Figure 8A). Nonetheless, only plants bearing the C-terminal part of AtCOI1 responded to JA-Ile like plants that express full-length AtCOI1. The hormone specificity determinants are therefore located in the C-terminus.

Alignments of available sequences of the C-terminal half of COI1 from several species (Matasci et al., 2014; Zhang et al., 2015b) showed a striking difference between bryophyte and tracheophyte sequences at AtCOI1 position 384. All vascular plants bear an alanine in this position, whereas bryophytes predominantly show valine or isoleucine, but never alanine (Figure 8B and Supplementary Figure S4). Available structural data showed that AtCOI1 Ala384 contacts the isoleucine side chain of JA-Ile (Sheard et al., 2010), which suggests that this difference between bryophytes and tracheophytes is important for ligand specification. We therefore mutated the Val in MpCOI1 to Ala and analysed the specificity of the resulting protein (MpCOI1^{V377A}). MpCOI1^{V377A} expression on the Mp*coi1-1* background restored OPDA sensitivity, indicating that the mutant protein MpCOI1^{V377A} is active and complements the Mp*coi1-1* mutation (Figure 8C). Strikingly, the transgenic plants were also able to perceive both JA-Ile and COR, similar to plants expressing At*COI1* in Mp*coi1-1* (Figure 8C and 7). A single amino acid change thus switches MpCOI1 ligand specificity to that of AtCOI1, which underlies the evolutionary divergence of the jasmonate ligand in early and late diverged plants.

The Val-to-Ala change enlarges the MpCOI1 pocket, allowing JA-Ile or COR binding. Since the MpCOI1 hormone-binding pocket is smaller than that of vascular plants, it is likely that the bryophyte hormone would also be smaller than JA-Ile.

OPDA is a precursor of the MpCOI1 ligand

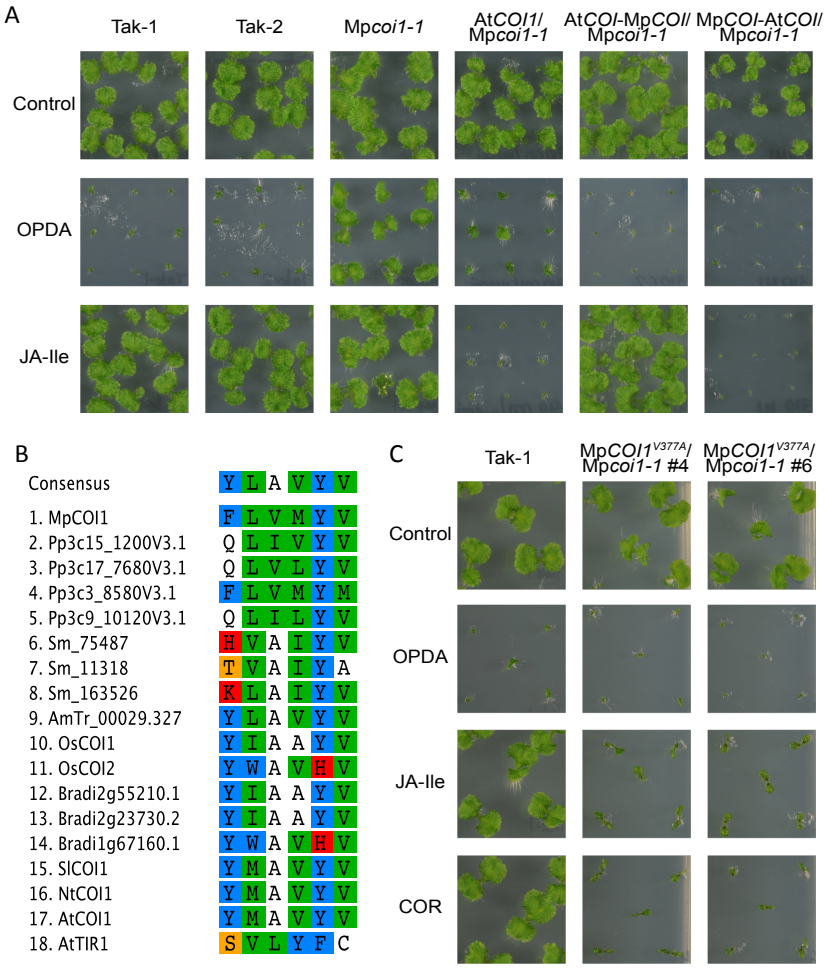

Figure 8: A single amino acid of COI1 determines ligand specificity. A) Growth inhibitory effect of OPDA and JA-Ile (both 50 µM) on 12-day-old *M. polymorpha* gemmalings of WT Tak-1 and Tak-2, the Mp*coi1-1* mutant, the complemented line $_{pro}$Mp*EF1*:At*COI1*/Mp*coi1-1* and the chimaeras $_{pro}$Mp*EF1*:At*COI1*$^{1\text{-}188}$-Mp*COI1*$^{188\text{-}581}$-flag/Mp*coi1-1* and $_{pro}$Mp*EF1*:Mp*COI1*$^{1\text{-}187}$-At*COI1*$^{189\text{-}592}$-flag/Mp*coi1-1*. B) Multiple sequence alignment (MSA) of amino acid sequences surrounding AtCOI1 Ala^{384} from various land plants (Mp, *Marchantia polymorpha*; Pp, *Physcomitrella patens*; Sm, *Selaginella moellendorfii*; AmTr; *Amborella trichopoda*; Os, *Oryza sativa*; Bradi; *Brachypodium distachyon*; Sl, *Solanum lycopersicum*; Nt, *Nicotiana tabacum*; At, *Arabidopsis thaliana*) showing the conservation of Ala^{384} in COI1 from all vascular plants, but not in bryophytes. The AtTIR1 sequence was included as an outgroup. MSA was performed with MUSCLE. C) The V377A mutation in MpCOI1 confers responsiveness to JA-Ile (both 50 µM) and COR (0.5 µM). Effect of OPDA, JA-Ile and COR on 13-day-old *M. polymorpha* gemmalings of WT Tak-1 and two lines of $_{pro}$Mp*EF1*:Mp*COI1*^{V377A}–flag/Mp*coi1-1*.

In Arabidopsis, AtCOI1 interacts with AtJAZ only in the presence of the hormone JA-Ile or its mimic, COR (Fonseca et al., 2009; Sheard et al., 2010). Since OPDA, but not JA or JA-Ile, accumulates after wounding in WT Marchantia plants, we tested whether OPDA is the MpCOI1/MpJAZ co-receptor ligand. We performed pull-down assays with OPDA, JA-Ile and COR, using AtCOI1/AtJAZ9 as a positive control. In contrast to JA-Ile or COR, OPDA did not induce the interaction between AtCOI1 and AtJAZ9, as described (Fonseca et al., 2009; Supplementary Figure S4A). OPDA, JA-Ile or COR were unable to induce the MpCOI1/MpJAZ interaction (Supplementary Figure S5B), which suggests

that the active hormone that binds the MpCOI1/MpJAZ co-receptor is not OPDA, but possibly an OPDA derivative.

Dinor-OPDA and dinor-*iso*-OPDA are OPDA products that accumulate after wounding

To identify the OPDA-derived ligand of MpCOI1 we used LC-MS to measure OPDA-related compounds previously identified in plants, for which we had available standards or were able to synthesize (compounds in bold in Supplementary Figure S6). In addition to OPDA, only dinor-OPDA (Weber et al., 1997) and to a higher level its isomer dinor-*iso*-OPDA accumulated in wounded plants, with kinetics similar to that of OPDA (Figure 9A). Consistent with this accumulation, in addition to OPDA only dinor-OPDA and dinor-*iso*-OPDA inhibited growth in a MpCOI1-dependent manner, while OPDA-Ile, 4,5-ddh-JA, 4,5-ddh-JA-Ile, MeJA, tetranor-*iso*-OPDA, 3,7-ddh-JA and 3,7-ddh-JA-Ile-Me produced no effect *in planta* (Supplementary Figure S7).

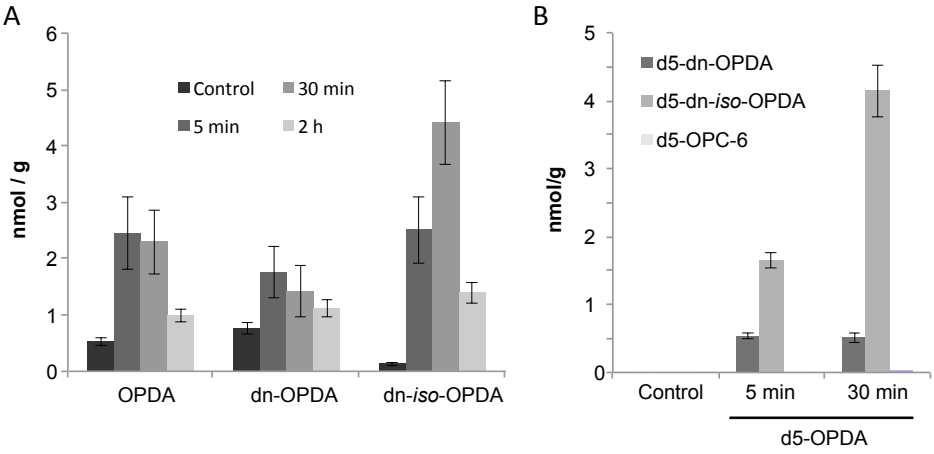

Figure 9: OPDA is a precursor of dinor-OPDA and both accumulate upon wounding. A) Time-course accumulation of OPDA, dinor-OPDA and dinor-*iso*-OPDA in WT Tak-1 in basal conditions or 5 min, 30 min and 2 h after mechanical wounding. B) Accumulation of deuterated d5-dn-OPDA, d5-dn-*iso*-OPDA and d5-OPC-6 in *M. polymorpha* WT Tak-1 plants 0, 5 and 30 min after treatment with d5-OPDA. Data shown as mean ± S.D.

It has long been assumed that the major source of dinor-OPDA in angiosperms is hexadecatrienoic acid, which is also abundant in Marchantia chloroplast membranes (Kajikawa et al., 2003; Weber et al., 1997). Conversion of OPDA into dn-OPDA and/or dn-*iso*-OPDA has not been reported yet. To test wether both hexadecatrienoic acid and OPDA can be dinor-OPDA precursors in Marchantia, we fed WT plants with deuterated OPDA (d5-OPDA), deuterated α-linolenic acid (d5-18:3; the OPDA precursor in vascular plants; Supplementary Figure S8), or deuterated hexadecatrienoic acid (d6-16:3), and used LC-MS to quantify plant production of deuterated derivatives. Both d5-dn-OPDA isomers accumulated after d5-OPDA treatment, which indicated that OPDA can be converted efficiently to dn-OPDA in Marchantia. The OPR3-mediated OPDA derivative OPC-6, was not detected, which confirmed lack of OPR3 activity in this plant. d5-OPDA and both d5-dn-OPDA isomers also accumulated after feeding plants with d5-18:3, which further supports the idea that

OPDA is converted into dn-OPDA and dn-*iso*-OPDA in Marchantia (Supplementary Figure S8A and B). Treatment with d6-16:3 resulted in rapid accumulation of both d5-dn-OPDA isomers, but not of d5-OPDA (Figure Supplementary S8C). These data confirm that both hexadecatrienoic and linolenic acids are dn-OPDA sources (Supplementary Figure S6). Non-deuterated OPDA and dn-OPDA isomers also accumulated after all three treatments with deuterated precursors, which indicates that synthesis

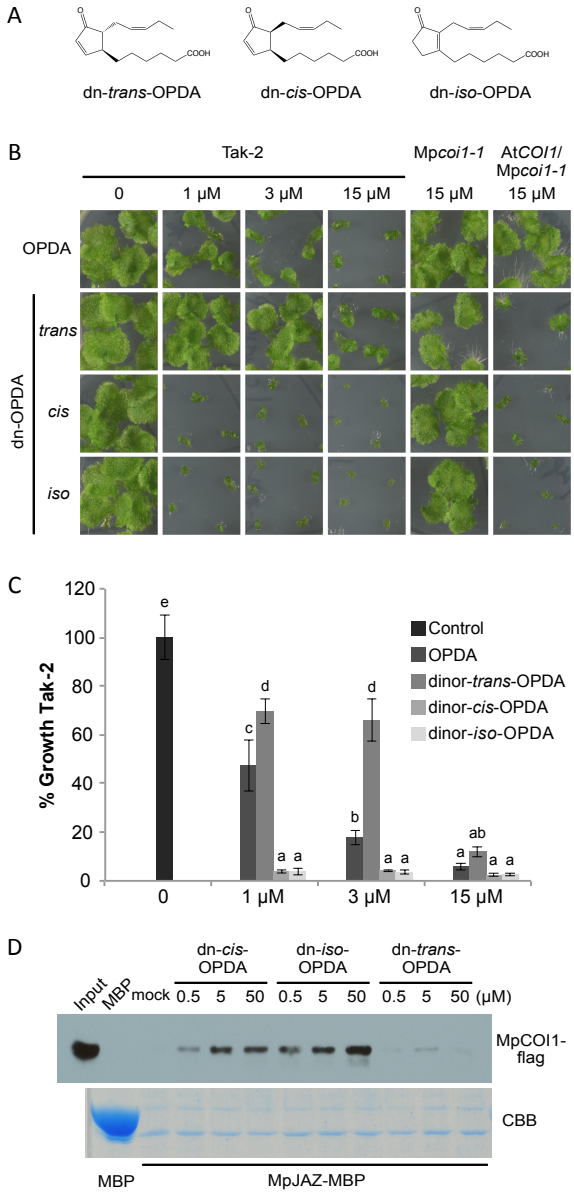

Figure 10: Dinor-OPDA is the bioactive ligand of MpCOI1 in *M. polymorpha*. A) Structures of dinor-OPDA isomers. B) Effect of various concentrations (1, 3 and 15 µM) of OPDA and dinor-OPDA isomers on gemmalings of WT Tak-2, Mp*coi1-1* and $_{pro}$Mp*EF1*:At*COI1*/Mp*coi1-1*. C) Growth percentage of plant area of Tak-2 by OPDA and dinor-OPDA isomers concentrations as in A. Data shown as mean ± S.D. D) Immunoblot (anti-flag antibody) of recovered MpCOI1-flag (from 35S:Mp*COI1*-flag Arabidopsis extracts) after pull-down reactions using recombinant MpJAZ-MBP protein alone or with the indicated dinor-OPDA isomers concentrations. Bottom, Coomassie blue staining of MpJAZ-MBP after Factor Xa cleavage.

of the hormone is subject to positive feedback, as is the case in angiosperms (Figure Supplementary S8D, E and F; Wasternack and Hause, 2013).

Dn-*iso*-OPDA and dn-*cis*-OPDA are MpCOI1 ligands

Although the *cis* and *trans* stereoisomers of dn-OPDA were not separated in our LC-MS assays, we prepared pure dn-*trans*-OPDA and tested the activity of the three possible isomers, dn-*cis*-OPDA, dn-*trans*-OPDA and dn-*iso*-OPDA (Figure 10A). Treatment of plants with similar concentrations of OPDA and dn-OPDA isomers showed that dn-*iso*-OPDA and dn-*cis*-OPDA have a greater inhibitory effect than OPDA in WT plants, and that this effect was completely MpCOI1-dependent (Figure 10B,C). Dn-*trans*-OPDA was barely active. To determine whether dn-*cis*-OPDA or dn-*iso*-OPDA are the bioactive hormone or yet other precursors, we used cell-free pull-down assays to test their capacity to trigger formation of the co-receptor MpCOI1/MpJAZ complex. Increasing dn-*cis*-OPDA and dn-*iso*-OPDA concentrations triggered retention by the immobilized MBP-MpJAZ protein of increasing amounts of MpCOI1 from plant cell-free extracts, whereas dn-*trans*-OPDA was almost inactive (Figure 10D). The activity of dn-*iso*-OPDA was about 5 fold stronger than that of dn-*cis*-OPDA, which together with the higher wound-induced accumulation of dn-*iso*-OPDA suggests that this isomer might be more relevant *in vivo*. Again, OPDA, JA-Ile and COR did not behave as ligands of MpCOI1/MpJAZ co-receptor (Supplementary Figure S9A). In contrast to Marchantia, Arabidopsis plants were only able to synthesize dn-*cis*-OPDA, but not dn-*iso*-OPDA (Supplementary Figure S9B), suggesting the presence in Marchantia of a dn-OPDA Δ^{10} to $\Delta^{9(13)}$ isomerase activity. We also tested whether dn-*cis*-OPDA stimulated the interaction between AtCOI1 and AtJAZ9 in the same conditions as MpCOI1/MpJAZ; we observed no interaction between these two proteins at the concentration tested (Supplementary Figure S9B). These results indicate that dn-*cis*-OPDA and dn-*iso*-OPDA are the MpCOI1 ligands and, therefore, the bioactive jasmonates in *M. polymorpha*.

Chapter 2:

Functional conservation of MpJAZ

Previous results of pull-down assays suggest that Mapoly0097s0021 is the orthologue JAZ protein in *M. polymorpha*. In this chapter we further characterize this gene to confirm its functional conservation. Moreover, an important problem to study JAZ function in Arabidopsis is the high redundancy of this family (Chini et al., 2016). In contrast to all the Embryophyta studied so far, where the JAZ family comprises several members, *M. polymorpha* only bears one homologous sequence for JAZ in its genome: Mapoly0097s0021 (MpJAZ; Bowman et al., 2017). Therefore, characterization of this family in a species with only one conserved family member should help to uncover novel JAZ-dependent functions.

Conservation of the TIFY family in the green lineage

JAZ proteins belong to the TIFY superfamily, which also contains ZIMs, PPDs and TIFY8 proteins (Vanholme et al., 2007). All TIFY superfamily members are characterized by the ZIM domain, which includes the TIFY motif (TIF[F/Y]XG). JAZ proteins differentiate from the other subfamilies by the presence of a specific Jas domain (Chini et al., 2016, 2007).

The evolution of the TIFY superfamily in land plants has already been studied (Bai et al., 2011), but little is known about this superfamily in algae. Although, previous analyses identified algal sequences as the so-called charophyte JAZ, these proteins lack the Jas domain and, therefore, are unlikely *bona fide* JAZ proteins (Wang et al., 2015). Moreover, recent genome sequencing projects suggest that JAZ proteins first appeared in the common ancestor of all land plants (Bowman et al., 2017). To clarify the evolutionary history of JAZ proteins we analysed the presence of TIFY family members in algal and bryophyte genomes. Blast searches in JGI and Marchantia community databases (http://phytozome.jgi.doe.gov and http://marchantia.info), sequence alignment and phylogenetic analyses (see Methods) identified the presence of ZIM and PPD sequences in charophytes but not in chlorophytes (Supplementary Figure S10). The only ZIM-related sequences in chlorophytes contain the GATA domain but not the ZIM, suggesting that GATA proteins might have been the precursors of ZIMs in charophytes. In contrast to ZIMs and PPDs, TIFY8 and JAZ sequences were absent in algae and only appear in extant early land plants (*Marchantia* and *Physcomitrella*). This indicates that JAZ was probably an acquisition during plant terrestrialization and that TIFY8 evolved simultaneously to JAZ (Supplementary Figure S10). Interestingly, we could not find homologue sequences for PPD in *Marchantia polymorpha*, but MpJAZ shows a partial conservation of the PPD domain (White, 2006; Supplementary Figure S10B). The lack of complete PPD in bryophytes suggests that PPD was either lost in bryophytes or evolved independently in Tracheophyta (Supplementary Figure S10C). These phylogenetic analyses place ZIM proteins as the ancestral TIFYs that evolved into the other members of the superfamily, including PPD, JAZ and TIFY8.

MpJAZ is a nuclear protein

Sequence conservation does not necessarily mean functional conservation. To confirm that JAZ function first appeared in land plants, we analysed conserved features of AtJAZs in MpJAZ. Genomic and transcriptomic data analyses of *M. polymorpha* in public databases showed putative Mp*JAZ* alternative splicing forms. JAZ spliced variants have been described in *Arabidopsis* and mainly affect the intron within the Jas domain (Chini et al., 2016; Chung et al., 2010). PCR amplification using specific primer combinations and sequencing of the amplified products confirmed that, the Jas region can be alternatively spliced in Mp*JAZ* transcripts, giving rise to a full-length protein containing the ZIM and Jas domains, and a shorter version lacking the Jas domain (MpJAZΔJas; Figure 11A). Q-PCR analyses revealed that the full-length version of MpJAZ (MpJAZ FL) had a higher basal expression and was induced by OPDA treatment, whereas expression of Mp*JAZΔJas* was lower and unaltered by the treatment (Figure 11B).

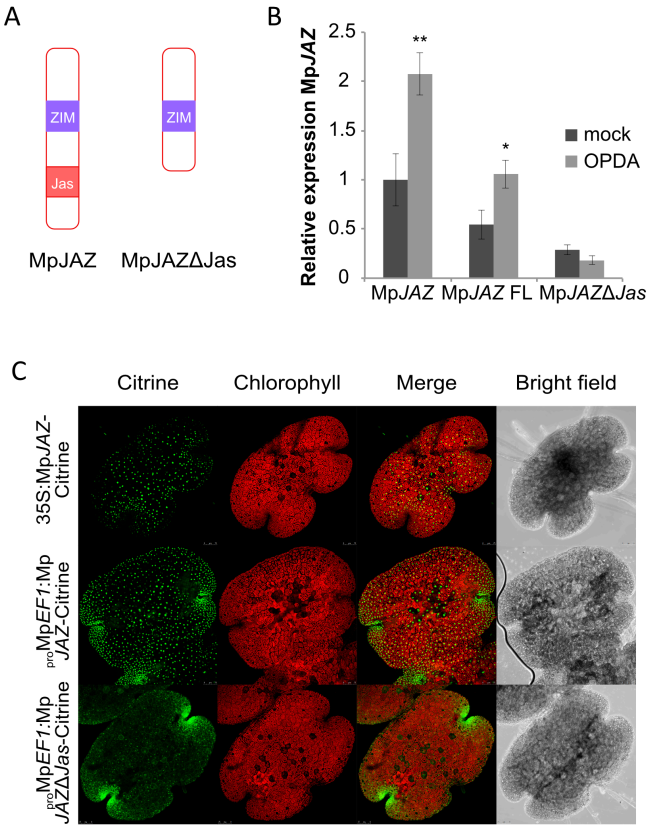

Figure 11: Mp*JAZ* has two different splicing versions with different subcellular localization. A) Scheme of MpJAZ, bearing ZIM and Jas domains, and MpJAZΔJas with just the ZIM domain. B) Relative expression by Q-PCR of total Mp*JAZ* and the two splicing forms: Mp*JAZ* full-length (FL) and Mp*JAZΔJas*. Data shown as mean ± S.D. * p <0.05; ** p < 0.01. C) MpJAZ and MpJAZΔJas subcellular localization by confocal imaging of 2-day-old 35S:Mp*JAZ*-Citrine, $_{pro}$Mp*EF1*:Mp*JAZ*-Citrine and $_{pro}$Mp*EF1*: Mp*JAZΔJas*-Citrine gemmalings

In Arabidopsis, the translocation of AtJAZ to the nucleus requires the physical interaction with MYC transcription factors, which is mediated mainly by the Jas domain (Withers et al., 2012). In *M. polymorpha*, the overexpression of Mp*JAZ* under two different promoters (35S and $_{pro}$Mp*EF1*) showed that MpJAZ is localized in the nucleus (Figure 11C, Supplementary Figure S11). MpJAZΔJas overexpression showed a dual localization in nuclei and cytoplasm, suggesting that, similar to AtJAZs, the lack of the Jas domain affects the nuclear localization of this protein (Figure 11C, Supplementary Figure S11).

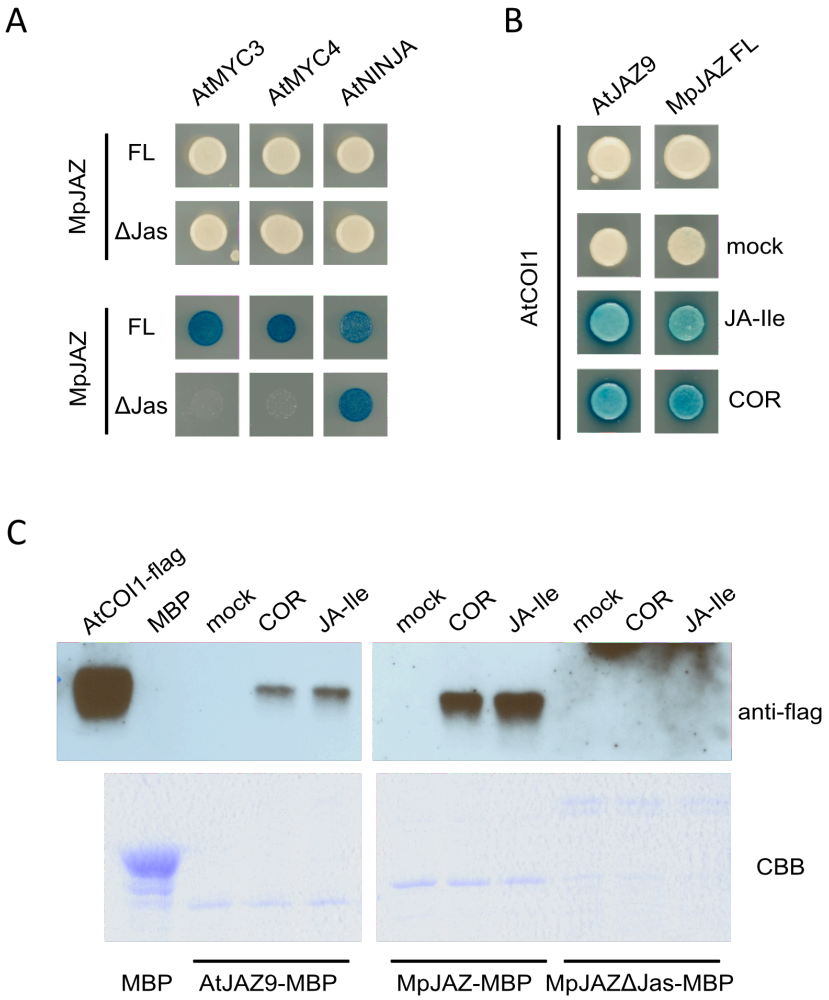

Figure 12: MpJAZ interacts with the partners of AtJAZ. A) Yeast two-hybrid assay between MpJAZ and MpJAZΔJas (fused to BD) and AtMYC3 and AtMYC4 (fused to AD). AtNINJA was fused to BD, and MpJAZ and MpJAZΔJas to AD. B) Yeast two-hybrid assay between AtJAZ9 and MpJAZ (fused to AD), and AtCOI1 (fused to BD) alone or with JA-Ile (300 µM) or COR (100 µM). Yeast growth on SD medium with glucose (top). Yeast growth on SD medium with galactose/raffinose (bottom). Blue color means interaction. C) Immunoblot (anti-flag antibody) of recovered AtCOI1-flag (from 35S:At*COI1*-flag *A. thaliana* extracts) after pull-down reactions using recombinant AtJAZ9-MBP, MpJAZ-MBP and MpJAZΔJas-MBP proteins alone or with JA-Ile (50 µM) or COR (0.5 µM). Coomassie blue staining of MpJAZ-MBP after Factor Xa cleavage (bottom).

Conserved interactions between MpJAZ and AtJAZs partners

To analyse functional conservation of Mp*JAZ*, we therefore checked if MpJAZ could interact with the same proteins as AtJAZs. The Jas domain of AtJAZ proteins mediates their interaction with AtMYC transcription factors in basal conditions, and with the hormone receptor AtCOI1 in the presence of the hormone (Chini et al., 2007; Fernández-Calvo et al., 2011; Fonseca et al., 2009; Katsir et al., 2008; Sheard et al., 2010). The ZIM domain is responsible for dimerization and interaction with the adaptor protein AtNINJA (Chini et al., 2009; Pauwels et al., 2010). Using yeast two-hybrid assays, we observed that full-length MpJAZ could interact with AtMYC3, AtMYC4 and AtNINJA, whereas MpJAZΔJas only interacted with AtNINJA (Figure 12A). These results suggest that, similar to AtJAZ proteins, the interaction with MYCs requires the Jas domain, whereas the interaction with NINJA occurs through the ZIM domain. We also observed that the ZIM domain mediates homo-dimerization of MpJAZ and hetero-dimerization between MpJAZ and AtJAZ3 (Supplementary Figure S12). MpJAZ also interacted with AtCOI1 exclusively in the presence of the hormone JA-Ile or its mimic coronatine (COR; Figure 12B). Using pull-down assays, we confirmed that the MpJAZ-AtCOI1 interaction requires the Jas domain (Figure 12C). These data indicate that despite 450 million years of separate evolution, the role of Jas and ZIM domains remain conserved between JAZ proteins from *M. polymorpha* and *A. thaliana* and can even mediate "interspecies" protein-protein interactions.

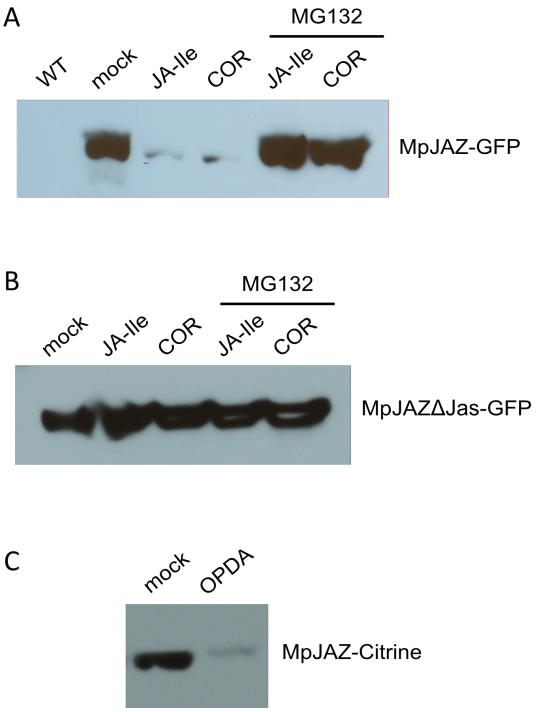

Figure 13: Degradation of MpJAZ and MpJAZΔJas *in planta*. Immunoblot (anti-GFP-HRP antibody) of MpJAZ (A) and MpJAZΔJas (B). 7-day-old *A. thaliana* 35S:Mp*JAZ*-GFP or 35S:Mp*JAZΔJas*-GFP seedlings were treated or not with JA-Ile (50 µM) +/- MG132 (100 µM) or COR (100 nM) +/- MG132 (100 µM) for 3 hours. C) Immunoblot (anti-GFP-HRP antibody) of MpJAZ degradation. 5-day-old *M. polymorpha* 35S:Mp*JAZ*-Citrine/35S:Mp*COI1*-flag gemmalings were treated or not with OPDA (50 µM) for 6 hours.

Hormone triggers MpJAZ degradation by the proteasome

In Arabidopsis, hormone-triggered recognition of AtJAZ proteins by the SCF^{COI1} complex leads to ubiquitination and subsequent degradation of the AtJAZ in the 26S proteasome (Chini et al., 2007). To

analyze whether the MpJAZ/AtCOI1 interaction described above can lead to MpJAZ degradation *in vivo*, we overexpressed both Mp*JAZ* and Mp*JAZΔJas* splicing versions independently in *A. thaliana*. Consistent with the requirement of the Jas domain for the interaction with AtCOI1, treatment of transgenic plants with either JA-Ile or COR promoted degradation of MpJAZ but not of MpJAZΔJas (Figure 13A and B). Moreover, concomitant treatment with the proteasome inhibitor MG132 completely blocked the degradation of MpJAZ, indicating that, as AtJAZs, MpJAZ is degraded through the 26S proteasome (Figure 13A). Bryophytes neither synthesize nor perceive JA-Ile and the active hormone is the OPDA-derivative dinor-OPDA (Chapter 1). Accordingly, MpJAZ was degraded by OPDA treatment in *M. polymorpha* (Figure 13C), suggesting that a similar mechanism to that of *A. thaliana* might be operating in *M. polymorpha* to destabilize MpJAZ in response to the hormone.

Mp*jaz* mutant shows severe developmental defects

To characterize Mp*JAZ* function *in vivo* in *M. polymorpha* we took advantage of conventional CRISPR/Cas9 technology (Sugano et al., 2014; see Methods) to generate Mp*jaz* mutants. As shown in

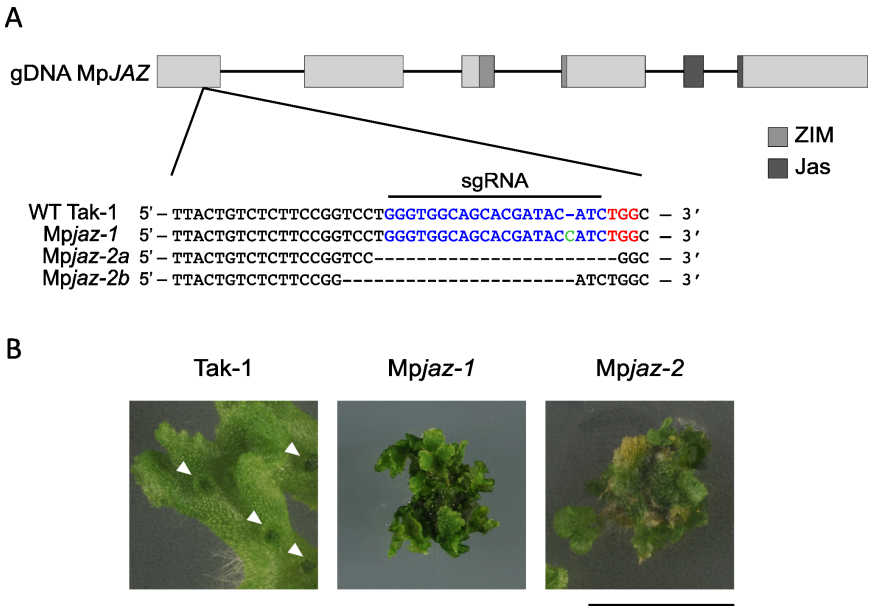

Figure 14: Generation of Mp*jaz* mutants by CRISPR/Cas9. A) Scheme of Mp*JAZ* locus. Light grey blocks, exons. ZIM and Jas domains are represented by two different shades of grey. Red, PAM sequence; blue, target sequence for the sgRNA. Sequencing revealed that Mp*jaz-1* mutant has one insertion (green) and Mp*jaz-2*, two deletions of different size (dashed lines; 22 and 23 bp). B) WT Tak-1 thallus and Mp*jaz* mutants phenotype. White triangles, gemma cups. Scale bar, 1 cm.

Figure 14A, we obtained two different alleles: Mp*jaz-1* and Mp*jaz-2*. Sequencing of Mp*jaz-1* showed an insertion of one nucleotide that generates a frame shift and therefore an aberrant and non-functional MpJAZ protein. Mp*jaz-2* was a chimaeric plant bearing at least two different deletions (Figure 14A). Both Mp*jaz-1* and Mp*jaz-2* were extremely dwarf and showed a similarly altered

morphology when compared to wild-type Tak-1 plants, including narrow branches of the thalli and absence of gemma cups (Figure 14B). Interestingly, parts of the thallus of the chimeric Mp*jaz-2* resumed growth. Sequencing of these growing parts confirmed that they carry the wild-type Mp*JAZ* sequence. Therefore, the lack of Mp*JAZ* severely reduces growth but this effect could be overcome in this chimaeric mutant by the proliferation of wild-type cells. This suggests that the MpJAZ-dependent signalling pathway has a cell-autonomous effect in *M. polymorpha*.

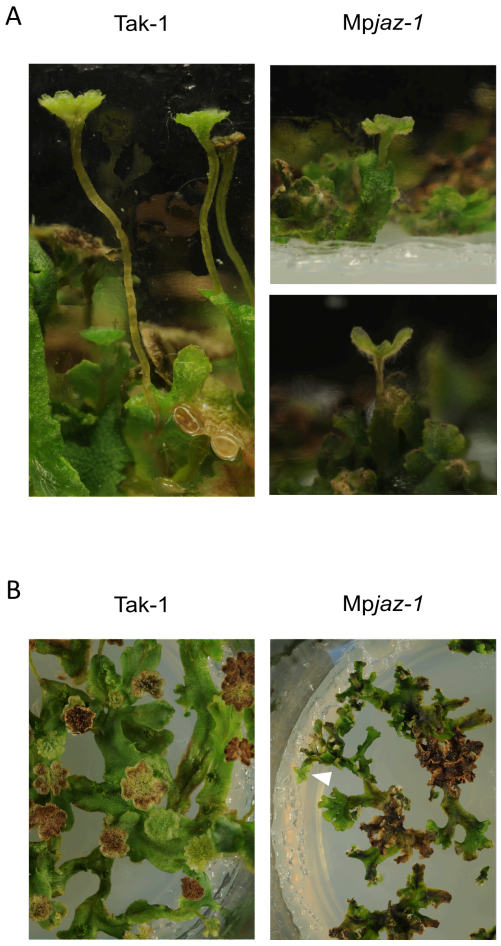

Figure 15: Mp*jaz-1* is affected in sexual reproduction. A) Mature Tak-1 antheridiophores and aberrant Mp*jaz-1* antheridiophores (18 and 22-day-old, respectively). B) WT Tak-1 and Mp*jaz-1* plants grown under white light and irradiated with FR light during 72 days. White triangle, antheridiophores in Mp*jaz-1* mutant (top right in A).

Mp*jaz-1* affects sexual and asexual reproduction

Growth-phase transition in *M. polymorpha* can be induced by supplementation of white light with far-red (Chiyoda et al., 2008; Kubota et al., 2014). To test whether Mp*jaz-1* mutant could undergo the transition to reproductive development, we grew pieces of Tak-1 and Mp*jaz-1* thalli *in vitro* for one week and then irradiated them with FR for several weeks. In the case of Tak-1, numerous antheridiophores started to emerge 12 days after the irradiation with FR, and 11 days after they were

fully developed (Supplementary Figure S13A). In contrast, Mp*jaz-1* only developed two antheridiophores after 34 and 54 days of FR irradiation (Figure 15A). The production of antheridiophores in Tak-1 72 days after FR irradiation was remarkable compared to the poor development of Mp*jaz-1* (Figure 15B). The morphology of Mp*jaz-1* antheridiophores was also different from that of WT, with aberrant formation of the antheridial receptacle, giving rise to two or four lobes instead of the WT eight lobes (Figure 15). The Mp*jaz-1* antheridiophores also displayed

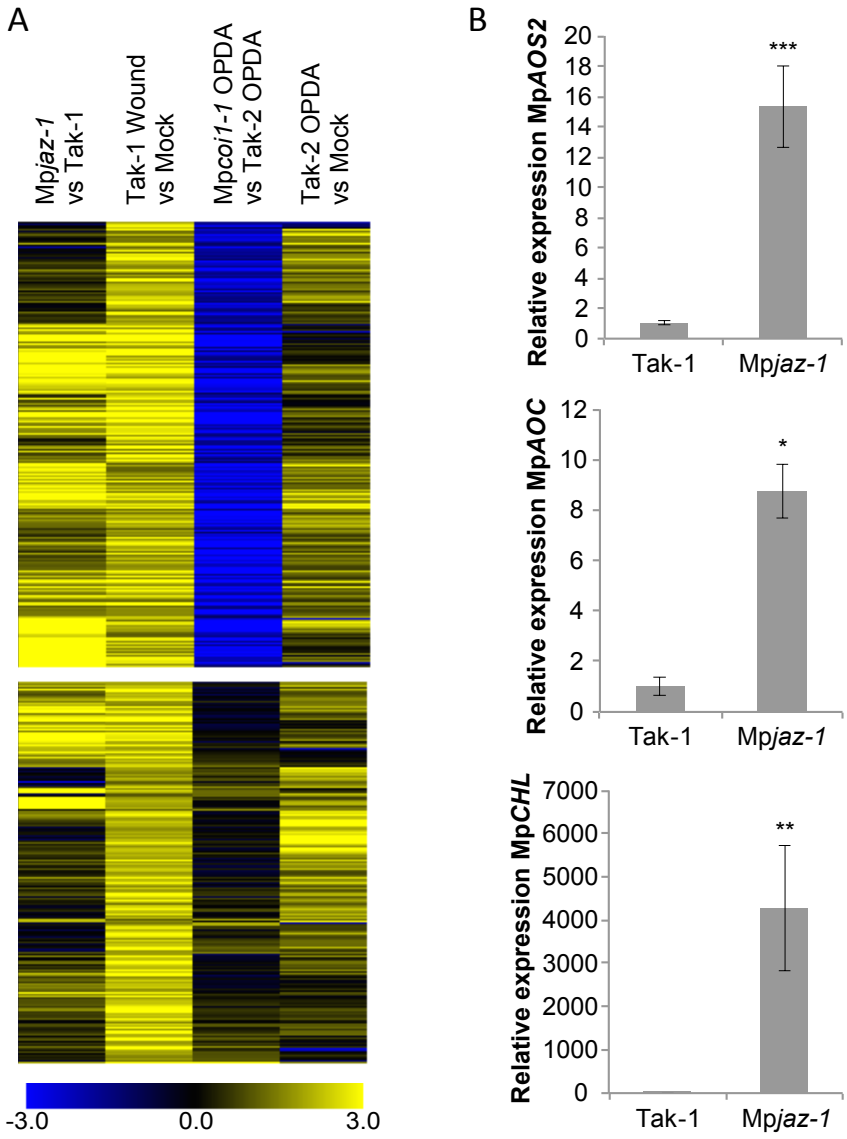

Figure 16: Mp*jaz-1* mutant shows a constitutive activation of MpCOI1-dependent pathway. A) Clustering analysis of genes upregulated by wounding (Tak-1 Wound vs Mock) selected by LogRatio > 1 and FDR (LIMMA) <0.05 compared to Mp*jaz-1* (Mp*jaz-1* vs Tak-1) and OPDA treatment in the WT (Tak-2 OPDA vs Mock) and in Mp*coi1-1* (Mp*coi1-1* OPDA vs Tak-2 OPDA). Analysis was set to two clusters, in which cluster 1 (top) correspond to MpCOI1-dependent genes and cluster 2 (bottom) to MpCOI1-independent genes. Total number of genes = 472. B) Q-PCR analyses of three OPDA-marker genes (Mp*AOS2*, Mp*AOC* and Mp*CHL*) in Tak-1 and Mp*jaz-1* mutant. Data shown as mean ± S.D. *p < 0.05; **p < 0.01; ***p < 0.001

reduced elongation of the stalk (Figure 15A) when compared to stage 5 Tak-1 antheridiophores, according to the shape of the antheridial receptacle (Higo et al., 2016).

Besides the production of sexual organs (antheridiophores and archegoniophores) *M. polymorpha* can reproduce asexually through the formation of clonal gemmae in the gemma cups located on the dorsal side of the mature thallus (Shimamura, 2016). No gemma cups were observed on Mp*jaz-1* thalli even when plants were grown on sucrose media, which induces gemma cup formation in the WT (Terui, 1981; Supplementary Figure S13A and B). Similar to the scarce formation of antheridiophores, one year-old plants developed one or two gemma cups, which produced viable gemmae.

Constitutive activation of the MpCOI1-dependent pathway in Mp*jaz* mutants

Mp*jaz* dwarf phenotype (Figure 14B) is consistent with a constitutive activation of the pathway, which leads to growth inhibition both in *Marchantia* and *Arabidopsis* (Chapter 1; Campos et al., 2016). Transcriptomic analyses using Marchantia microarrays designed in our laboratory (Chapter 1) showed a constitutive upregulation of genes induced by wounding and OPDA treatment in Mp*jaz-1* mutant compared to WT Tak-1 (Figure 16A). Although more than half of these genes were MpCOI1-dependent, Mp*jaz* exhibited an upregulation of a set of genes induced by wounding and OPDA but MpCOI1-independent (Figure 16A, bottom).

Q-PCR analysis of three genes differentially expressed according to microarray data (Mp*AOS2,* Mp*AOC* and Mp*CHL*; Chapter 1) confirmed their upregulation in Mp*jaz-1* (Figure 16B). Given that MpAOS2 and MpAOC are involved in OPDA and dinor-OPDA biosynthesis (Koeduka et al., 2015; Yamamoto et al., 2015), we measured the accumulation of these molecules in the mutant and the WT. Mp*jaz-1* accumulates enormous amounts of OPDA, dn-OPDA and dn-*iso*-OPDA (Figure 17). These high levels support the conservation of the positive feedback loop of hormone biosynthesis described in Arabidopsis (Wasternack and Hause, 2013).

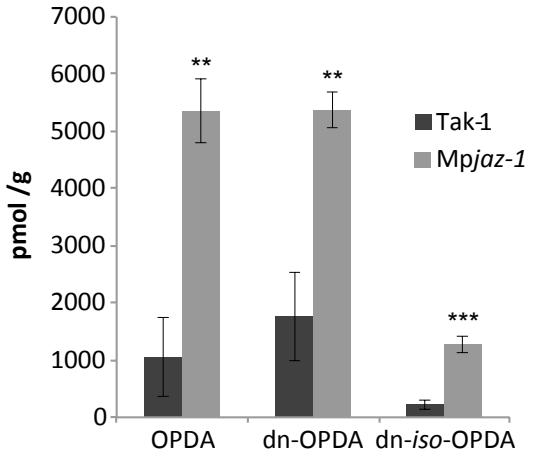

Figure 17: Mp*jaz-1* produces higher levels of OPDA and dinor-OPDA/dinor-*iso*-OPDA than the WT. Accumulation of OPDA, dinor-OPDA and dinor-*iso*-OPDA in WT Tak-1 and Mp*jaz-1* in basal conditions. Data shown as mean ± S.D. **p < 0.01; ***p < 0.001

Mp*jaz* complementation by Mp*JAZ* and At*JAZ*

Consistent with the dwarf phenotype of mature thalli, Mp*jaz-1* gemmalings showed a reduced growth compared to WT Tak-1 in basal conditions and were hypersensitive to OPDA treatments (Figure 18). Expression of a Cas9-resistant version of Mp*JAZ* (see Methods and Supplementary Figure S14) into the Mp*jaz-1* background, fully restored the WT phenotype of thalli as well as the production of gemmae in gemma cups, indicating that the Mp*jaz-1* mutation was responsible for the developmental defects of the mutant. Mp*JAZ*/Mp*jaz-1* gemmae showed WT phenotype in basal conditions and were more resistant to OPDA than the WT (Figure 18). This increased OPDA resistance is consistent with a higher expression of the transgene compared to the endogenous Mp*JAZ* and with its function as a repressor.

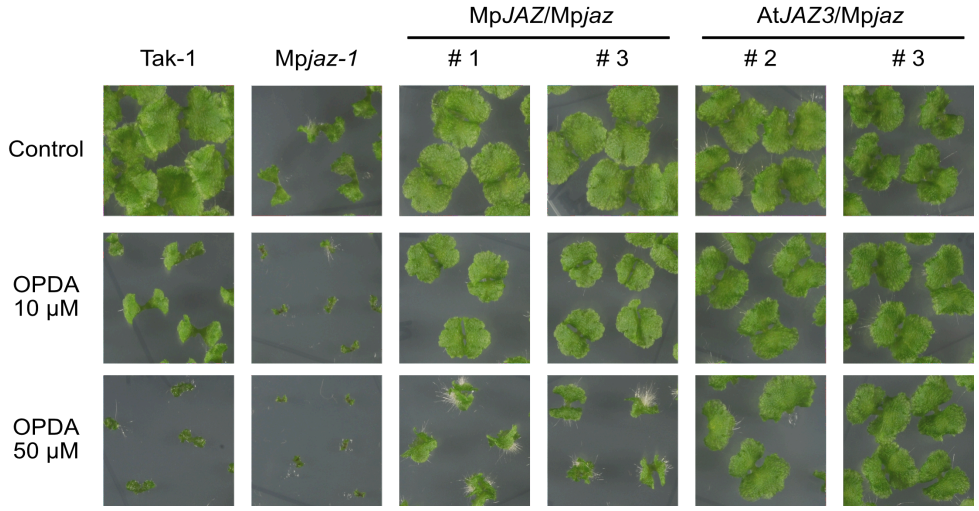

Figure 18: Mp*JAZ* and At*JAZ3* complement Mp*jaz-1* mutant and confer OPDA resistance. Effect of OPDA (10 and 50 µM) on 15-day-old WT Tak-1, Mp*jaz-1*, $_{pro}$Mp*EF1*:Mp*JAZ*^{Cas9R}-Citrine/Mp*jaz-1* (#1 and #3) and $_{pro}$Mp*EF1*:At*JAZ3*-Citrine/Mp*jaz-1* (#2 and #3) gemmalings.

To confirm whether JAZ function is conserved between *M. polymorpha* and *A. thaliana*, we attempted to complement Mp*jaz-1* with At*JAZ3*. At*JAZ3* constitutive expression ($_{pro}$Mp*EF1*:At*JAZ3*/Mp*jaz-1*) effectively restored the WT phenotype in the Mp*jaz-1* mutant, indicating that JAZ function is conserved in land plants (Figure 18). In addition, gemmae of the transgenic plants $_{pro}$Mp*EF1*:At*JAZ3*/Mp*jaz-1* were fully insensitive to OPDA (Figure 18). This result indicates that AtJAZ3 can actively repress the pathway in *M. polymorpha* but it is unable to form a functional co-receptor with MpCOI1 and the active hormone dinor-OPDA.

Chapter 3:
Rational design of a ligand-based antagonist of jasmonate perception

Analyses of the roles of JA during development and in response to stress have been so far carried out by genetic approaches or exogenous treatments of the hormone or precursors. However, loss-of-function mutants are limited tools for the analysis of JA-dependent responses in particular tissues or developmental times. Temporal and spatial analyses of the roles of JA have been hindered by the lack of JA-Ile antagonist molecules that could be used to manipulate or repress the pathway in particular tissues or developmental stages without compromising the whole JA response of the plant in other tissues or stages. Moreover, the dissection of the roles of JA pathway in species distantly related to Arabidopsis has also been hampered by the lack of genetic tools, problem that can now be overcome by the use of JA antagonists (Böhm et al., 2016).

Rational design of JA-Ile co-receptor antagonists

We aimed to design a direct antagonist that could compete with JA-Ile for binding to its co-receptor (AtCOI1-AtJAZ) and prevent the hormone-triggered interaction between AtCOI1 and the AtJAZ repressors. Given that the keto and carboxyl groups of the hormone are exposed to the solvent when JA-Ile binds AtCOI1(Sheard et al., 2010), we reasoned that a stable modification on either group of the hormone would prevent the interaction with AtJAZ proteins for stereochemical reasons without compromising the specific binding to AtCOI1 (Supplementary Figure S15). Thus, we modified the keto with a methyloxime group because of the ease of chemical synthesis and its stability. Moreover, the absence of any polar group should avoid any disturbance of binding to its receptor. In the case of the carboxyl group, we chose a methyl esterification because it was easily chemically synthesized.

We synthesized the *O*-methyloxime derivatives of (–)-JA (JA-MO, **1**), (–)-JA-L-Ile (JA-Ile-MO, **2**) and COR (COR-MO, **3**; Figure 19A) as well as the methyl esters of JA-Ile and COR and analyzed their effects *in vivo* and *in vitro*. The two methyl esters did not show any antagonistic effect in our tests (pull-down, activation of $_{pro}$At*JAZ2:GUS* expression and degradation of AtJAZ1:GUS; not shown), possibly owing to the existence of plant esterases that could cleave the ester to produce COR or JA-Ile. Similarly, JA-MO did not show any effect, possibly because the modification could prevent JAR1 from conjugating with isoleucine to produce JA-Ile-MO. Therefore we focused on the analysis of the JA-Ile-MO and COR-MO derivatives.

COR-MO and JA-Ile-MO modulate JA-mediated phenotypes

Anthocyanin accumulation and inhibition of root growth are two of the best-characterized plant responses to JA-Ile (or its mimic COR). Increasing concentrations of COR induce a dose-dependent increase in anthocyanin content (Figure 19B and Supplementary Figure S16). In contrast, plants grown in the presence of different combinations of COR and COR-MO concentrations showed a strong, dose-dependent reduction of this COR effect (Figure 19 and Supplementary Figure S16). The half-maximum inhibitory concentration (IC_{50}) of COR-MO was 0.43 µM for a concentration of 0.5 µM

COR and 0.7 µM for a concentration of 1 µM COR, underscoring the potency of COR-MO (Figure 19C and Supplementary Figure S16). Notably, COR-MO treatment alone did not have any noticeable effect on anthocyanin accumulation even at concentrations of 30 µM, supporting its specificity and lack of toxicity (Figure 19B, C and Supplementary Figure S16).

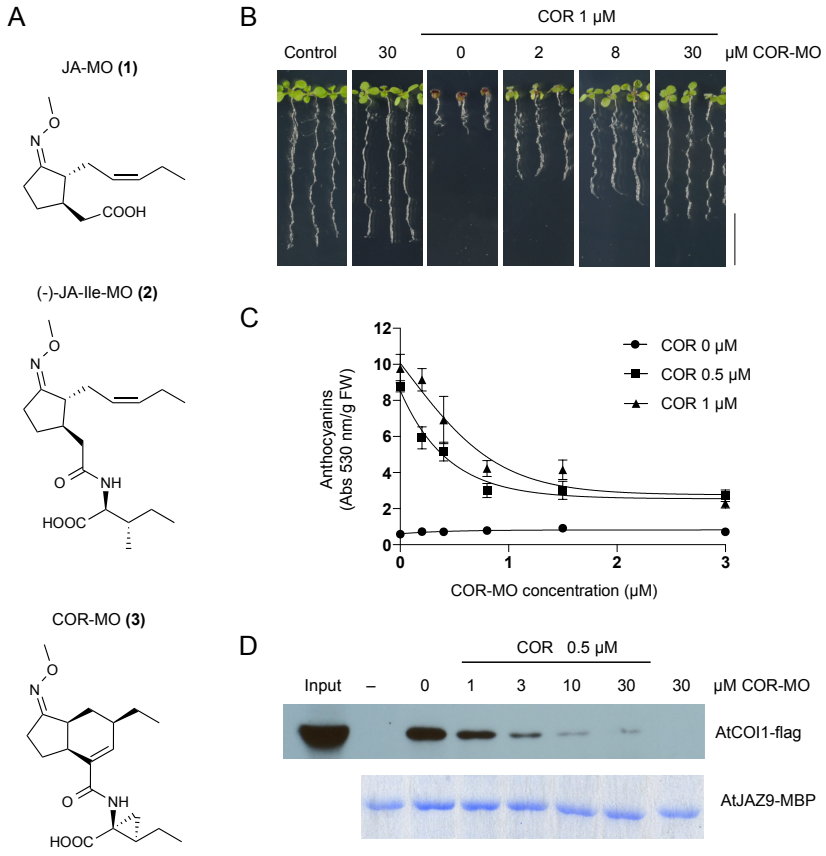

Figure 19: Effect of COR-MO on COR-dependent anthocyanin accumulation, root growth inhibition and AtCOI1/AtJAZ9 interaction. A) Structures of JA-MO, JA-Ile-MO and COR-MO. B) Arabidopsis WT seedlings grown for 10 d on Johnson medium supplemented with COR-MO and/or COR at the indicated concentrations. Scale bar, 1 cm. C) Quantification of anthocyanin accumulation of 10-day-old WT seedlings grown on different combinations of COR and COR-MO. Abs, absorbance; FW, fresh weight. Data shown as mean ± S.D. D) Immunoblot (anti-flag antibody) of recovered AtCOI1-flag (from 35S:At*COI1*-flag *A. thaliana* extracts) after pull-down reactions using recombinant JAZ9-MBP protein alone or with different combinations of COR and COR-MO. Coomassie blue staining of AtJAZ9-MBP after Factor Xa cleavage (bottom).

Similarly to its effect on anthocyanins, COR-MO reduced the inhibition of root growth by COR in a dose-dependent manner, with an IC_{50} of 0.8 µM for a concentration of COR of 1 µM (Supplementary Figure S16), and even high concentrations (30 µM) of COR-MO alone did not alter root growth (Figure 19b and Supplementary Figure S16).

The inhibitory effect of COR-MO was not restricted to COR activity; it also inhibited the effects of JA treatments on anthocyanin accumulation and root growth (Supplementary Figure S17). These are

remarkably strong effects, considering that the plants had been grown continuously in the presence of the agonists since their germination.

JA-Ile-MO also reduced root growth inhibition and anthocyanin accumulation by JA (Supplementary Figure S18), but this effect was milder compared to that of COR-MO. When lower concentrations of JA-Ile-MO were used for shorter periods of time, the effect of JA-Ile-MO was not appreciable (Supplementary Figure S18C). These results indicate that both methyloxime derivatives inhibit these hormone-regulated processes and that COR-MO is a much more potent antagonist than JA-Ile-MO. Therefore, we focused our analyses on COR-MO.

COR-MO reduces AtCOI1-AtJAZ interaction

To test whether the rationally designed antagonist could effectively interfere with the COR-mediated formation of the AtCOI1–AtJAZ co- receptor complex, we performed pull-down assays using recombinant AtJAZ9-MBP protein and plant extracts expressing AtCOI1-flag. In the presence of COR, AtCOI1 binds AtJAZ9, as shown by AtCOI1-flag detection after the pull-down reaction (Figure 19D). However, when COR-MO was added to the pull-down reaction, it reduced the COR-dependent AtCOI1-AtJAZ9 interaction in a concentration-dependent manner (IC_{50} = 1.53 µM for a concentration of 0.5 µM COR; Figure 19D and Supplementary Figure S19). COR-MO was unable to induce the AtCOI1-AtJAZ9 interaction in the absence of COR (Figure 19D). These results suggest that COR-MO competitively inhibits binding of COR to the AtCOI1-AtJAZ co-receptor.

COR-MO reduces AtJAZ degradation

Hormone-triggered AtJAZ binding to the SCF^{AtCOI1} complex induces polyubiquitination and subsequent proteasome degradation of JAZ repressors. Because of the inhibitory effect of COR-MO

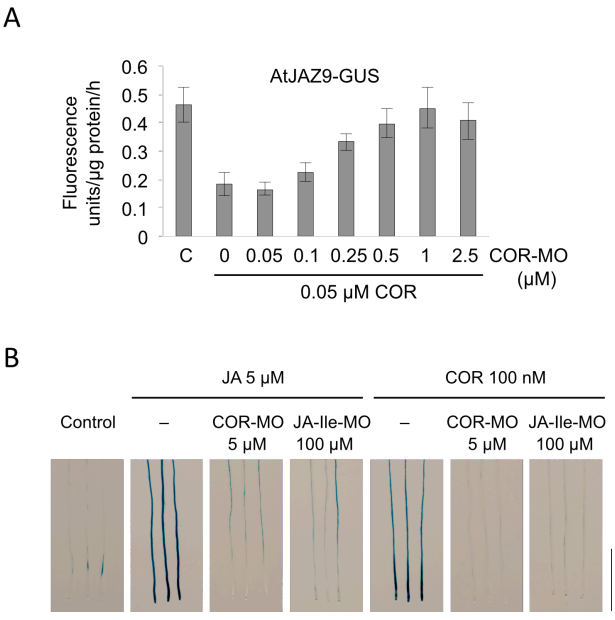

Figure 20: Effect of COR-MO on COR-mediated JAZ9 degradation and JA- and COR-dependent At*JAZ2* gene expression.
A) Quantification of GUS activity in roots of 7-day-old transgenic Arabidopsis 35S:At*JAZ9*-GUS. Seedlings were pretreated with the indicated concentrations of COR-MO for 1 h and then treated with COR 50 nM for 1 h. Data shown as mean ± S.D. B) 7-day-old Arabidopsis $_{prom}$At*JAZ2*:GUS seedlings were concurrently treated for 1 h with either JA (5 µM) or COR (100 nM) plus COR-MO (5 µM) or JA-Ile-MO (100 µM). Scale bar, 0.5 cm

on the receptor complex formation described above, we next studied the COR-MO effect on the hormone-triggered degradation of several AtJAZ proteins (AtJAZ1, AtJAZ9 and AtJAZ10) in seedlings of transgenic *Arabidopsis* 35S:At*JAZ1*-GUS, 35S:At*JAZ9*-GUS and 35S:At*JAZ10*-GUS lines. Treatment of transgenic seedlings with COR (or JA) triggered the degradation of the three AtJAZ-GUS proteins, as observed by reduced GUS activity (Figure 20A and Supplementary Figure S20). In contrast, pretreatment with COR-MO prevented the degradation of these proteins in a concentration-dependent manner. The effect was stronger in the cases of AtJAZ9 and AtJAZ10 (Figure 20A and Supplementary Figure S20). These results indicate that the effect of COR-MO is not restricted to a particular AtCOI1/AtJAZ co-receptor complex.

Consistent with previous results from the phenotypic analyses, JA-Ile-MO treatment also prevented the degradation of AtJAZ1 but required a concentration much higher than COR-MO (Supplementary Figure S20B).

COR-MO prevents JA-dependent gene expression

JAZ genes are among the earliest JA-responsive genes; therefore, to test the effect of COR-MO on JA-dependent gene expression, we first generated an *Arabidopsis* transgenic line carrying the promoter region of At*JAZ2* fused to the GUS marker. JA or COR highly induced the expression of At*JAZ2*, as shown by GUS accumulation (Figure 20B). The concomitant treatment with COR-MO or JA-Ile-MO prevented hormone-induced gene expression of $_{pro}$At*JAZ2*:*GUS*. We concluded that both COR-MO and JA-Ile-MO prevent JA- and COR- dependent gene expression. Similar to previous results, COR-MO required a 20-fold lower concentration than JA-Ile-MO to obtain similar effects.

To address the specificity and magnitude of COR-MO's inhibitory effect, we next obtained whole-genome transcriptomic profiles of wild-type (WT) seedlings untreated or treated with COR, COR-MO or both simultaneously, using two-color microarrays. Differentially expressed genes were selected as those showing a fold change ≥2 or ≤-2 and a false discovery rate (FDR) < 0.05 (see Methods). Profiles obtained comparing COR- treated versus COR- plus COR-MO–treated plants render a total of 62 genes with increased expression and 386 genes with reduced expression due to COR-MO treatment. Remarkably, analysis of JA regulation data of those genes from public databases (Bio-Analytic Resource for Plant Biology; http://bar.utoronto.ca/) revealed that a high percentage of the genes with reduced expression by COR-MO treatment (in the COR versus COR plus COR-MO comparison) were genes induced by JA (55.44% observed versus 1.97% expected; Supplementary Figure S21). None of them, however, were repressed by the hormone (Supplementary Figure S21). Similarly, a high percentage of the genes with increased expression by COR-MO correspond to genes repressed by JA, and none of them correspond to genes induced by the hormone (21% observed versus 0.49% expected; Supplementary Figure S21).

COR-MO alone did not promote any significant (FDR < 0.05) change in gene expression after 2 h of treatment compared to untreated plants, indicating that COR-MO does not have off-target effects in the absence of the agonist (microarray data code in Gene Expression Omnibus: GSE56027).

Altogether, these results indicate that COR-MO has a strong effect in inhibiting the modulation of gene expression by COR at the whole-genome scale and support a strong specificity of COR- MO activity.

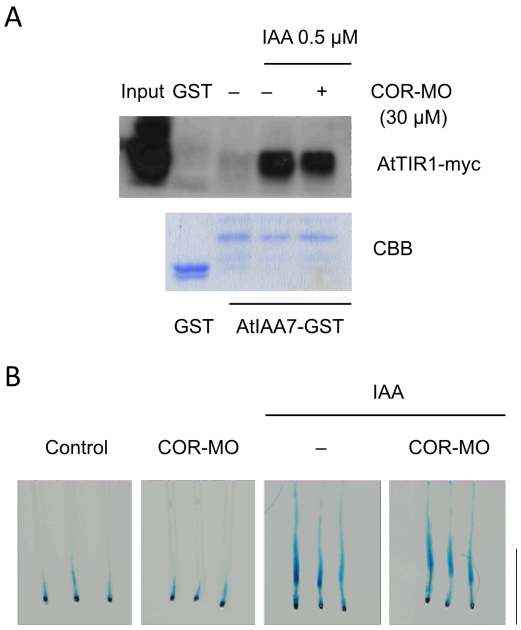

Figure 21: COR-MO does not affect auxin perception and signalling. A) Immunoblot (anti–myc-HRP antibody) of recovered AtTIR1-myc (from Dexp:At*TIR1*-myc/At*tir1-1*) after pull-down reactions using recombinant GST and AtIAA7-GST protein, alone (–), with IAA (0.5 µM) or with IAA plus COR-MO. Coomassie blue staining of the GST and AtIAA7-GST (bottom). B) Effect of COR-MO on auxin-responsive DR5:GUS reporter gene expression. 6-day-old seedlings were pretreated with COR-MO (10 µM) for 1 h and then treated with IAA (5 µM) for 80 min. Scale bar, 0.25 cm.

JA derivatives such as JA-Trp have been shown to influence auxin responses by (indirectly) interfering with the AtTIR1 and AtTIR1-related auxin co-receptors (Staswick, 2009; Staswick et al., 2017). The auxin co-receptor AtTIR1 is, phylogenetically, the closest protein to AtCOI1 (Chico et al., 2008; Katsir et al., 2008; Tan et al., 2007), and auxin and JA-Ile act similarly as molecular glues between their co-receptor proteins (Chico et al., 2008; Fonseca et al., 2009; Katsir et al., 2008; Tan et al., 2007). To further discard any off-target effect of COR-MO, we assessed several auxin responses. First, we analyzed the auxin-mediated interaction between AtTIR1 and AtIAA7 by pull-down assays. IAA induced the interaction between AtTIR1-myc from plant extracts and recombinant AtIAA7-GST (Figure 21A). The addition of COR-MO to the pull-down reaction did not affect the interaction between these two proteins, supporting its specificity for the JA-Ile receptor complex (Figure 21A).

Next, we studied the effect of COR-MO on auxin-induced gene expression using the auxin marker DR5. DR5:GUS seedlings treated with COR-MO show DR5:GUS expression in roots similar to that in non-treated seedlings (Figure 21B). Moreover, the auxin induction of DR5:GUS expression in seedlings was not altered by treatment with COR-MO. These results showed that COR-MO does not affect DR5:GUS expression or the AtTIR1/AtIAA7 interaction, which is the closest receptor complex to AtCOI1/AtJAZ, therefore supporting the specificity of COR-MO on the AtCOI1/AtJAZ system.

COR-MO modulates JA-mediated pathogen defences

Activation of the JA signalling pathway is required for plant defences against necrotrophic pathogens, and therefore we next analyzed the effect of COR-MO treatment on JA-dependent defences against *Botrytis cinerea*. Four-week-old WT *Arabidopsis* plants were challenged with 5×10^5 spores of the fungus, and infection symptoms were scored 4 d after inoculation. Simultaneous application of the spores and COR-MO promoted a shift of symptoms from mild to severe, indicating that the antagonist reduces the activation of JA-dependent defences, therefore increasing the susceptibility to the necrotrophic fungus (Figure 22A). Similarly, quantification of spores produced after 4 d of infection revealed that COR-MO treatment increases plant susceptibility, enhancing spore production by approximately twofold (Figure 22B).

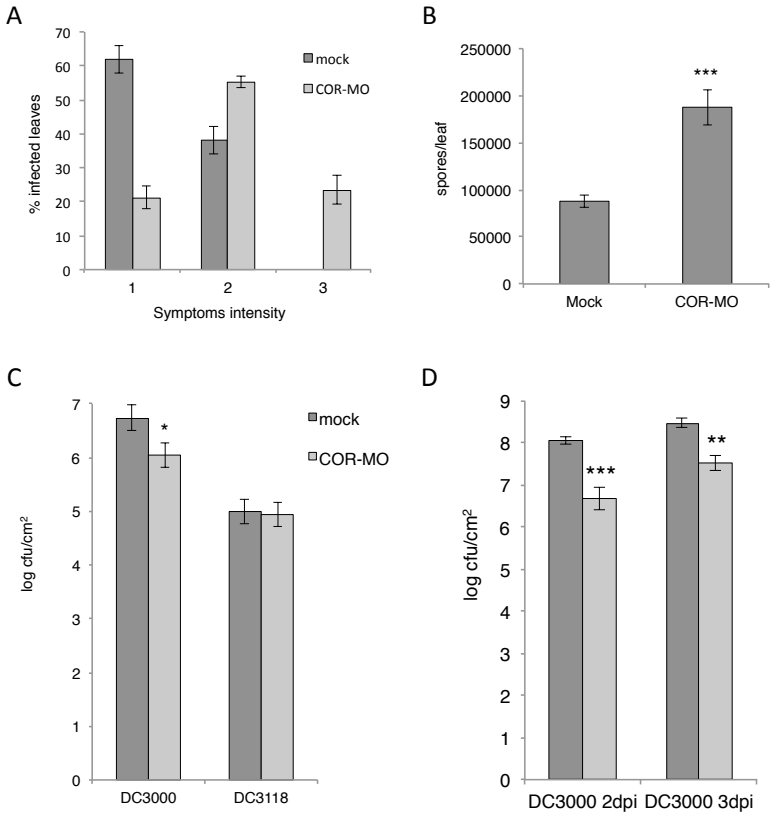

Figure 22: Effect of COR-MO on the infection by the necrotrophic pathogen *B. cinerea* and the bacterial hemibiotroph strains Pst DC3000 and DC3118 (COR⁻). A) Quantification of symptoms 4 d after inoculation of Arabidopsis WT plants with *B. cinerea* (5×10^5 spores per ml). COR-MO (10 μM) was included in the spore suspension when indicated. Symptoms were divided in three stages depending on the size of the necrotic lesion (1: <10 mm^2 , 2: 10–20 mm^2 or 3: >20 mm^2). Data shown as mean ± S.D. B) Determination of *B. cinerea* spore number 4 d after inoculation of Arabidopsis WT plants. Data shown as mean ± S.D. C) Bacterial growth on WT Arabidopsis plants (infiltrated with COR-MO 24 h before inoculation) 2 d after spray inoculation with Pst DC3000 or DC3118. D) Bacterial growth on *N. benthamiana* leaves (infiltrated with COR-MO 24 h before inoculation) 2 d and 3 d post spray inoculation (2dpi and 3dpi, respectively) with Pst DC3000. Bacterial counts are expressed as log(CFU cm^{-2}). Data shown as mean ± SEM. *$p < 0.05$; **$p < 0.01$; ***$p < 0.001$ by Student's t-test.

In biotrophic or hemibiotrophic pathogens, such as *Pseudomonas syringae*, JA-Ile promotes susceptibility owing to its well-documented antagonistic effect on the SA pathway (Gimenez-Ibanez and Solano, 2013; Robert-Seilaniantz et al., 2011). To test the biotechnological potential of COR-MO, we analyzed whether its antagonistic activity could be sufficient to overcome the effect of COR produced by *P. syringae* during infection. In our bioassays, we used two different strains of *P. syringae* pv. *tomato* (Pst): DC3000, which produces COR, and DC3118, a COR-deficient isogenic Pst DC3000 strain commonly known as Cor^{-}, because it is impaired in COR synthesis (Brooks et al., 2004). We infiltrated COR-MO together with the bacterial strains DC3000 and DC3118 into *Arabidopsis* leaves. Five days after infection, COR-MO reduced the symptoms produced by DC3000 but did not show any effect upon infection with DC3118 (Supplementary Figure S22). Moreover, COR-MO strongly reduced the COR-dependent symptoms caused by DC3118 supplemented with the phytotoxin (Supplementary Figure S22).

We also performed the infection assays by infiltration of COR-MO 24 h before spray application of either Pst DC3000 or DC3118. The results of this assay agreed with those of the infiltration assay (Figure 22C). The use of COR-MO reduced bacterial growth by one logarithmic unit of colony-forming units (CFU) cm^{-2}. Notably, pretreatment with COR-MO and subsequent spray infection with Pst DC3118 did not affect bacterial growth of this strain. This suggests that COR-MO directly targets the JA signalling pathway, which is activated by COR produced by DC3000.

To further explore the biotechnological potential of COR-MO, we analyzed its effect on a solanaceous species (*Nicotiana benthamiana*). COR-MO reduced bacterial growth by over one logarithmic unit, confirming that the antagonist is effective in different plant-pathogen interactions (Figure 22D).

Discussion

Ligand-receptor co-evolution shaped the jasmonate pathway in land plants

In this work, we identified a new hormone, dn-OPDA, with two active isoforms in *Marchantia polymorpha*, and show that bryophytes and vascular plants share a conserved signalling machinery that is activated by different molecules (dn-*iso*-OPDA/dn-*cis*-OPDA or JA-Ile).

Genome sequences available from a myriad sequencing projects provide an unprecedented opportunity to study the conservation of pathways among different plant lineages and to understand how representative of plant diversity is the knowledge obtained in eudicot models. More importantly, comparative genomics should help to identify mechanisms that may be hidden by gene redundancy in vascular plants, in which their complex and redundant genomes slow down discovery of such mechanisms.

Our results provide an example of the power of comparative genomics and the usefulness of the new model system *Marchantia polymorpha*. Liverworts are considered the sister lineage to all other land plants. Therefore the presence in its genome of single copies of each of the core components of the JA pathway and the functional conservation shown here indicate that this pathway appeared in the first common ancestor of all extant land plants (Bowman et al., 2017). Liverworts and mosses lack two key enzymes, namely OPR3 and JAR1, involved in the biosynthesis of the vascular plant hormone JA-Ile and should not be able to synthesize it (this work; Stumpe et al., 2010; Yamamoto et al., 2015). Therefore the hormones activating this pathway should be different in bryophytes and vascular plants. Consistent with this hypothesis, we found that JA-Ile is neither synthesized nor perceived by bryophytes, but rather that *M. polymorpha* produces two isomers of dn-OPDA, dn-*cis*-OPDA and dn-*iso*-OPDA, as the bioactive ligands of its COI1 receptor. The wound-induced accumulation of OPDA and dn-OPDA isomers indicates that the chloroplastic steps of JA biosynthesis are conserved between bryophytes and vascular plants, and should therefore be present in their common ancestor. In eudicots, the major sources of these compounds are α-linolenic (18:3) and hexadecatrienoic (16:3) acids, respectively (Wasternack and Hause, 2013). These two fatty acids are abundant in Marchantia chloroplastic membranes (Kajikawa et al., 2003). However, the observation that OPDA inhibits growth in Marchantia coupled with the finding that only dn-OPDA isomers and not OPDA, are MpCOI1 ligands suggested that OPDA should be an additional source of dn-OPDA. Our results using deuterated α-linolenic and deuterated OPDA demonstrate that this conversion exists in Marchantia and clarifies the biosynthetic steps to the bioactive hormone formation in this plant.

Additionally, dn-OPDA can be transformed into dn-*iso*-OPDA, an isomer that is not present in eudicots such as Arabidopsis. The most similar compound identified in plants is *iso*-OPDA, which is naturally synthesized in stressed barley leaves and mosses from the genus *Dicranum* (Ichikawa et al., 1984; Kramell et al., 2000). Certain herbivore insects have evolved an enzyme to convert OPDA into *iso*-OPDA, although a similar enzyme has not been identified in plants (Dabrowska et al., 2009). Feeding experiments with *iso*-OPDA have shown that many plant species and even yeasts can

transform *iso*-OPDA into cis-jasmone, being dn-*iso*-OPDA one of the intermediates (Dabrowska and Boland, 2007). However, we were unable to detect any *iso*-OPDA in *M. polymorpha*, so dn-*iso*-OPDA likely comes from dn-OPDA originated from either OPDA or 16:3, according to our feeding experiments with deuterated precursors.

The adaptive insect mechanism to convert OPDA into *iso*-OPDA suggests that besides the role of OPDA as precursor of signalling molecules or as a signalling molecule itself, it might exhibit some direct deterrent effects on the insects. This could be related to the presence of an α,β-unsaturated carbonyl, a very reactive chemical group also present in other Reactive Electrophile Species (RES). Therefore, the COI1-independent transcriptional response to OPDA might be at least partially due to the presence of this chemical group, since RES are known to upregulate genes related to detoxification and heat shock proteins (this work; Farmer and Mueller, 2013; Taki et al., 2005).

The discovery of the active hormone in bryophytes and the fact that one single amino acid in MpCOI1 switches the ligand specificity towards that of AtCOI1 suggest a simple evolutionary path from the ancestral land plants to the extant vascular plants. It seems likely that the appearance of vascular plants exerted a selective pressure to the evolution of a more polar hormone, which would facilitate movement through the vasculature. Another difference between JA and dn-OPDA/dn-*iso*-OPDA is the absence of an α,β-unsaturated carbonyl, that could have some deleterious effects through a COI1-independent pathway. The detection of trace amounts of the JA-Ile precursor JA and its lack of activity indicate that JA had not been co-opted yet for the synthesis of a functional hormone in liverworts, and that JA could be a catabolic product of dn-OPDA that might exist in the ancestral land plant. The appearance of the new hormone JA-Ile only required two enzymes, OPR3 and JAR1, from pre-extant functions. OPR3 facilitated the entrance of OPDA and dn-OPDA into the peroxisomal β-oxidation to enhance JA production and could evolve from existing cytoplasmic OPR genes (Supplementary Figure S1; Han, 2017; Li et al., 2009). More critically, JAR1-mediated conjugation of JA to Ile provided the polarity to the molecule required for spreading through the vasculature. JAR1 belongs to a family of GH3 enzymes with poor substrate specificity and mainly involved in auxin conjugation with amino acids (Staswick et al., 2005). JA-Ile is slightly bigger than dn-OPDA, but the change of a single amino acid in the ancestral COI1 easily allowed the accommodation of the newly evolved hormone. In summary, only three changes (one amino acid in COI1 and modification of two pre-existing enzymes) were sufficient for the evolution of a new hormone and the adaptation of its signalling pathway in vascular plants.

Dn-OPDA is currently considered just a precursor of the hormone from vascular plants, JA-Ile. Our results suggest that dn-OPDA may also have a hormonal role in vascular plants. However, the transformation of dn-OPDA into JA-Ile, the absence of dn-*iso*-OPDA in eudicots and the inability of dn-OPDA to induce AtCOI1/AtJAZ9 interaction suggest that this ligand might be active just in bryophytes. Certainly, it will be interesting to test if dn-OPDA could be the ligand of the co-receptor

formed by AtCOI1 and one of the other 12 AtJAZ and therefore could be regulating specific processes related to those AtJAZ and their interactors.

Despite the single amino acid in COI1 that determines ligand specificity, COI1 function is conserved in land plants and AtCOI1 can still perceive the active hormone from bryophytes. This conservation implies that AtCOI1 can form an active co-receptor with MpJAZ in *M. polymorpha*. Even when AtCOI1 is overexpressed under a strong constitutive promoter in *M. polymorpha*, the OPDA-induced growth inhibition is not as strong as in the wild-type. Additionally, both JA-Ile and COR strongly inhibit growth of these transgenic plants. This suggests that the affinity of AtCOI1 for the ancestral hormone is much lower than the affinity for their ligands JA-Ile and COR (Fonseca et al., 2009; Sheard et al., 2010). Although dn-OPDA/dn-*iso*-OPDA can still fit in the binding pocket of AtCOI1, they may not establish the same interactions as in MpCOI1.

The COI1/JAZ pathway regulates growth and defence in bryophytes as it does in vascular plants. Fertility is a developmental trait regulated by JAs in eudicots and also in *P. patens* (Stumpe et al., 2010; Wasternack and Hause, 2013). However, our results show that Mp*coi1* mutant plants do not exhibit altered fertility. Perhaps the regulation of fertility by JAs was acquired by mosses but was still absent in liverworts. Analyses of other members of the three bryophyte lineages will be required to clarify the involvement of JAs in fertility along evolution. The transcriptomic analyses of *M. polymorpha* in response to wounding and OPDA revealed that a high number of differentially expressed genes in both conditions depend on MpCOI1. Among them there are genes involved in defence, OPDA biosynthesis and secondary metabolism. In the promoters of these genes there is an over-representation of the G-box, the cis-element recognized and bound by AtMYC (Godoy et al., 2011), suggesting that the MYC DNA-binding sites are conserved in land plants. Since MYC TFs were already present in algae and were recruited for JAs signalling pathway during land plant colonization, it would be interesting to study if algal MYC can regulate a similar set of genes through binding to the G-box.

MpJAZ contains the two canonical domains ZIM and Jas that define the JAZ family (Vanholme et al., 2007). Additionally, MpJAZ seems to harbor a PPD-like domain in its N-terminus, suggesting that MpJAZ could have some PPD-related activities since *PPD* genes are not present in bryophytes. ZIM and Jas from MpJAZ mediate the same interactions as their counterparts from AtJAZ. MpJAZ forms homo- and hetero-dimers and binds to AtNINJA through the ZIM domain (Chini et al., 2009; Pauwels et al., 2010), whereas Jas is involved in the interaction with AtMYC in basal conditions and with AtCOI1 exclusively in the presence of JA-Ile or COR (Chini et al., 2007; Katsir et al., 2008). Accordingly, in Arabidopsis MpJAZ but not MpJAZΔJas is degraded through the 26S proteasome upon perception of the hormone.

However, in MpJAZ the lack of a CMID to bind MYC when the Jas domain is not present could explain why MpJAZΔJas does not act as a constitutive repressor of the pathway (Moreno et al., 2013).

Conversely, the different localization of MpJAZ and MpJAZΔJas suggests that the reduced nuclear localization of the truncated version could be due to the dimerization with MpJAZ, which probably interacts with MpMYC and is imported into the nucleus (Withers et al., 2012).

In addition to the conserved interactions, we have demonstrated that JAZ function is conserved in land plants, since At*JAZ3* could complement the Mp*jaz-1* mutant. In *A. thaliana*, there is redundancy among the 13 members of the JAZ family (Chini et al., 2016). A genetic approach to knock-out 13 genes is a laborious task but recently, a quintuple At*jaz* mutant has been obtained (Campos et al., 2016). Similar to Mp*jaz*, this mutant displays a constitutive activation of the pathway and reduced growth. Mp*jaz* shows an upregulation of MpCOI1-dependent genes and increased accumulation of OPDA, dn-OPDA and dn-*iso*-OPDA, consistent with the upregulation of OPDA biosynthetic genes. The upregulation of MpCOI1-independent genes in Mp*jaz* might be due to the accumulation of OPDA, since OPDA treatment can also induce the expression of MpCOI1-independent genes. The overall activation of the MpCOI1 pathway results in a maintained stressed situation for the plant that impacts in different pathways. For instance, Mp*jaz-1* shows an upregulation of chlorophyllase, a marker of JA-dependent senescence (Tsuchiya et al., 1999). Indeed, Mp*jaz-1* plants has a reduced growth rate and often generates dead tissue instead of growing into a fully-developed thallus with marked dichotomous branching (Shimamura, 2016). Mp*jaz-1* is severely affected in sexual and asexual reproduction. Both production of gemma cups and antheridiophores are scarce. While the few gemmae produced by Mp*jaz-1* are perfectly viable although show the typical reduced size of Mp*jaz-1*, the antheridiophores show aberrant antheridial receptacle and short stalks.

Both Mp*JAZ* and At*JAZ3* could effectively complement the Mp*jaz-1* mutant. The introduction of either gene in the mutant background resulted in WT-like plants, although the effect of the overexpression of MpJAZ under a strong constitutive promoter rendered the plants more resistant to OPDA than the WT. In turn, mutant plants overexpressing At*JAZ3* were fully OPDA-insensitive. This is probably because AtJAZ3 could repress the MYC orthologues in *M. polymorpha* but failed to form an active co-receptor with MpCOI1, acting as a constitutive repressor that cannot be degraded in a hormone-dependent manner.

The use of *M. polymorpha* as a model plant has proven to be an excellent opportunity to characterize a signalling pathway with a minimal set of components. The discovery of a new hormone activating this pathway has been the result of a collaborative approach with experts in chemical synthesis and oxylipins measurements. Now that we have identified that the signalling module in *M. polymorpha* works similarly to that of eudicots we will continue the characterization of the other conserved components (MYCs, NINJA) and more importantly, we will exploit the unique features of *M. polymorpha* to uncover new regulatory mechanisms and downstream players involved in this pathway.

Rational design of a ligand-based antagonist of jasmonate perception

The identification of antagonists by chemical biology approaches is of great interest to manipulate pathways in particular tissues, developmental stages or in species where mutants are not available (Fonseca et al., 2014b). However, in most cases, the compounds identified show undesired off-target effects, leading to toxicity that compromises the application of these chemicals on crops (Lamberth et al., 2013). Structural data of receptor-ligand interactions allow a ligand-based rational design, a strategy widely used in the biomedical field, whose application to agrochemical design lags behind (Lamberth et al., 2013; Marcos et al., 2008). The rational design of antagonist molecules based on receptor ligands allows improvement of their properties in terms of specificity, reduced toxicity, greater stability or modulation of the spectrum of action compared to non-ligands (Lamberth et al., 2013; Marcos et al., 2008).

On the basis of previous structural studies of the AtCOI1-ligand-AtJAZ degron complex (Sheard et al., 2010), we hypothesized that stable modifications of the keto group of the ligand would still allow its binding to AtCOI1 but would prevent binding of the AtJAZ degron peptide, thus blocking AtCOI1 function. Our results show that one of the designed antagonists (COR-MO) inhibits all of the tested AtCOI1-mediated responses to JA-Ile (or COR) from the molecular to the whole-plant level. Thus, we demonstrated that COR-MO competes with the hormone (or its mimic COR) for the formation of the co-receptor complexes, although demonstration of direct binding of COR-MO to the hormone binding pocket of the co-receptor awaits further testing. COR-MO prevented the degradation of the JAZ repressor and therefore blocked responses to the hormone. Remarkably, this inhibition occurred at very low ratios of the antagonist versus agonist concentrations (IC_{50} 0.4 µM and 0.8 µM of COR-MO for concentrations of COR 0.5 µM and 1 µM, respectively), underscoring the efficiency and strength of this molecule, which constitutes a powerful tool to manipulate the JA pathway. Indeed, COR-MO has been used to study COI1-dependent processes in the Venus flytrap *Dionaea muscipula*, where JA pathway is involved in the trap closure and secretion of enzymes for prey digestion in the green stomach (Böhm et al., 2016).

The toxicity of current pesticides potentially poses serious threats to human health and the environment. As a consequence, there is an increasing demand for safer agrochemicals that can support a sustainable agriculture (Enserink et al., 2013; Lamberth et al., 2013). In addition to its use in plant biology research, we envision the agronomical application of COR-MO to potentiate crop defences against biotrophic and hemibiotrophic pathogens. In a simplified view, jasmonates are key hormones regulating plant defences against necrotrophs, whereas the SA pathway orchestrates defences against biotrophs (Gimenez-Ibanez and Solano, 2013; Robert-Seilaniantz et al., 2011). The antagonism between these two pathways is well documented and, thus, activation of the JA pathway reduces resistance to biotrophic pathogens and *vice versa* (Gimenez-Ibanez and Solano, 2013; Robert-Seilaniantz et al., 2011; Xin and He, 2013). Indeed, COR is a paradigmatic example of how

evolution has provided *P. syringae* strains with the ability to manipulate the host hormonal network to enhance susceptibility (Bender et al., 1999; Gimenez-Ibanez et al., 2014, 2016b; Jiang et al., 2013; Uppalapati et al., 2007). We found that inhibition of the JA pathway by COR-MO counteracts this strategy of *P. syringae* and enhances resistance to biotrophic pathogens.

So far, efforts to develop plants with broad-spectrum resistance by genetic manipulation of defence pathway genes have had limited success owing to the antagonism between defence pathways (Boyd et al., 2013; Gimenez-Ibanez and Solano, 2013; Robert-Seilaniantz et al., 2011). Besides, public resistance to the production of genetically modified plants is still an important factor to consider. This could be a drawback for the application of the point mutation of AtCOI1 A384V that uncoupled JA-Ile and COR perception by the AtCOI1/AtJAZ co-receptor (Zhang et al., 2015b). The modification of the plant receptor generated plants that could still perceived JA-Ile but were insensitive to COR and therefore impaired in *P. syringae*-dependent activation of the JA pathway. The use of agrochemicals instead of genetic strategies to improve plant resistance has the advantage that chemical treatments can be tissue specific and transient (tissue controlled and time controlled), therefore reducing the tissue and time windows of weakness and exposure to opportunistic pathogens. For instance, JA-insensitive plants become susceptible to soil-borne microorganisms, which in many cases are not even pathogenic for WT plants (Adie et al., 2007; Staswick et al., 1998; Vijayan et al., 1998). Therefore, the use of JA-insensitive plants to enhance resistance to foliar pathogens such as *P. syringae* would face the threat of susceptibility to soil-borne pathogens. However, this problem could be overcome by the use of specific JA pathway antagonists (*i.e.* COR-MO or jarin-1; Meesters et al., 2014) on crop leaves, which should not affect the JA sensitivity of the roots, at least in transient applications. Moreover, a small molecule can be easily applied and taken in by the plant. Of course, this potential use needs to be tested.

COR-MO is a much more efficient antagonist than JA-Ile-MO, probably because the JA-Ile-MO used was based on the (–)-JA-Ile isomer rather than the bioactive (+)-7-*iso*-JA-Ile. This is also in line with studies of auxin antagonists and consistent with the higher affinity of COR than JA-Ile for AtCOI1 binding (Fonseca et al., 2009; Hayashi et al., 2008, 2012; Sheard et al., 2010). In the case of auxin, the AtTIR1-IAA complex is stabilized by its interaction with the AtAUX/IAA degron peptide (Tan et al., 2007). IAA derivatives (for example, BH-IAA) that prevent the interaction of AtTIR1 ligand with the AtAUX/IAA peptide are unable to stabilize the receptor complex and have a lower overall affinity for AtTIR1, therefore behaving as weak antagonists (Hayashi et al., 2008). However, modifications of the IAA moiety that increase the affinity for AtTIR1, resulting in molecules such as auxinole, markedly enhance the antagonistic activity of the derivative (Hayashi et al., 2012). Similar to AtTIR1-auxin-AtAUX/IAA, the AtCOI1-JA-Ile complex is stabilized by binding to the AtJAZ degron peptide, and the cyclopentanone ring shared by COR and JA-Ile establish similar interactions with Phe89 and Tyr444 of AtCOI1 (Sheard et al., 2010; Tan et al., 2007). However, the cyclohexene ring of COR provides a

stronger interaction surface than the corresponding pentenyl side chain of JA-Ile, explaining the higher affinity of COR than JA-Ile for AtCOI1 (Sheard et al., 2010). This higher affinity also explains why COR-MO is a more efficient antagonist of the hormone than JA-Ile-MO.

COR-MO is to our knowledge the first compound of a new type of small-molecule inhibitors of AtCOI1 receptor-ligand interactions, but it is not the only JA pathway antagonist, since jarin-1 is a small molecule developed to antagonize AtJAR1 (Meesters et al., 2014). The use of higher alkyloximes as well as aryloximes of COR is a further possibility for designing new antagonists. However, a large alkyl or a phenyl group might disturb receptor binding, reducing their effectiveness as inhibitors, and this was the reason for choosing the methyloxime. Alternatively, modifications of the COR moiety that increase binding to AtCOI1 should also increase its antagonistic activity, similarly to the case of auxinole (Hayashi et al., 2012). In summary, we have developed a powerful and specific dissection tool for JA biology with important biotechnological and agronomical potential.

Conclusions

- The COI1/JAZ signalling pathway is conserved in land plants although the hormone from bryophytes, dn-*cis*-OPDA/dn-*iso*-OPDA, is different from that of vascular plants, JA-Ile

- One single amino acid in COI1 determines hormone specificity

- JA-Ile and COI1 emergence in vascular plants from their ancestral counterparts required co-evolution of hormone biosynthetic complexity and receptor specificity

- COR-MO is a potent and specific antagonist that prevents the interaction between COI1 and their ligands JA-Ile or COR

- La ruta de señalización de COI1/JAZ está conservada en plantas terrestres, aunque la hormona de briófitos, dn-*cis*-OPDA/dn-*iso*-OPDA, es diferente de la de plantas vasculares, JA-Ile

- Un único aminoácido en COI1 determina la especificidad de hormona

- La aparición del JA-Ile y de COI1 en plantas vasculares a partir de sus ortólogos ancestrales requirió la coevolución de la complejidad de la biosíntesis hormonal y de la especificidad del receptor.

- COR-MO es un antagonista específico y potente que previene la interacción entre COI1 y sus ligandos, JA-Ile o COR.

References

Adie, B.A.T., Pérez-Pérez, J., Pérez-Pérez, M.M., Godoy, M., Sánchez-Serrano, J.-J., Schmelz, E.A., and Solano, R. (2007). ABA is an essential signal for plant resistance to pathogens affecting JA biosynthesis and the activation of defenses in Arabidopsis. Plant Cell **19**: 1665–81.

Aldridge, D.C., Galt, S., Giles, D., and Turner, W.B. (1971). Metabolites of *Lasiodiplodia theobromae*. J. Chem. Soc. C Org.: 1623.

Asamitsu, Y., Nakamura, Y., Ueda, M., Kuwahara, S., and Kiyota, H. (2006). Synthesis and odor description of both enantiomers of methyl 4,5-didehydrojasmonate, a component of jasmin absolute. Chem. Biodivers. **3**: 654–659.

Bai, Y., Meng, Y., Huang, D., Qi, Y., and Chen, M. (2011). Origin and evolutionary analysis of the plant-specific TIFY transcription factor family. Genomics **98**: 128–136.

Bender, C.L., Alarcón-Chaidez, F., and Gross, D.C. (1999). *Pseudomonas syringae* phytotoxins: mode of action, regulation, and biosynthesis by peptide and polyketide synthetases. Microbiol. Mol. Biol. Rev. **63**: 266–92.

Böhm, J. et al. (2016). The Venus flytrap *Dionaea muscipula* counts prey-induced action potentials to induce sodium uptake. Curr. Biol. **26**: 286–295.

Boter, M., Golz, J.F., Giménez-Ibañez, S., Fernandez-Barbero, G., Franco-Zorrilla, J.M., and Solano, R. (2015). FILAMENTOUS FLOWER is a direct target of JAZ3 and modulates responses to Jasmonate. Plant Cell **27**: 3160–3174.

Boter, M., Ruíz-Rivero, O., Abdeen, A., and Prat, S. (2004). Conserved MYC transcription factors play a key role in jasmonate signaling both in tomato and Arabidopsis. Genes Dev. **18**: 1577–91.

Bowman, J.L. (2016). A brief history of Marchantia from Greece to genomics. Plant Cell Physiol. **57**: 210–229.

Bowman, J.L., Floyd, S.K., and Sakakibara, K. (2007). Green Genes-Comparative Genomics of the Green Branch of Life. Cell **129**: 229–234.

Bowman, J.L. et al. (2017). Insights into land plant evolution garnered from the *Marchantia polymorpha* genome. Cell (under revision).

Boyd, L.A., Ridout, C., O'Sullivan, D.M., Leach, J.E., and Leung, H. (2013). Plant–pathogen interactions: disease resistance in modern agriculture. Trends Genet. **29**: 233–240.

Brodhun, F., Cristobal-Sarramian, A., Zabel, S., Newie, J., Hamberg, M., and Feussner, I. (2013). An iron 13S-Lipoxygenase with an α-Linolenic Acid specific Hydroperoxidase activity from *Fusarium oxysporum*. PLoS One **8**: e64919.

Broekaert, W.F., Delauré, S.L., De Bolle, M.F.C., and Cammue, B.P.A. (2006). The role of Ethylene in host-pathogen interactions. Annu. Rev. Phytopathol. **44**: 393–416.

Brooks, D.M., Hernández-Guzmán, G., Kloek, A.P., Alarcón-Chaidez, F., Sreedharan, A., Rangaswamy, V., Peñaloza-Vázquez, A., Bender, C.L., and Kunkel, B.N. (2004). Identification and characterization of a well-defined series of Coronatine biosynthetic mutants of *Pseudomonas syringae* pv. *tomato* DC3000. Mol. Plant-Microbe Interact. **17**: 162–174.

Browse, J. and Howe, G.A. (2008). New weapons and a rapid response against insect attack. Plant Physiol. **146**: 832–8.

Caillaud, M.-C., Asai, S., Rallapalli, G., Piquerez, S., Fabro, G., and Jones, J.D.G. (2013). A downy mildew effector attenuates Salicylic Acid–triggered immunity in Arabidopsis by interacting with the host mediator complex. PLoS Biol. **11**: e1001732.

Campos, M.L., Yoshida, Y., Major, I.T., de Oliveira Ferreira, D., Weraduwage, S.M., Froehlich, J.E., Johnson, B.F., Kramer, D.M., Jander, G., Sharkey, T.D., and Howe, G.A. (2016). Rewiring of jasmonate and phytochrome B signalling uncouples plant growth-defense tradeoffs. Nat. Commun. **7**: 12570.

Causier, B., Ashworth, M., Guo, W., and Davies, B. (2012). The TOPLESS interactome: a framework for gene repression in Arabidopsis. Plant Physiol. **158**: 423–38.

Chang, C., Bowman, J.L., and Meyerowitz, E.M. (2016). Field guide to plant model systems. Cell **167**: 325–339.

Chapuis, C., Büchi, G.H., and Wüest, H. (2005). Synthesis of cis-Hedione® and Methyl Jasmonate via cascade Baylis-Hillman reaction and Claisen ortho ester rearrangement. Helv. Chim. Acta **88**: 3069–3088.

Cheng, Z., Sun, L., Qi, T., Zhang, B., Peng, W., Liu, Y., and Xie, D. (2011). The bHLH transcription factor MYC3 interacts with the Jasmonate ZIM-domain proteins to mediate Jasmonate response in Arabidopsis. Mol. Plant **4**: 279–288.

Chico, J.-M., Fernandez-Barbero, G., Chini, A., Fernandez-Calvo, P., Diez-Diaz, M., and Solano, R. (2014). Repression of Jasmonate-dependent defenses by shade involves differential regulation of protein stability of MYC transcription factors and their JAZ repressors in Arabidopsis. Plant Cell **26**: 1967–1980.

Chico, J.M., Chini, A., Fonseca, S., and Solano, R. (2008). JAZ repressors set the rhythm in jasmonate signaling. Curr. Opin. Plant Biol. **11**: 486–494.

Chini, A., Fonseca, S., Chico, J.M., Fernández-Calvo, P., and Solano, R. (2009). The ZIM domain mediates homo- and heteromeric interactions between Arabidopsis JAZ proteins. Plant J. **59**: 77–87.

References

Chini, A., Fonseca, S., Fernández, G., Adie, B., Chico, J.M., Lorenzo, O., García-Casado, G., López-Vidriero, I., Lozano, F.M., Ponce, M.R., Micol, J.L., and Solano, R. (2007). The JAZ family of repressors is the missing link in jasmonate signalling. Nature **448**: 666–671.

Chini, A., Gimenez-Ibanez, S., Goossens, A., and Solano, R. (2016). Redundancy and specificity in jasmonate signalling. Curr. Opin. Plant Biol. **33**: 147–156.

Chiyoda, S., Ishizaki, K., Kataoka, H., Yamato, K.T., and Kohchi, T. (2008). Direct transformation of the liverwort *Marchantia polymorpha* L. by particle bombardment using immature thalli developing from spores. Plant Cell Rep. **27**: 1467–1473.

Chung, H.S., Cooke, T.F., Depew, C.L., Patel, L.C., Ogawa, N., Kobayashi, Y., and Howe, G.A. (2010). Alternative splicing expands the repertoire of dominant JAZ repressors of jasmonate signaling. Plant J. **63**: 613–622.

Chung, H.S. and Howe, G.A. (2009). A critical role for the TIFY motif in repression of jasmonate signaling by a stabilized splice variant of the JASMONATE ZIM-domain protein JAZ10 in Arabidopsis. Plant Cell **21**: 131–45.

Chung, H.S., Niu, Y., Browse, J., and Howe, G.A. (2009). Top hits in contemporary JAZ: An update on jasmonate signaling. Phytochemistry **70**: 1547–1559.

Clough, S.J. and Bent, A.F. (1998). Floral dip: a simplified method for *Agrobacterium*-mediated transformation of *Arabidopsis thaliana*. Plant J. **16**: 735–743.

Cole, S.J., Yoon, A.J., Faull, K.F., and Diener, A.C. (2014). Host perception of jasmonates promotes infection by *Fusarium oxysporum* formae speciales that produce isoleucine- and leucine-conjugated jasmonates. Mol. Plant Pathol. **15**: 589–600.

Cuéllar, A.P., Pauwels, L., De Clercq, R., and Goossens, A. (2013). Yeast Two-Hybrid analysis of Jasmonate signaling proteins. In Jasmonate Signaling: Methods and Protocols, A. Goossens and L. Pauwels, eds, Methods in Molecular Biology. (Humana Press: Totowa, NJ), pp. 173–185.

Dabrowska, P. and Boland, W. (2007). iso-OPDA: An early precursor of cis-Jasmone in plants? ChemBioChem **8**: 2281–2285.

Dabrowska, P., Freitak, D., Vogel, H., Heckel, D.G., and Boland, W. (2009). The phytohormone precursor OPDA is isomerized in the insect gut by a single, specific glutathione transferase. Proc. Natl. Acad. Sci. U. S. A. **106**: 16304–16309.

Dang, H.T., Lee, Y.M., Kang, G.J., Yoo, E.S., Hong, J., Lee, S.M., Lee, S.K., Pyee, Y., Chung, H.-J., Moon, H.R., Kim, H.S., and Jung, J.H. (2012). In vitro stability and in vivo anti-inflammatory efficacy of synthetic jasmonates. Bioorg. Med. Chem. **20**: 4109–16.

Dathe, W., Miersch, O., and Schmidt, J. (1989). Occurrence of Jasmonic Acid, related compounds and Abscisic Acid in fertile and sterile fronds of three Equisetum species. Biochem. und Physiol. der Pflanz. **185**: 83–92.

Dathe, W., Rönsch, H., Preiss, A., Schade, W., Sembdner, G., and Schreiber, K. (1981). Endogenous plant hormones of the broad bean, *Vicia faba* L. (-)-jasmonic acid, a plant growth inhibitor in pericarp. Planta **153**: 530–5.

Demianski, A.J., Chung, K.M., and Kunkel, B.N. (2012). Analysis of Arabidopsis JAZ gene expression during *Pseudomonas syringae* pathogenesis. Mol. Plant Pathol. **13**: 46–57.

Demole, E., Lederer, E., and Mercier, D. (1962). Isolement et détermination de la structure du jasmonate de méthyle, constituant odorant caractéristique de l'essence de jasmin. Helv. Chim. Acta **45**: 675–685.

Dombrecht, B., Xue, G.P., Sprague, S.J., Kirkegaard, J.A., Ross, J.J., Reid, J.B., Fitt, G.P., Sewelam, N., Schenk, P.M., Manners, J.M., and Kazan, K. (2007). MYC2 differentially modulates diverse jasmonate-dependent functions in Arabidopsis. Plant Cell **19**: 2225–45.

Enserink, M., Hines, P.J., Vignieri, S.N., Wigginton, N.S., and Yeston, J.S. (2013). The pesticide paradox. Science **341**: 728–729.

Fan, X., Mattheis, J.P., and Fellman, J.K. (1998). A role for jasmonates in climacteric fruit ripening. Planta **204**: 444–449.

Farmer, E.E. (2014). Leaf defence (Oxford University Press: Oxford).

Farmer, E.E., Alméras, E., and Krishnamurthy, V. (2003). Jasmonates and related oxylipins in plant responses to pathogenesis and herbivory. Curr. Opin. Plant Biol. **6**: 372–8.

Farmer, E.E. and Mueller, M.J. (2013). ROS-Mediated Lipid Peroxidation and RES-Activated Signaling. Annu. Rev. Plant Biol. **64**: 429–450.

Farmer, E.E. and Ryan, C.A. (1990). Interplant communication: airborne methyl jasmonate induces synthesis of proteinase inhibitors in plant leaves. Proc. Natl. Acad. Sci. U. S. A. **87**: 7713–6.

Fernández-Calvo, P. et al. (2011). The Arabidopsis bHLH transcription factors MYC3 and MYC4 are targets of JAZ repressors and act additively with MYC2 in the activation of jasmonate responses. Plant Cell **23**: 701–715.

Feys, B., Benedetti, C.E., Penfold, C.N., and Turner, J.G. (1994). Arabidopsis mutants selected for resistance to the phytotoxin Coronatine are male sterile, insensitive to Methyl Jasmonate, and resistant to a bacterial pathogen. Plant Cell **6**: 751–759.

Figueroa, P. and Browse, J. (2015). Male sterility in Arabidopsis induced by overexpression of a MYC5-SRDX chimeric repressor. Plant J. **81**: 849–860.

Floková, K., Feussner, K., Herrfurth, C., Miersch, O., Mik, V., Tarkowská, D., Strnad, M., Feussner, I., Wasternack, C., and Novák, O. (2016). A previously undescribed jasmonate compound in flowering *Arabidopsis thaliana* – The identification of cis-(+)-OPDA-Ile. Phytochemistry **122**: 230–237.

Flores-Sandoval, E., Eklund, D.M., and Bowman, J.L. (2015). A simple auxin transcriptional response system regulates multiple morphogenetic processes in the liverwort *Marchantia polymorpha*. PLoS Genet. **11**: e1005207.

Fonseca, S., Chini, A., Hamberg, M., Adie, B., Porzel, A., Kramell, R., Miersch, O., Wasternack, C., and Solano, R. (2009). (+)-7-iso-Jasmonoyl-L-isoleucine is the endogenous bioactive jasmonate. Nat. Chem. Biol. **5**: 344–350.

Fonseca, S., Fernández-Calvo, P., Fernández, G.M., Díez-Díaz, M., Gimenez-Ibanez, S., López-Vidriero, I., Godoy, M., Fernández-Barbero, G., Van Leene, J., De Jaeger, G., Franco-Zorrilla, J.M., and Solano, R. (2014a). bHLH003, bHLH013 and bHLH017 are new targets of JAZ repressors negatively regulating JA responses. PLoS One **9**: 1–12.

Fonseca, S., Rosado, A., Vaughan-Hirsch, J., Bishopp, A., and Chini, A. (2014b). Molecular locks and keys: the role of small molecules in phytohormone research. Front. Plant Sci. **5**: 709.

Fonseca, S. and Solano, R. (2013). Pull-Down analysis of interactions among Jasmonic Acid core signaling proteins. In Jasmonate Signaling: Methods and Protocols, A. Goossens and L. Pauwels, eds, Methods in Molecular Biology. (Humana Press: Totowa, NJ), pp. 159–171.

Frerigmann, H., Berger, B., and Gigolashvili, T. (2014). bHLH05 is an interaction partner of MYB51 and a novel regulator of glucosinolate biosynthesis in Arabidopsis. Plant Physiol. **166**: 349–369.

Gimenez-Ibanez, S., Boter, M., Fernández-Barbero, G., Chini, A., Rathjen, J.P., and Solano, R. (2014). The bacterial effector HopX1 targets JAZ transcriptional repressors to activate Jasmonate signaling and promote infection in Arabidopsis. PLoS Biol. **12**: e1001792.

Gimenez-Ibanez, S., Boter, M., Ortigosa, A., García-Casado, G., Chini, A., Lewsey, M.G., Ecker, J.R., Ntoukakis, V., and Solano, R. (2017). JAZ2 controls stomata dynamics during bacterial invasion. New Phytol. **213**: 1378–1392.

Gimenez-Ibanez, S., Chini, A., and Solano, R. (2016). How microbes twist Jasmonate signaling around their little fingers. Plants **5**: 9.

Gimenez-Ibanez, S. and Solano, R. (2013). Nuclear jasmonate and salicylate signaling and crosstalk in defense against pathogens. Front. Plant Sci. **4**: 72.

Glazebrook, J. (2005). Contrasting mechanisms of defense against biotrophic and necrotrophic pathogens. Annu. Rev. Phytopathol. **43**: 205–227.

Göbel, C. and Feussner, I. (2009). Methods for the analysis of oxylipins in plants. Phytochemistry **70**: 1485–1503.

Godoy, M., Franco-Zorrilla, J.M., Pérez-Pérez, J., Oliveros, J.C., Lorenzo, Ó., and Solano, R. (2011). Improved protein-binding microarrays for the identification of DNA-binding specificities of transcription factors. Plant J. **66**: 700–711.

Guo, C.Q., Edwards, D., Wu, P.C., Duckett, J.G., Hueber, F.M., and Li, C. Sen (2012). *Riccardiothallus devonicus* gen. et sp. nov., the earliest simple thalloid liverwort from the Lower Devonian of Yunnan, China. Rev. Palaeobot. Palynol. **176–177**: 35–40.

Hamberg, M. (1998). Stereochemistry of oxygenation of linoleic acid catalyzed by prostaglandin-endoperoxide H synthase-2. Arch. Biochem. Biophys. **349**: 376–80.

Hamberg, M. and Fahlstadius, P. (1990). Allene oxide cyclase: a new enzyme in plant lipid metabolism. Arch. Biochem. Biophys. **276**: 518–26.

Hamberg, M. and Gardner, H.W. (1992). Oxylipin pathway to jasmonates: Biochemistry and biological significance. Biochim. Biophys. Acta - Lipids Lipid Metab. **1165**: 1–18.

Han, G. (2017). Evolution of jasmonate biosynthesis and signaling mechanisms. J. Exp. Bot. **68**: 1323–1331.

Hao, B.-Z. and Wu, J.-L. (2000). Laticifer differentiation in *Hevea brasiliensis*: induction by exogenous Jasmonic Acid and Linolenic Acid. Ann. Bot. **85**: 37–43.

Harholt, J., Moestrup, Ø., and Ulvskov, P. (2016). Why plants were terrestrial from the beginning. Trends Plant Sci. **21**: 96–101.

Hayashi, K.-I., Tan, X., Zheng, N., Hatate, T., Kimura, Y., Kepinski, S., and Nozaki, H. (2008). Small-molecule agonists and antagonists of F-box protein-substrate interactions in auxin perception and signaling. Proc. Natl. Acad. Sci. U. S. A. **105**: 5632–7.

References

Hayashi, K., Neve, J., Hirose, M., Kuboki, A., Shimada, Y., Kepinski, S., and Nozaki, H. (2012). Rational design of an auxin antagonist of the SCF TIR1 auxin receptor complex. ACS Chem. Biol. **7**: 590–598.

Heil, M., Koch, T., Hilpert, A., Fiala, B., Boland, W., and Linsenmair, K. (2001). Extrafloral nectar production of the ant-associated plant, *Macaranga tanarius*, is an induced, indirect, defensive response elicited by jasmonic acid. Proc. Natl. Acad. Sci. U. S. A. **98**: 1083–8.

Heitz, T., Widemann, E., Lugan, R., Miesch, L., Ullmann, P., Desaubry, L., Holder, E., Grausem, B., Kandel, S., Miesch, M., Werck-Reichhart, D., and Pinot, F. (2012). Cytochromes P450 CYP94C1 and CYP94B3 catalyze two successive oxidation steps of plant hormone Jasmonoyl-isoleucine for catabolic turnover. J. Biol. Chem. **287**: 6296–6306.

Higo, A. et al. (2016). Transcriptional framework of male gametogenesis in the liverwort *Marchantia polymorpha* L. Plant Cell Physiol. **57**: 325–338.

Hong, F., Breitling, R., McEntee, C.W., Wittner, B.S., Nemhauser, J.L., and Chory, J. (2006). RankProd: a bioconductor package for detecting differentially expressed genes in meta-analysis. Bioinformatics **22**: 2825–7.

Hou, X., Lee, L.Y.C., Xia, K., Yan, Y., and Yu, H. (2010). DELLAs modulate Jasmonate signaling via competitive binding to JAZs. Dev. Cell **19**: 884–894.

Howe, G.A. and Jander, G. (2008). Plant Immunity to Insect Herbivores. Annu. Rev. Plant Biol. **59**: 41–66.

Howe, G.A., Lightner, J., Browse, J., and Ryan, C.A. (1996). An octadecanoid pathway mutant (JL5) of tomato is compromised in signaling for defense against insect attack. Plant Cell **8**: 2067–77.

Hu, Y., Jiang, L., Wang, F., and Yu, D. (2013). Jasmonate regulates the inducer of cbf expression-C-repeat binding factor/DRE binding factor1 cascade and freezing tolerance in Arabidopsis. Plant Cell **25**: 2907–24.

Hulsen, T., de Vlieg, J., and Alkema, W. (2008). BioVenn - a web application for the comparison and visualization of biological lists using area-proportional Venn diagrams. BMC Genomics **9**: 488.

Ichikawa, T., Yamada, K., Namikawa, M., Sakai, K., and Kondo, K. (1984). New cyclopentenonyl fatty acids from Japanese mosses. J. Hattori Bot. Lab. **56**: 209–213.

Inoue, K., Nishihama, R., Kataoka, H., Hosaka, M., Manabe, R., Nomoto, M., Tada, Y., Ishizaki, K., and Kohchi, T. (2016). Phytochrome signaling Is mediated by PHYTOCHROME INTERACTING FACTOR in the liverwort *Marchantia polymorpha*. Plant Cell **28**: 1406–1421.

Ishizaki, K., Chiyoda, S., Yamato, K.T., and Kohchi, T. (2008). *Agrobacterium*-mediated transformation of the haploid liverwort *Marchantia polymorpha* L., an emerging model for plant biology. Plant Cell Physiol. **49**: 1084–1091.

Ishizaki, K., Johzuka-Hisatomi, Y., Ishida, S., Iida, S., and Kohchi, T. (2013). Homologous recombination-mediated gene targeting in the liverwort *Marchantia polymorpha* L. Sci. Rep. **3**: 1532.

Ishizaki, K., Nishihama, R., Ueda, M., Inoue, K., Ishida, S., Nishimura, Y., Shikanai, T., and Kohchi, T. (2015). Development of gateway binary vector series with four different selection markers for the liverwort *Marchantia polymorpha*. PLoS One **10**: 1–13.

Jiang, S., Yao, J., Ma, K.-W., Zhou, H., Song, J., He, S.Y., and Ma, W. (2013). Bacterial Effector Activates Jasmonate Signaling by Directly Targeting JAZ Transcriptional Repressors. PLoS Pathog. **9**: e1003715.

Kagale, S., Links, M.G., and Rozwadowski, K. (2010). Genome-wide analysis of ethylene-responsive element binding factor-associated amphiphilic repression motif-containing transcriptional regulators in Arabidopsis. Plant Physiol. **152**: 1109–34.

Kaiser, R. and Lamparsky, D. (1974). New cyclopentanoid constituents from jasmine absolute. Tetrahedron Lett. **15**: 3413–3416.

Kajikawa, M., Yamato, K.T., Kanamaru, H., Sakuradani, E., Shimizu, S., Fukuzawa, H., Sakai, Y., and Ohyama, K. (2003). MpFAE3, a beta-ketoacyl-CoA synthase gene in the liverwort *Marchantia polymorpha* L., is preferentially involved in elongation of palmitic acid to stearic acid. Biosci. Biotechnol. Biochem. **67**: 1667–74.

Kato, H., Ishizaki, K., Kouno, M., Shirakawa, M., Bowman, J.L., Nishihama, R., and Kohchi, T. (2015). Auxin-mediated transcriptional system with a minimal set of components is critical for morphogenesis through the life cycle in *Marchantia polymorpha*. PLoS Genet. **11**: e1005084.

Katsir, L., Schilmiller, A.L., Staswick, P.E., He, S.Y., and Howe, G.A. (2008). COI1 is a critical component of a receptor for jasmonate and the bacterial virulence factor coronatine. Proc. Natl. Acad. Sci. U. S. A. **105**: 7100–7105.

Kienow, L., Schneider, K., Bartsch, M., Stuible, H.-P., Weng, H., Miersch, O., Wasternack, C., and Kombrink, E. (2008). Jasmonates meet fatty acids: functional analysis of a new acyl-coenzyme A synthetase family from *Arabidopsis thaliana*. J. Exp. Bot. **59**: 403–419.

Kiyota, H., Yoneta, Y., and Oritani, T. (1997). Synthesis and biological activities of methyl 3,7- and 4,5-didehydrojasmonates. Phytochemistry **46**: 983–986.

Kloek, A.P., Verbsky, M.L., Sharma, S.B., Schoelz, J.E., Vogel, J., Klessig, D.F., and Kunkel, B.N. (2001). Resistance to *Pseudomonas syringae* conferred by an *Arabidopsis thaliana* coronatine-insensitive (coi1) mutation occurs through two distinct mechanisms. Plant J. **26**: 509–522.

Koch, T., Bandemer, K., and Boland, W. (1997). Biosynthesis of cis-jasmone: a pathway for the inactivation and the disposal of the plant stress hormone jasmonic acid to the gas phase? Helv. Chim. Acta **80**: 838–850.

Koeduka, T., Ishizaki, K., Mwenda, C.M., Hori, K., Sasaki-Sekimoto, Y., Ohta, H., Kohchi, T., and Matsui, K. (2015). Biochemical characterization of allene oxide synthases from the liverwort *Marchantia polymorpha* and green microalgae *Klebsormidium flaccidum* provides insight into the evolutionary divergence of the plant CYP74 family. Planta **242**: 1175–1186.

Koo, A.J.K., Cooke, T.F., and Howe, G. a (2011). Cytochrome P450 CYP94B3 mediates catabolism and inactivation of the plant hormone jasmonoyl-L-isoleucine. Proc. Natl. Acad. Sci. U. S. A. **108**: 9298–303.

Kramell, R., Miersch, O., Atzorn, R., Parthier, B., and Wasternack, C. (2000). Octadecanoid-derived alteration of gene expression and the "oxylipin signature" in stressed barley leaves. Implications for different signaling pathways. Plant Physiol. **123**: 177–188.

Kubota, A., Ishizaki, K., Hosaka, M., and Kohchi, T. (2013). Efficient *Agrobacterium*-mediated transformation of the liverwort *Marchantia polymorpha* using regenerating thalli. Biosci. Biotechnol. Biochem. **77**: 167–172.

Kubota, A., Kita, S., Ishizaki, K., Nishihama, R., Yamato, K.T., and Kohchi, T. (2014). Co-option of a photoperiodic growth-phase transition system during land plant evolution. Nat. Commun. **5**: 3668.

Lamberth, C., Jeanmart, S., Luksch, T., and Plant, A. (2013). Current challenges and trends in the discovery of agrochemicals. Science **341**: 742–746.

Laurie-Berry, N., Joardar, V., Street, I.H., and Kunkel, B.N. (2006). The *Arabidopsis thaliana* JASMONATE INSENSITIVE 1 gene is required for suppression of Salicylic Acid-dependent defenses during infection by *Pseudomonas syringae*. Mol. Plant-Microbe Interact. **19**: 789–800.

Lewis, L.A. and McCourt, R.M. (2004). Green algae and the origin of land plants. Am. J. Bot. **91**: 1535–1556.

Li, C., Schilmiller, A.L., Liu, G., Lee, G.I., Jayanty, S., Sageman, C., Vrebalov, J., Giovannoni, J.J., Yagi, K., Kobayashi, Y., and Howe, G.A. (2005). Role of beta-oxidation in jasmonate biosynthesis and systemic wound signaling in tomato. Plant Cell **17**: 971–86.

Li, L., Zhao, Y., McCaig, B.C., Wingerd, B.A., Wang, J., Whalon, M.E., Pichersky, E., and Howe, G.A. (2004). The tomato homolog of CORONATINE-INSENSITIVE1 is required for the maternal control of seed maturation, jasmonate-signaled defense responses, and glandular trichome development. Plant Cell **16**: 126–43.

Li, Q., Zheng, J., Li, S., Huang, G., Skilling, S.J., Wang, L., Li, L., Li, M., Yuan, L., and Liu, P. (2017). Transporter-mediated nuclear entry of Jasmonoyl-Isoleucine is essential for Jasmonate signaling. Mol. Plant **10**: 695–708.

Li, R. et al. (2014). Virulence factors of geminivirus interact with MYC2 to subvert plant resistance and promote vector performance. Plant Cell **26**: 4991–5008.

Li, W., Liu, B., Yu, L., Feng, D., Wang, H., and Wang, J. (2009). Phylogenetic analysis, structural evolution and functional divergence of the 12-oxo-phytodienoate acid reductase gene family in plants. BMC Evol. Biol. **9**: 90.

Lorenzo, O., Chico, J.M., Sánchez-Serrano, J.J., and Solano, R. (2004). JASMONATE-INSENSITIVE1 encodes a MYC transcription factor essential to discriminate between different jasmonate-regulated defense responses in Arabidopsis. Plant Cell **16**: 1938–50.

Ludwig-Müller, J., Jülke, S., Bierfreund, N.M., Decker, E.L., and Reski, R. (2009). Moss (*Physcomitrella patens*) GH3 proteins act in auxin homeostasis. New Phytol. **181**: 323–38.

Mafli, A., Goudet, J., and Farmer, E.E. (2012). Plants and tortoises: mutations in the Arabidopsis jasmonate pathway increase feeding in a vertebrate herbivore. Mol. Ecol. **21**: 2534–41.

Mandaokar, A., Thines, B., Shin, B., Markus Lange, B., Choi, G., Koo, Y.J., Yoo, Y.J., Choi, Y.D., Choi, G., and Browse, J. (2006). Transcriptional regulators of stamen development in Arabidopsis identified by transcriptional profiling. Plant J. **46**: 984–1008.

Maor, R., Jones, A., Nuhse, T.S., Studholme, D.J., Peck, S.C., and Shirasu, K. (2007). Multidimensional Protein Identification Technology (MudPIT) analysis of ubiquitinated proteins in plants. Mol. Cell. Proteomics **6**: 601–610.

Marcos, J.F., Muñoz, A., Pérez-Payá, E., Misra, S., and López-García, B. (2008). Identification and rational design of novel antimicrobial peptides for plant protection. Annu. Rev. Phytopathol. **46**: 273–301.

Matasci, N. et al. (2014). Data access for the 1,000 Plants (1KP) project. Gigascience **3**: 17.

Matthes, M.C., Bruce, T.J.A., Ton, J., Verrier, P.J., Pickett, J.A., and Napier, J.A. (2010). The transcriptome of cis-jasmone-induced resistance in *Arabidopsis thaliana* and its role in indirect defence. Planta **232**: 1163–1180.

References

Medina-Rivera, A. et al. (2015). RSAT 2015: Regulatory Sequence Analysis Tools. Nucleic Acids Res. **43**: W50–W56.

Meesters, C., Mönig, T., Oeljeklaus, J., Krahn, D., Westfall, C.S., Hause, B., Jez, J.M., Kaiser, M., and Kombrink, E. (2014). A chemical inhibitor of jasmonate signaling targets JAR1 in *Arabidopsis thaliana*. Nat. Chem. Biol. **10**: 830–836.

Melotto, M., Mecey, C., Niu, Y., Chung, H.S., Katsir, L., Yao, J., Zeng, W., Thines, B., Staswick, P., Browse, J., Howe, G.A., and He, S.Y. (2008). A critical role of two positively charged amino acids in the Jas motif of Arabidopsis JAZ proteins in mediating coronatine- and jasmonoyl isoleucine-dependent interactions with the COI1 F-box protein. Plant J. **55**: 979–988.

Melotto, M., Underwood, W., Koczan, J., Nomura, K., and He, S.Y. (2006). Plant stomata function in innate immunity against bacterial invasion. Cell **126**: 969–980.

Miersch, O., Bohlmann, H., and Wasternack, C. (1999). Jasmonates and related compounds from *Fusarium oxysporum*. Phytochemistry **50**: 517–523.

Miersch, O., Schmidt, J., Sembdner, G., and Schreiber, K. (1989). Jasmonic acid-like substances from the culture filtrate of *Botryodiplodia theobromae*. Phytochemistry **28**: 1303–1305.

Moreno, J.E., Shyu, C., Campos, M.L., Patel, L.C., Chung, H.S., Yao, J., He, S.Y., and Howe, G.A. (2013). Negative feedback control of Jasmonate signaling by an alternative splice variant of JAZ10. Plant Physiol. **162**: 1006–1017.

Nakamura, Y., Paetz, C., Brandt, W., David, A., Rendón-Anaya, M., Herrera-Estrella, A., Mithöfer, A., and Boland, W. (2014). Synthesis of 6-substituted 1-oxoindanoyl Isoleucine conjugates and modeling studies with the COI1-JAZ co-receptor complex of lima bean. J. Chem. Ecol. **40**: 687–699.

Nakata, M., Mitsuda, N., Herde, M., Koo, A.J.K., Moreno, J.E., Suzuki, K., Howe, G. A, and Ohme-Takagi, M. (2013). A bHLH-type transcription factor, ABA-INDUCIBLE BHLH-TYPE TRANSCRIPTION FACTOR/JA-ASSOCIATED MYC2-LIKE1, acts as a repressor to negatively regulate Jasmonate signaling in Arabidopsis. Plant Cell **25**: 1641–1656.

Niu, Y., Figueroa, P., and Browse, J. (2011). Characterization of JAZ-interacting bHLH transcription factors that regulate jasmonate responses in Arabidopsis. J. Exp. Bot. **62**: 2143–2154.

Ogorodnikova, A. V., Mukhitova, F.K., and Grechkin, A.N. (2015). Oxylipins in the spikemoss *Selaginella martensii*: Detection of divinyl ethers, 12-oxophytodienoic acid and related cyclopentenones. Phytochemistry **118**: 42–50.

El Oirdi, M., El Rahman, T.A., Rigano, L., El Hadrami, A., Rodriguez, M.C., Daayf, F., Vojnov, A., and Bouarab, K. (2011). *Botrytis cinerea* manipulates the antagonistic effects between immune pathways to promote disease development in tomato. Plant Cell **23**: 2405–2421.

Okada, M., Ito, S., Matsubara, A., Iwakura, I., Egoshi, S., and Ueda, M. (2009). Total syntheses of coronatines by exo-selective Diels–Alder reaction and their biological activities on stomatal opening. Org. Biomol. Chem. **7**: 3065.

Park, J.-H., Halitschke, R., Kim, H.B., Baldwin, I.T., Feldmann, K.A., and Feyereisen, R. (2002). A knock-out mutation in allene oxide synthase results in male sterility and defective wound signal transduction in Arabidopsis due to a block in jasmonic acid biosynthesis. Plant J. **31**: 1–12.

Patkar, R.N., Benke, P.I., Qu, Z., Constance Chen, Y.Y., Yang, F., Swarup, S., and Naqvi, N.I. (2015). A fungal monooxygenase-derived jasmonate attenuates host innate immunity. Nat. Chem. Biol. **11**: 733–740.

Pauwels, L. et al. (2010). NINJA connects the co-repressor TOPLESS to jasmonate signalling. Nature **464**: 788–91.

Pauwels, L. et al. (2015). The RING E3 ligase KEEP ON GOING modulates JASMONATE ZIM-DOMAIN12 stability. Plant Physiol. **169**: 1405–1417.

Pauwels, L., Morreel, K., De Witte, E., Lammertyn, F., Van Montagu, M., Boerjan, W., Inzé, D., and Goossens, A. (2008). Mapping methyl jasmonate-mediated transcriptional reprogramming of metabolism and cell cycle progression in cultured Arabidopsis cells. Proc. Natl. Acad. Sci. U. S. A. **105**: 1380–5.

Plett, J.M., Daguerre, Y., Wittulsky, S., Vayssieres, A., Deveau, A., Melton, S.J., Kohler, A., Morrell-Falvey, J.L., Brun, A., Veneault-Fourrey, C., and Martin, F. (2014). Effector MiSSP7 of the mutualistic fungus *Laccaria bicolor* stabilizes the Populus JAZ6 protein and represses jasmonic acid (JA) responsive genes. Proc. Natl. Acad. Sci. U. S. A. **111**: 8299–8304.

Ponce de León, I., Hamberg, M., and Castresana, C. (2015). Oxylipins in moss development and defense. Front. Plant Sci. **6**: 483.

Ponce De León, I., Schmelz, E.A., Gaggero, C., Castro, A., Álvarez, A., and Montesano, M. (2012). *Physcomitrella patens* activates reinforcement of the cell wall, programmed cell death and accumulation of evolutionary conserved defence signals, such as salicylic acid and 12-oxo-phytodienoic acid, but not jasmonic acid, upon *Botrytis cinerea* infection. Mol. Plant Pathol. **13**: 960–974.

Pratiwi, P., Tanaka, G., Takahashi, T., Xie, X., Yoneyama, K., Matsuura, H., and Takahashi, K. (2017). Identification of Jasmonic Acid and Jasmonoyl-Isoleucine, and characterization of AOS, AOC, OPR and JAR1 in the model lycophyte *Selaginella moellendorffii*. Plant Cell Physiol. **58**: 789–801.

Proust, H., Honkanen, S., Jones, V.A.S., Morieri, G., Prescott, H., Kelly, S., Ishizaki, K., Kohchi, T., and Dolan, L. (2016). RSL class I genes controlled the development of epidermal structures in the common ancestor of land plants. Curr. Biol. **26**: 93–99.

Provart, N.J. et al. (2016). 50 years of Arabidopsis research: highlights and future directions. New Phytol. **209**: 921–944.

Qi, T., Huang, H., Song, S., and Xie, D. (2015). Regulation of Jasmonate-mediated stamen development and seed production by a bHLH-MYB complex in Arabidopsis. Plant Cell **27**: 1620–1633.

Qi, T., Song, S., Ren, Q., Wu, D., Huang, H., Chen, Y., Fan, M., Peng, W., Ren, C., and Xie, D. (2011). The Jasmonate-ZIM-domain proteins interact with the WD-Repeat/bHLH/MYB complexes to regulate Jasmonate-mediated anthocyanin accumulation and trichome initiation in *Arabidopsis thaliana*. Plant Cell **23**: 1795–1814.

Quinlan, A.R. and Hall, I.M. (2010). BEDTools: a flexible suite of utilities for comparing genomic features. Bioinformatics **26**: 841–2.

Ran, F.A., Hsu, P.D., Lin, C.-Y., Gootenberg, J.S., Konermann, S., Trevino, A.E., Scott, D.A., Inoue, A., Matoba, S., Zhang, Y., and Zhang, F. (2013). Double nicking by RNA-guided CRISPR Cas9 for enhanced genome editing specificity. Cell **154**: 1380–9.

Reymond, P., Weber, H., Damond, M., and Farmer, E.E. (2000). Differential gene expression in response to mechanical wounding and insect feeding in Arabidopsis. Plant Cell **12**: 707–20.

Robert-Seilaniantz, A., Grant, M., and Jones, J.D.G. (2011). Hormone crosstalk in plant disease and defense: more than just JASMONATE-SALICYLATE antagonism. Annu. Rev. Phytopathol. **49**: 317–343.

Sabovljević, M., Vujičić, M., and Sabovljević, A. (2014). Plant growth regulators in bryophytes. Bot. Serbica **38**: 99–107.

Samuelsson, B. and Ställberg, G. (1963). Structure and synthesis of a derivative of Prostaglandin E1. Prostaglandins and related factors 16. Acta Chem. Scand. **17**: 810–816.

Saracco, S.A., Hansson, M., Scalf, M., Walker, J.M., Smith, L.M., and Vierstra, R.D. (2009). Tandem affinity purification and mass spectrometric analysis of ubiquitylated proteins in Arabidopsis. Plant J. **59**: 344–358.

Sasaki-Sekimoto, Y., Jikumaru, Y., Obayashi, T., Saito, H., Masuda, S., Kamiya, Y., Ohta, H., and Shirasu, K. (2013). Basic Helix-Loop-Helix transcription factors JASMONATE-ASSOCIATED MYC2-LIKE1 (JAM1), JAM2, and JAM3 are negative regulators of Jasmonate responses in Arabidopsis. Plant Physiol. **163**: 291–304.

Schaller, F., Biesgen, C., Müssig, C., Altmann, T., and Weiler, E.W. (2000). 12-Oxophytodienoate reductase 3 (OPR3) is the isoenzyme involved in jasmonate biosynthesis. Planta **210**: 979–984.

Scholz, J., Brodhun, F., Hornung, E., Herrfurth, C., Stumpe, M., Beike, A.K., Faltin, B., Frank, W., Reski, R., and Feussner, I. (2012). Biosynthesis of allene oxides in *Physcomitrella patens*. BMC Plant Biol **12**: 228.

Schweizer, F., Fernández-Calvo, P., Zander, M., Diez-Diaz, M., Fonseca, S., Glauser, G., Lewsey, M.G., Ecker, J.R., Solano, R., and Reymond, P. (2013). Arabidopsis basic helix-loop-helix transcription factors MYC2, MYC3, and MYC4 regulate glucosinolate biosynthesis, insect performance, and feeding behavior. Plant Cell **25**: 3117–32.

Sehr, E.M., Agusti, J., Lehner, R., Farmer, E.E., Schwarz, M., and Greb, T. (2010). Analysis of secondary growth in the Arabidopsis shoot reveals a positive role of jasmonate signalling in cambium formation. Plant J. **63**: 811–822.

Seo, H.S., Song, J.T., Cheong, J.-J., Lee, Y.-H., Lee, Y.-W., Hwang, I., Lee, J.S., and Choi, Y.D. (2001). Jasmonic acid carboxyl methyltransferase: A key enzyme for jasmonate-regulated plant responses. Proc. Natl. Acad. Sci. U. S. A. **98**: 4788–4793.

Sheard, L.B. et al. (2010). Jasmonate perception by inositol-phosphate-potentiated COI1–JAZ co-receptor. Nature **468**: 400–405.

Shimamura, M. (2016). *Marchantia polymorpha* : Taxonomy, Phylogeny and Morphology of a Model System. Plant Cell Physiol. **57**: 230–256.

Shyu, C., Figueroa, P., Depew, C.L., Cooke, T.F., Sheard, L.B., Moreno, J.E., Katsir, L., Zheng, N., Browse, J., and Howe, G.A. (2012). JAZ8 lacks a canonical degron and has an EAR motif that mediates transcriptional repression of jasmonate responses in Arabidopsis. Plant Cell **24**: 536–50.

Smyth, G.K. (2004). Linear models and empirical Bayes methods for assessing differential expression in microarray experiments. Stat. Appl. Genet. Mol. Biol. **3**: Article3.

Solly, J.E., Cunniffe, N.J., and Harrison, C.J. (2017). Regional growth rate differences specified by apical notch activities regulate liverwort thallus shape. Curr. Biol. **27**: 16–26.

Song, S., Huang, H., Gao, H., Wang, J., Wu, D., Liu, X., Yang, S., Zhai, Q., Li, C., Qi, T., and Xie, D. (2014). Interaction between MYC2 and ETHYLENE INSENSITIVE3 modulates antagonism between Jasmonate and Ethylene signaling in Arabidopsis. Plant Cell **26**: 263–279.

Song, S., Qi, T., Fan, M., Zhang, X., Gao, H., Huang, H., Wu, D., Guo, H., and Xie, D. (2013). The bHLH subgroup IIId factors negatively regulate Jasmonate-mediated plant defense and development. PLoS Genet. **9**: e1003653.

Song, S., Qi, T., Huang, H., Ren, Q., Wu, D., Chang, C., Peng, W., Liu, Y., Peng, J., and Xie, D. (2011). The Jasmonate-ZIM domain proteins interact with the R2R3-MYB transcription factors MYB21 and MYB24 to affect Jasmonate-regulated stamen development in Arabidopsis. Plant Cell **23**: 1000–13.

Soukas, A., Cohen, P., Socci, N.D., and Friedman, J.M. (2000). Leptin-specific patterns of gene expression in white adipose tissue. Genes Dev. **14**: 963–80.

Spoel, S.H. et al. (2003). NPR1 modulates cross-talk between salicylate- and jasmonate-dependent defense pathways through a novel function in the cytosol. Plant Cell **15**: 760–70.

Staswick, P. (2009). Plant hormone conjugation: a signal decision. Plant Physiol. **150**: 1310–1321.

Staswick, P., Rowe, M., Spalding, E.P., and Splitt, B.L. (2017). Jasmonoyl-L-Tryptophan disrupts IAA activity through the AUX1 Auxin Permease. Front. Plant Sci. **8**: 1–10.

Staswick, P.E., Serban, B., Rowe, M., Tiryaki, I., Maldonado, M.T., Maldonado, M.C., and Suza, W. (2005). Characterization of an Arabidopsis enzyme family that conjugates amino acids to indole-3-acetic acid. Plant Cell **17**: 616–27.

Staswick, P.E., Su, W., and Howell, S.H. (1992). Methyl jasmonate inhibition of root growth and induction of a leaf protein are decreased in an *Arabidopsis thaliana* mutant. Proc. Natl. Acad. Sci. U. S. A. **89**: 6837–40.

Staswick, P.E. and Tiryaki, I. (2004). The oxylipin signal jasmonic acid is activated by an enzyme that conjugates it to isoleucine in Arabidopsis. Plant Cell **16**: 2117–27.

Staswick, P.E., Tiryaki, I., and Rowe, M.L. (2002). Jasmonate response locus JAR1 and several related Arabidopsis genes encode enzymes of the firefly luciferase superfamily that show activity on jasmonic, salicylic, and indole-3-acetic acids in an assay for adenylation. Plant Cell **14**: 1405–15.

Staswick, P.E., Yuen, G.Y., and Lehman, C.C. (1998). Jasmonate signaling mutants of Arabidopsis are susceptible to the soil fungus *Pythium irregulare*. Plant J. **15**: 747–754.

Stelmach, B.A., Müller, A., Hennig, P., Gebhardt, S., Schubert-Zsilavecz, M., and Weiler, E.W. (2001). A novel class of oxylipins, sn1-O-(12-oxophytodienoyl)-sn2-O-(hexadecatrienoyl)-monogalactosyl Diglyceride, from *Arabidopsis thaliana*. J. Biol. Chem. **276**: 12832–8.

Stintzi, A. and Browse, J. (2000). The Arabidopsis male-sterile mutant, opr3, lacks the 12-oxophytodienoic acid reductase required for jasmonate synthesis. Proc. Natl. Acad. Sci. U. S. A. **97**: 10625–30.

Stumpe, M., Göbel, C., Faltin, B., Beike, A.K., Hause, B., Himmelsbach, K., Bode, J., Kramell, R., Wasternack, C., Frank, W., Reski, R., and Feussner, I. (2010). The moss *Physcomitrella patens* contains cyclopentenones but no jasmonates: mutations in allene oxide cyclase lead to reduced fertility and altered sporophyte morphology. New Phytol. **188**: 740–749.

Sugano, S.S., Shirakawa, M., Takagi, J., Matsuda, Y., Shimada, T., Hara-Nishimura, I., and Kohchi, T. (2014). CRISPR/Cas9-mediated targeted mutagenesis in the liverwort *Marchantia polymorpha* L. Plant Cell Physiol. **55**: 475–481.

Suza, W.P., Rowe, M.L., Hamberg, M., and Staswick, P.E. (2010). A tomato enzyme synthesizes (+)-7-iso-jasmonoyl-L-isoleucine in wounded leaves. Planta **231**: 717–28.

Taki, N., Sasaki-sekimoto, Y., Obayashi, T., Kikuta, A., and Kobayashi, K. (2005). 12-Oxo-Phytodienoic Acid Triggers Expression of a Distinct Set of Genes and Plays a Role in Wound-Induced Gene Expression in Arabidopsis. Plant Physiol. **139**: 1268–1283.

Tan, X., Calderon-Villalobos, L.I., Sharon, M., Zheng, C., Robinson, C. V, Estelle, M., and Zheng, N. (2007). Mechanism of auxin perception by the TIR1 ubiquitin ligase. Nature **446**: 640–645.

Tanaka, M., Esaki, T., Kenmoku, H., Koeduka, T., Kiyoyama, Y., Masujima, T., Asakawa, Y., and Matsui, K. (2016). Direct evidence of specific localization of sesquiterpenes and marchantin A in oil body cells of *Marchantia polymorpha* L. Phytochemistry **130**: 77–84.

Terui, K. (1981). Growth and gemma-cup formation in relation to archegoniophore protrusion in *Marchantia polymorpha* L. Ann. Rep. Fac. Educ., Iwate Univ **40**: 19–28.

Theodoulou, F.L., Job, K., Slocombe, S.P., Footitt, S., Holdsworth, M., Baker, A., Larson, T.R., and Graham, I.A. (2005). Jasmonic acid levels are reduced in COMATOSE ATP-binding cassette transporter mutants. Implications for transport of jasmonate precursors into peroxisomes. Plant Physiol. **137**: 835–40.

Thilmony, R., Underwood, W., and He, S.Y. (2006). Genome-wide transcriptional analysis of the *Arabidopsis thaliana* interaction with the plant pathogen *Pseudomonas syringae* pv. *tomato* DC3000 and the human pathogen *Escherichia coli* O157:H7. Plant J. **46**: 34–53.

Thines, B., Katsir, L., Melotto, M., Niu, Y., Mandaokar, A., Liu, G., Nomura, K., He, S.Y., Howe, G.A., and Browse, J. (2007). JAZ repressor proteins are targets of the SCF(COI1) complex during jasmonate signalling. Nature **448**: 661–665.

Thireault, C., Shyu, C., Yoshida, Y., St. Aubin, B., Campos, M.L., and Howe, G.A. (2015). Repression of jasmonate signaling by a non-TIFY JAZ protein in Arabidopsis. Plant J. **82**: 669–679.

Toda, Y. et al. (2013). RICE SALT SENSITIVE3 forms a ternary complex with JAZ and class-C bHLH factors and regulates Jasmonate-induced gene expression and root cell elongation. Plant Cell **25**: 1709–1725.

de Torres Zabala, M., Zhai, B., Jayaraman, S., Eleftheriadou, G., Winsbury, R., Yang, R., Truman, W., Tang, S., Smirnoff, N., and Grant, M. (2016). Novel JAZ co-operativity and unexpected JA dynamics underpin Arabidopsis defence responses to *Pseudomonas syringae* infection. New Phytol. **209**: 1120–34.

Tsuchiya, T., Ohta, H., Okawa, K., Iwamatsu, A., Shimada, H., Masuda, T., and Takamiya, K. (1999). Cloning of chlorophyllase, the key enzyme in chlorophyll degradation: finding of a lipase motif and the induction by methyl jasmonate. Proc. Natl. Acad. Sci. U. S. A. **96**: 15362–7.

Turner, J.G., Ellis, C., and Devoto, A. (2002). The jasmonate signal pathway. Plant Cell **14 Suppl**: S153-64.

Ueda, J. and Kato, J. (1980). Isolation and identification of a senescence-promoting substance from wormwood (*Artemisia absinthium* L.). Plant Physiol. **66**: 246–9.

Uppalapati, S.R., Ayoubi, P., Weng, H., Palmer, D.A., Mitchell, R.E., Jones, W., and Bender, C.L. (2005). The phytotoxin coronatine and methyl jasmonate impact multiple phytohormone pathways in tomato. Plant J. **42**: 201–217.

Uppalapati, S.R., Ishiga, Y., Wangdi, T., Kunkel, B.N., Anand, A., Mysore, K.S., and Bender, C.L. (2007). The phytotoxin Coronatine contributes to pathogen fitness and is required for suppression of Salicylic Acid accumulation in tomato inoculated with *Pseudomonas syringae* pv. *tomato* DC3000. Mol. Plant-Microbe Interact. **20**: 955–965.

Vanholme, B., Grunewald, W., Bateman, A., Kohchi, T., and Gheysen, G. (2007). The tify family previously known as ZIM. Trends Plant Sci. **12**: 239–244.

Vick, B.A., Zimmerman, D.C., and Weisleder, D. (1979). Thermal alteration of a cyclic fatty acid produced by a flaxseed extract. Lipids **14**: 734–740.

Vijayan, P., Shockey, J., Lévesque, C.A., Cook, R.J., and Browse, J. (1998). A role for jasmonate in pathogen defense of Arabidopsis. Proc. Natl. Acad. Sci. U. S. A. **95**: 7209–14.

Wang, C., Liu, Y., Li, S.-S., and Han, G.-Z. (2015). Insights into the origin and evolution of the plant hormone signaling machinery. Plant Physiol. **167**: 872–886.

Wasternack, C. (2015). How jasmonates earned their laurels: past and present. J. Plant Growth Regul. **34**: 761–794.

Wasternack, C. (2007). Jasmonates: An update on biosynthesis, signal transduction and action in plant stress response, growth and development. Ann. Bot. **100**: 681–697.

Wasternack, C. and Hause, B. (2013). Jasmonates: Biosynthesis, perception, signal transduction and action in plant stress response, growth and development. An update to the 2007 review in Annals of Botany. Ann. Bot. **111**: 1021–1058.

Weber, H., Vick, B.A., and Farmer, E.E. (1997). Dinor-oxo-phytodienoic acid: a new hexadecanoid signal in the jasmonate family. Proc. Natl. Acad. Sci. U. S. A. **94**: 10473–8.

Wellman, C.H., Osterloff, P.L., and Mohiuddin, U. (2003). Fragments of the earliest land plants. Nature **425**: 282–285.

White, D.W.R. (2006). PEAPOD regulates lamina size and curvature in Arabidopsis. Proc. Natl. Acad. Sci. U. S. A. **103**: 13238–13243.

Wickett, N.J. et al. (2014). Phylotranscriptomic analysis of the origin and early diversification of land plants. Proc. Natl. Acad. Sci. U. S. A. **111**: E4859–E4868.

Widemann, E., Miesch, L., Lugan, R., Holder, E., Heinrich, C., Aubert, Y., Miesch, M., Pinot, F., and Heitz, T. (2013). The Amidohydrolases IAR3 and ILL6 contribute to Jasmonoyl-Isoleucine hormone turnover and generate 12-Hydroxyjasmonic Acid upon wounding in Arabidopsis leaves. J. Biol. Chem. **288**: 31701–31714.

Withers, J., Yao, J., Mecey, C., Howe, G.A., Melotto, M., and He, S.Y. (2012). Transcription factor-dependent nuclear localization of a transcriptional repressor in jasmonate hormone signaling. Proc. Natl. Acad. Sci. U. S. A. **109**: 20148–53.

Wu, K., Zhang, L., Zhou, C., Yu, C.-W., and Chaikam, V. (2008). HDA6 is required for jasmonate response, senescence and flowering in Arabidopsis. J. Exp. Bot. **59**: 225–234.

Xie, D.X., Feys, B.F., James, S., Nieto-Rostro, M., and Turner, J.G. (1998). COI1: an Arabidopsis gene required for jasmonate-regulated defense and fertility. Science. **280**: 1091–4.

Xin, X.-F. and He, S.Y. (2013). *Pseudomonas syringae* pv. *tomato* DC3000: a model pathogen for probing disease susceptibility and hormone signaling in plants. Annu. Rev. Phytopathol. **51**: 473–98.

References

Yamamoto, Y., Ohshika, J., Takahashi, T., Ishizaki, K., Kohchi, T., Matusuura, H., and Takahashi, K. (2015). Functional analysis of allene oxide cyclase, MpAOC, in the liverwort *Marchantia polymorpha*. Phytochemistry **116**: 48–56.

Yan, Y., Stolz, S., Chételat, A., Reymond, P., Pagni, M., Dubugnon, L., and Farmer, E.E. (2007). A downstream mediator in the growth repression limb of the jasmonate pathway. Plant Cell **19**: 2470–83.

Yang, D.-L. et al. (2012). Plant hormone jasmonate prioritizes defense over growth by interfering with gibberellin signaling cascade. Proc. Natl. Acad. Sci. U. S. A. **109**: E1192-200.

Yukimune, Y., Tabata, H., Higashi, Y., and Hara, Y. (1996). Methyl jasmonate-induced overproduction of paclitaxel and baccatin III in Taxus cell suspension cultures. Nat. Biotechnol. **14**: 1129–32.

Záveská Drábková, L., Dobrev, P.I., and Motyka, V. (2015). Phytohormone profiling across the bryophytes. PLoS One **10**: e0125411.

Zhang, F. et al. (2015a). Structural basis of JAZ repression of MYC transcription factors in jasmonate signalling. Nature **525**: 269–273.

Zhang, F., Ke, J., Zhang, L., Chen, R., Sugimoto, K., Howe, G.A., Xu, H.E., Zhou, M., He, S.Y., and Melcher, K. (2017). Structural insights into alternative splicing-mediated desensitization of jasmonate signaling. Proc. Natl. Acad. Sci. U. S. A. **114**: 1720–1725.

Zhang, L., Yao, J., Withers, J., Xin, X.-F., Banerjee, R., Fariduddin, Q., Nakamura, Y., Nomura, K., Howe, G.A., Boland, W., Yan, H., and He, S.Y. (2015b). Host target modification as a strategy to counter pathogen hijacking of the jasmonate hormone receptor. Proc. Natl. Acad. Sci. U. S. A. **112**: 14354–14359.

Zhao, Y., Thilmony, R., Bender, C.L., Schaller, A., He, S.Y., and Howe, G.A. (2003). Virulence systems of *Pseudomonas syringae* pv. *tomato* promote bacterial speck disease in tomato by targeting the jasmonate signaling pathway. Plant J. **36**: 485–499.

Zhou, C., Zhang, L., Duan, J., Miki, B., and Wu, K. (2005). HISTONE DEACETYLASE19 is involved in jasmonic acid and ethylene signaling of pathogen response in Arabidopsis. Plant Cell **17**: 1196–204.

Zhou, Z., Wu, Y., Yang, Y., Du, M., Zhang, X., Guo, Y., Li, C., and Zhou, J.-M. (2015). An Arabidopsis plasma membrane proton ATPase modulates JA signaling and is exploited by the *Pseudomonas syringae* effector protein AvrB for stomatal invasion. Plant Cell **27**: 2032–41.

Zhu, W., Wei, W., Fu, Y., Cheng, J., Xie, J., Li, G., Yi, X., Kang, Z., Dickman, M.B., and Jiang, D. (2013). A secretory protein of necrotrophic fungus *Sclerotinia sclerotiorum* that suppresses host resistance. PLoS One **8**: e53901.

Zhu, Z. et al. (2011). Derepression of ethylene-stabilized transcription factors (EIN3/EIL1) mediates jasmonate and ethylene signaling synergy in Arabidopsis. Proc. Natl. Acad. Sci. U. S. A. **108**: 12539–12544.

Zimmerman, D.C. and Vick, B.A. (1970). Hydroperoxide Isomerase: a new enzyme of lipid metabolism. Plant Physiol. **46**: 445–453.

Supplementary data

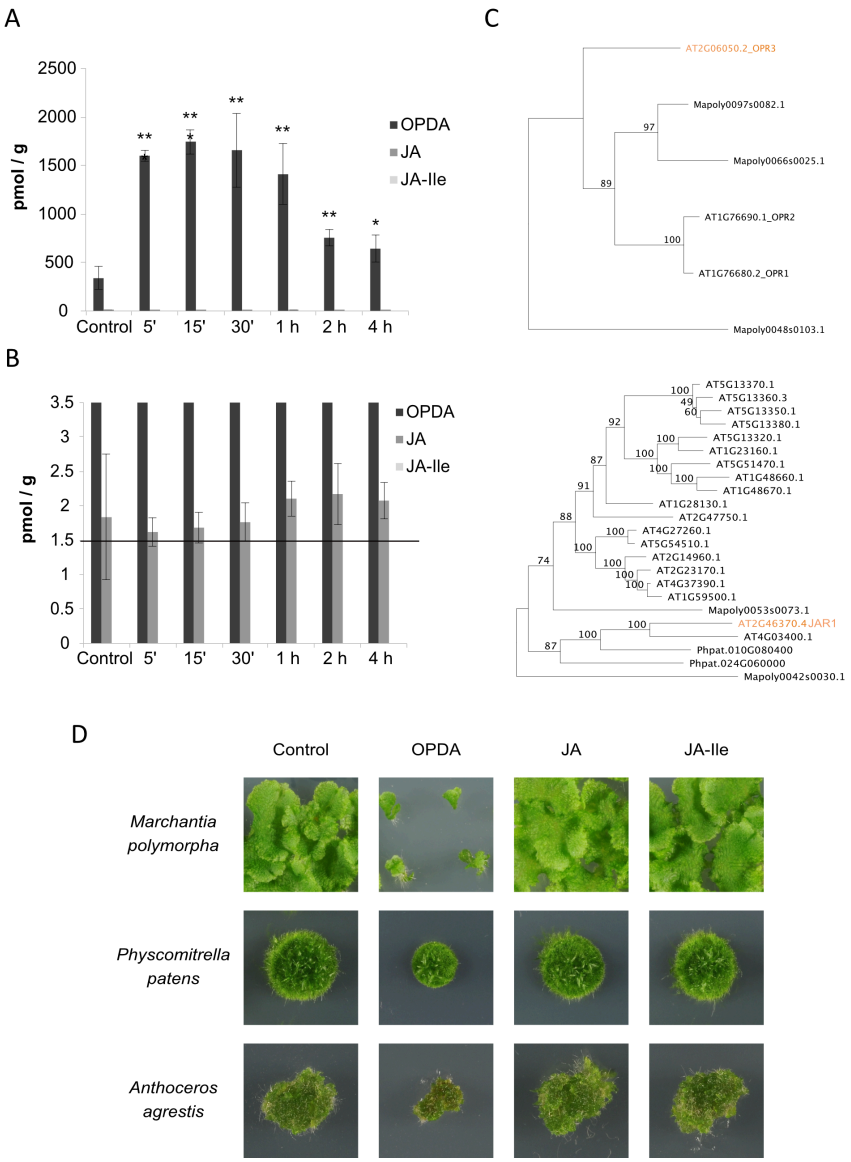

Supplementary Figure S1. OPDA accumulates after wounding and inhibits growth in bryophytes. A) Time-course of OPDA, JA and JA-Ile accumulation in *M. polymorpha* WT Tak-1 at different times after mechanical wounding. B) Magnification of A to show that JA levels detected in *M. polymorpha* were near the detection limit (black horizontal line). Data shown as mean ± S.D. C) Phylogenetic analyses of OPR3 (top) and JAR1 (bottom) in *M. polymorpha* and *A. thaliana*. For the JAR1 tree, *Physcomitrella patens* sequences were included as a reference of bryophyte auxin-conjugating GH3. D) Effect of OPDA, JA and JA-Ile on *M. polymorpha* WT Tak-1, the moss *Physcomitrella patens* and the liverwort *Anthoceros agrestis* growth. Concentration was 50 µM for all molecules.

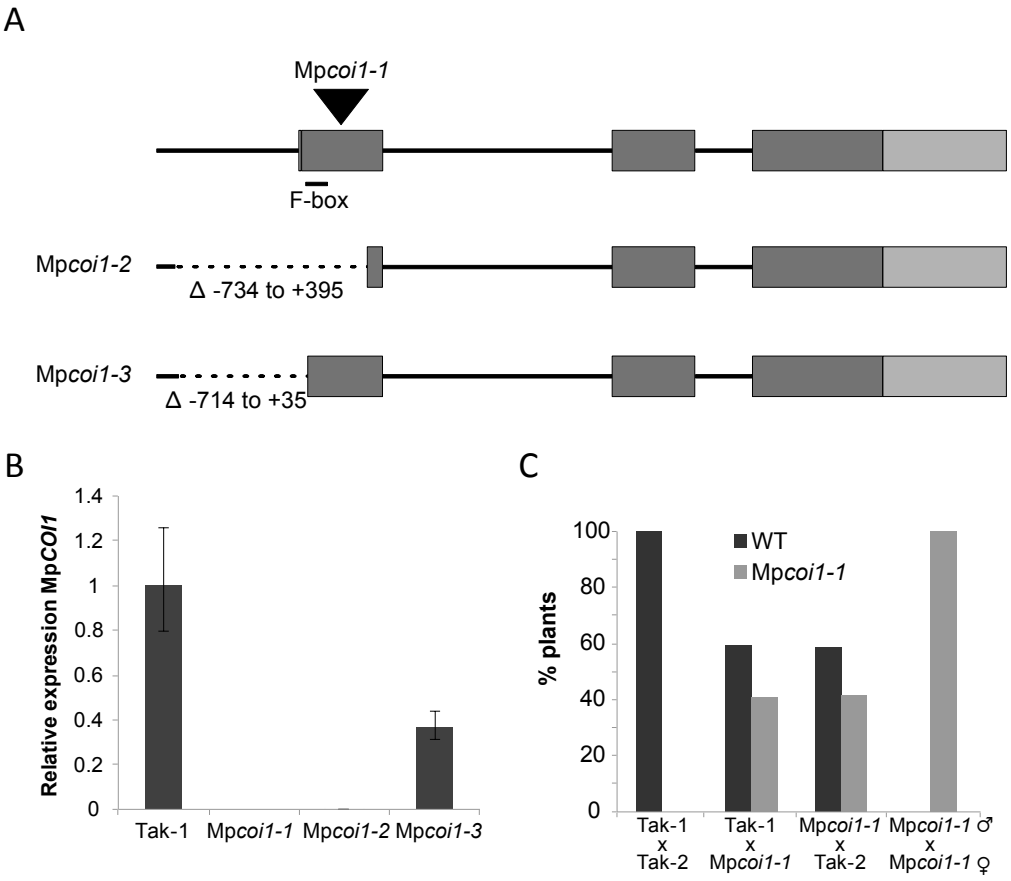

Supplementary Figure S2. Mp*coi1* mutant alleles. A) Scheme of the Mapoly0025s0025 (Mp*COI1*) locus and mutant alleles. Dark grey blocks, exons; light grey, 3′ UTR regions; triangle, T-DNA insertion in Mp*coi1-1* allele, which disrupts the first exon by gene targeting-mediated homologous recombination. Dashed lines indicate deletions in Mp*coi1-2* and Mp*coi1-3* mutants obtained by CRISPR/Cas9 nickase. Numbers correspond to nucleotide position of each deletion relative to ATG. B) Relative expression of Mp*COI1* by Q-PCR in WT Tak-1 and the three alleles Mp*coi1-1*, Mp*coi1-2* and Mp*coi1-3*. Primers were designed in the first exon. Data shown as mean ± S.D. C) Segregation of Mpcoi1-1 mutation after crossing parental lines Tak-1 ♂ x Tak-2 ♀, Tak-1 ♂ x Mpcoi1-1 ♀, Mpcoi1-1 ♂ x Tak-2 ♀, and Mpcoi1-1 ♂ x Mpcoi1-1 ♀. 20-30 plants were analysed per cross.

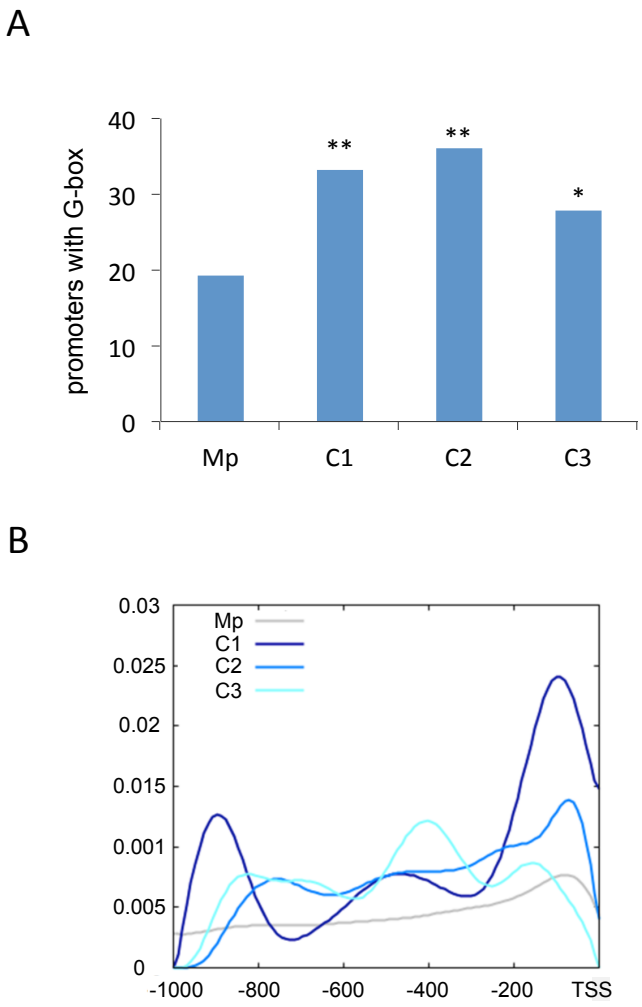

Supplementary Figure S3. A) Over-representation of G-box (CACGTG; target sequence of MYC-related transcription factors) in OPDA/COI1-regulated gene promoters. Percentage of G-box-containing promoter regions in the complete set of *Marchantia* genes (Mp) and the genes in each of the clusters in Figure 3B (C1, C2 and C3). Clusters 1 and 2 are particularly enriched in G-boxes. Asterisks indicate statistical significance between the proportions within each cluster and the proportion of the G-box in the complete set of *Marchantia* promoters (hypergeometric test, * $p<0.05$; ** $p<0.005$). B) G-boxes are enriched in proximal promoters. Density plot of G-boxes in promoter regions (number of DNA motifs at each position per number of promoters, 1000 bp upstream of the transcription start site, TSS) of *Marchantia* genes (Mp) and the genes in each cluster. G-boxes are particularly enriched in the proximal promoters near the TSS of genes from clusters 1 and 2.

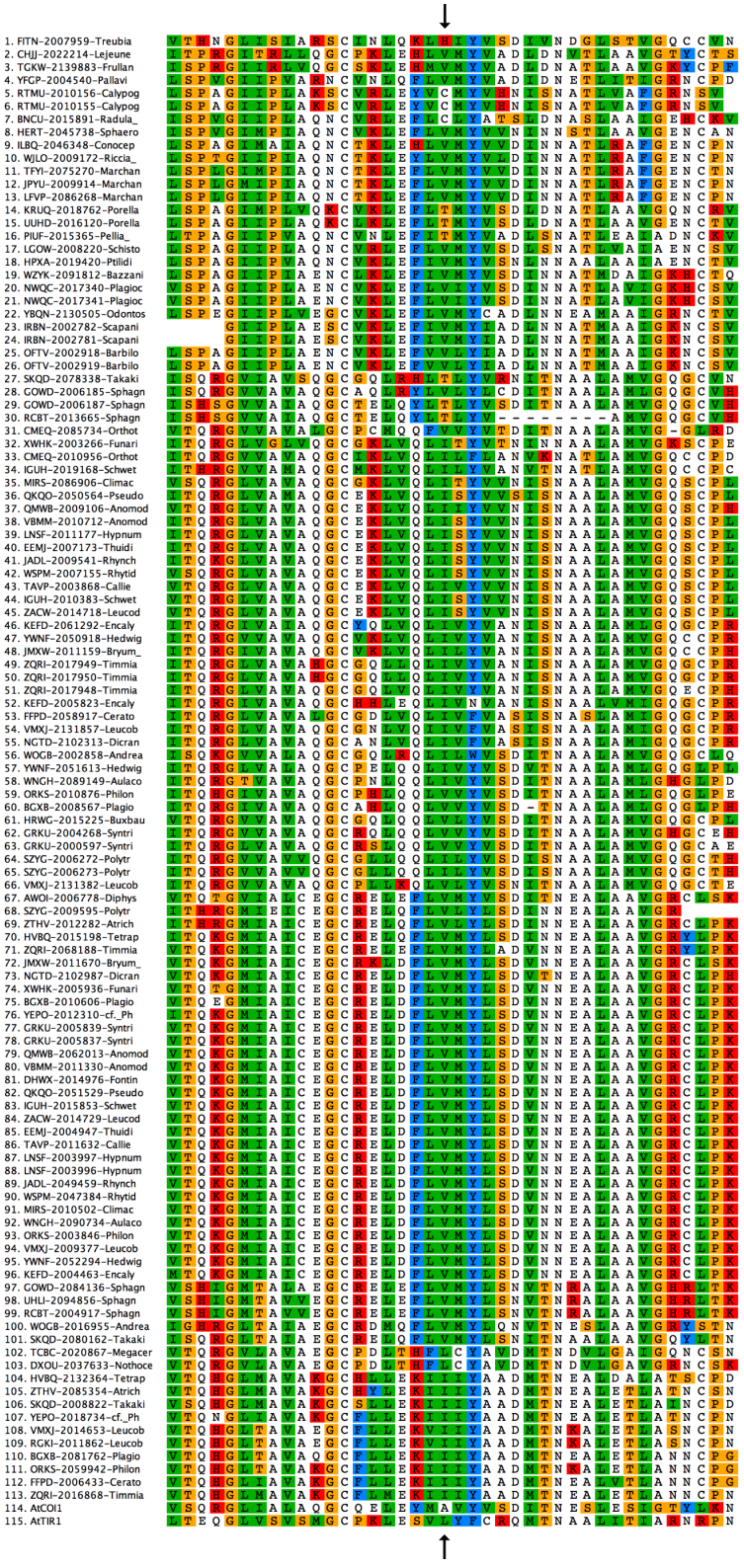

Supplementary Figure S4: No available bryophyte COI1 sequences have an alanine at the position equivalent to AtCOI1^{A384}. Multiple sequence alignment of the predicted bryophyte COI1 amino acid sequences from OneKP database (see Matasci et al., 2014 for full species name and corresponding codes). AtCOI1 and AtTIR1 sequences are included for comparison (bottom). Arrows indicate the position at which AtCOI1 has an alanine, whereas all bryophytes have a residue other than alanine.

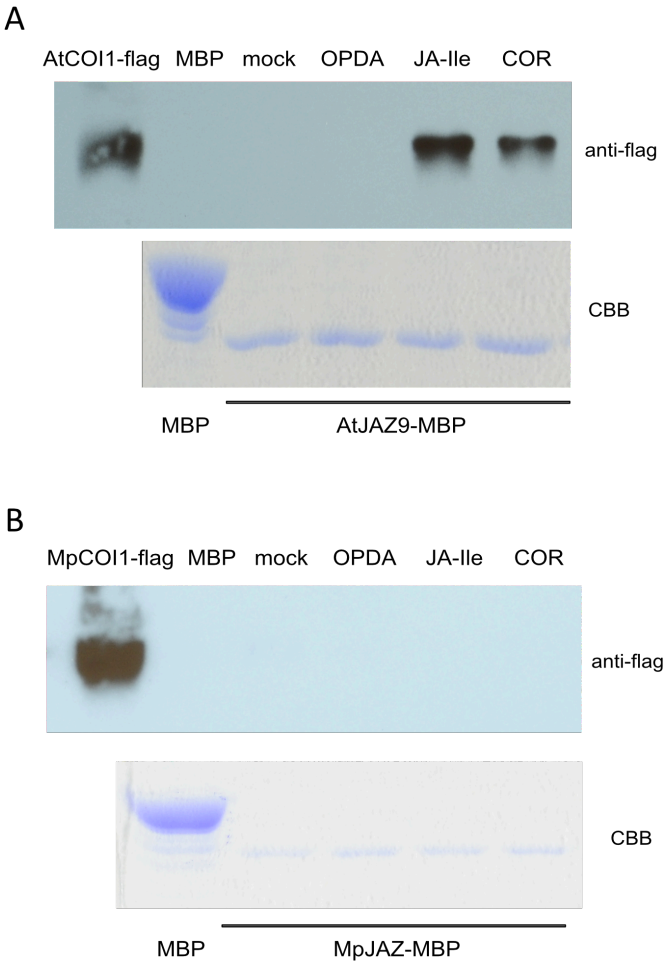

Supplementary Figure S5: The COI-JAZ co-receptor has distinct hormone specificities in *Arabidopsis* and *Marchantia*. A) Immunoblot (anti-flag antibody) of recovered AtCOI1-flag (from 35S:At*COI1*-flag Arabidopsis extracts) after pull-down reactions using recombinant AtJAZ9-MBP protein alone or with different molecules: OPDA (50 µM), JA-Ile (50 µM), COR (0.5 µM). Coomassie blue staining of AtJAZ9-MBP after Factor Xa cleavage (bottom). B) Immunoblot of MpCOI-flag (from 35S:Mp*COI1*-flag Arabidopsis extracts) after pull-down reactions using recombinant MpJAZ-MBP protein alone or with OPDA (50 µM), JA-Ile (50 µM) and COR (0.5 µM).

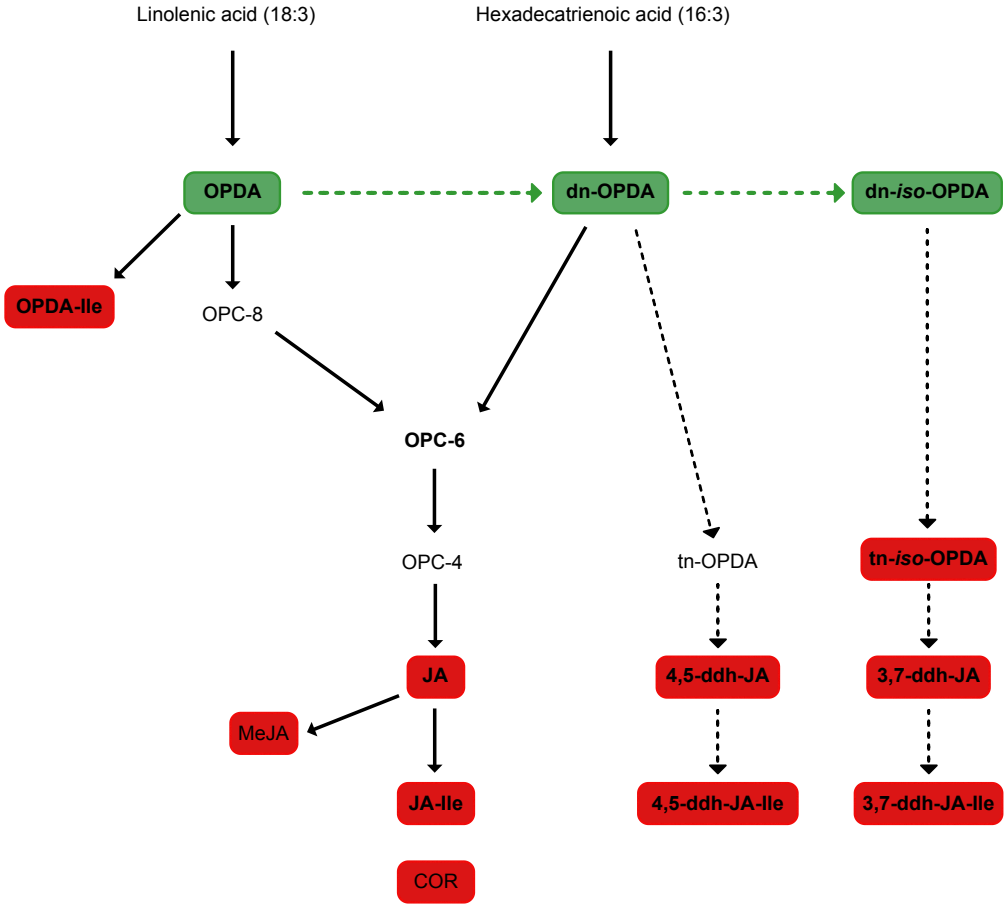

Supplementary Figure S6: Biosynthetic pathways of JA-Ile and related oxylipins. Black arrows indicate steps described in tracheophytes. Black dashed lines indicate hypothetic alternative reactions not yet described in plants. Red indicates inactive molecules that do not inhibit growth in *M. polymorpha*, green indicates active molecules that inhibit growth in *M. polymorpha* (OPDA, dn-OPDA and dn-*iso*-OPDA). Green dashed line indicates the OPDA-to-dinor-OPDA-to-dinor-*iso*-OPDA conversion in *M. polymorpha* described in this study. Bold letters indicate molecules used as internal standards in *M. polymorpha* (OPDA, dn-OPDA, OPDA-Ile, OPC-6, JA, JA-Ile, 4,5-ddh-JA, 4,5-ddh-JA-Ile, tetranor-*iso*-OPDA, 3,7-ddh-JA and 3,7-ddh-JA-Ile-Me).

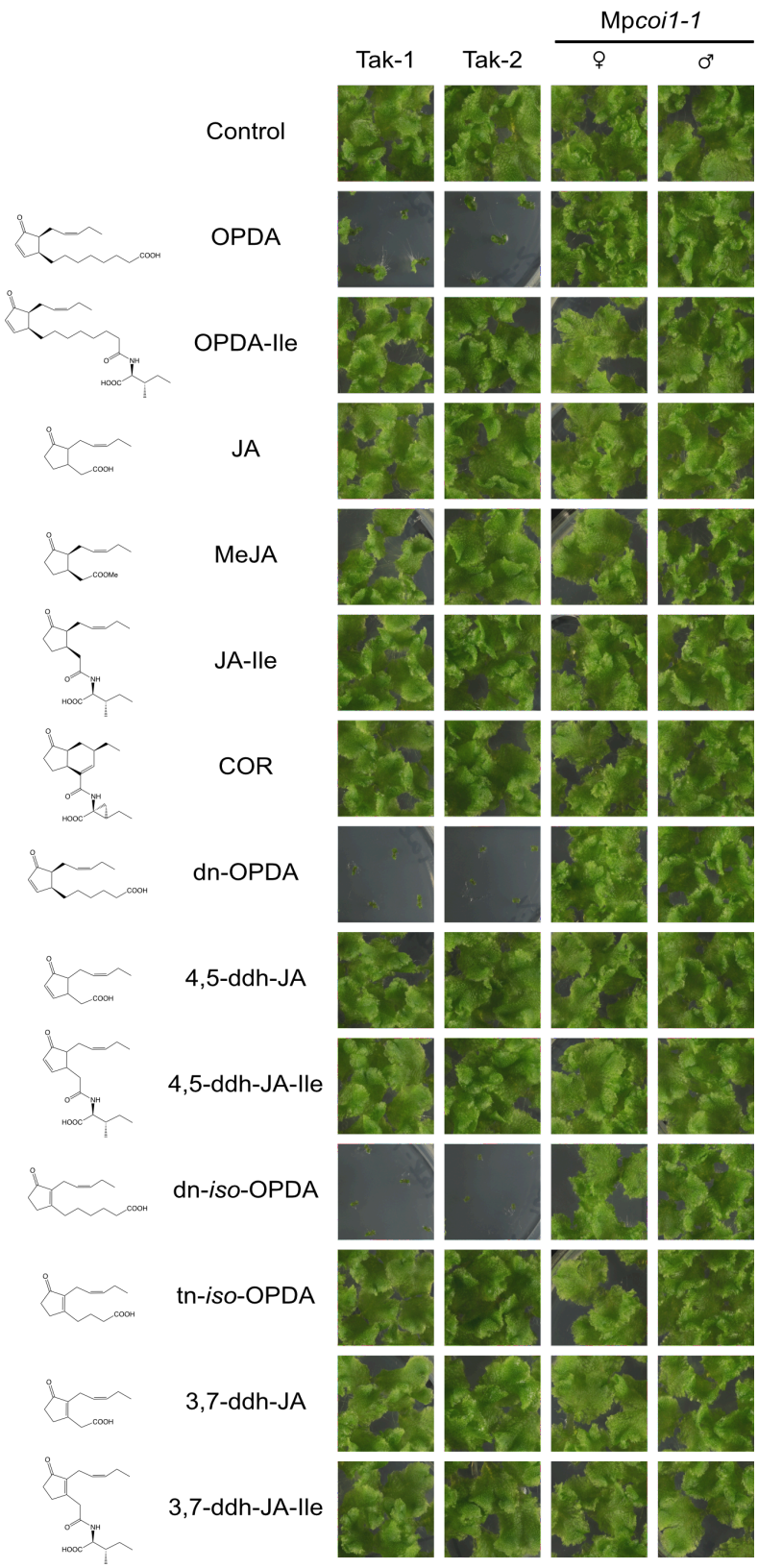

Supplementary Figure S7: Only OPDA, dinor-OPDA and dinor-*iso*-OPDA inhibit growth in *M. polymorpha* and this inhibition is Mp*COI1*-dependent. Effect of various oxylipins (OPDA, OPDA-Ile, JA, MeJA, JA-Ile, dinor-*cis*-OPDA, 4,5-ddh-JA, 4,5-ddh-JA-Ile, dinor-*iso*-OPDA, tetranor-*iso*-OPDA, 3,7-ddh-JA and 3,7-ddh-JA-Ile-Me; all 50 µM) and coronatine (0.5 µM) on 11-day-old *M. polymorpha* WT Tak-1 and Tak-2 and Mp*coi1-1* male and female mutants.

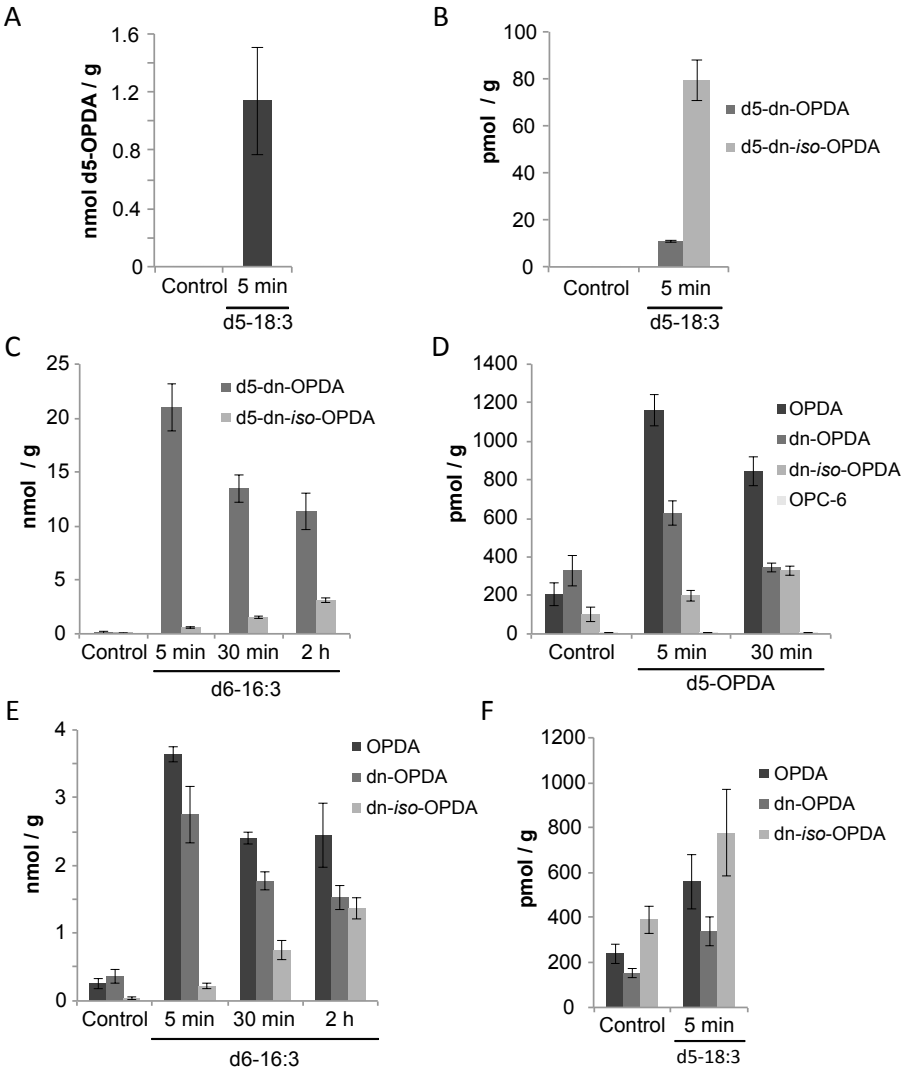

Supplementary Figure S8: 16:3 and 18:3 are dn-OPDA precursors and the oxylipin biosynthesis feedback loop is conserved in *M. polymorpha*. A) Accumulation of deuterated OPDA (d5-OPDA) in Tak-1 upon 5 min treatment with deuterated linolenic acid (d5-18:3). B) Accumulation of d5-dinor-OPDA and d5-dinor-*iso*-OPDA in Tak-1 after 5 min d5-18:3 treatment. C) Accumulation of d5-dinor-OPDA and d5-dinor-*iso*-OPDA in Tak-1 after treatment with deuterated hexadecatrienoic acid (d6-16:3) for 5 min, 30 min and 2 h. D) Accumulation of non-deuterated OPDA, dinor-OPDA, dinor-*iso*-OPDA and OPC-6 in Tak-1 plants in basal conditions and 5 or 30 min after d5-OPDA treatment. E) Accumulation of non-deuterated OPDA, dinor-OPDA and dinor-*iso*-OPDA in Tak-1 plants in basal conditions and 5 min, 30 min and 2 h after treatment with d6-16:3. F) Accumulation of non-deuterated OPDA, dinor-OPDA and dinor-*iso*-OPDA in Tak-1 plants in basal conditions and 5 min after treatment with d5-18:3. Data shown as mean ± S.D.

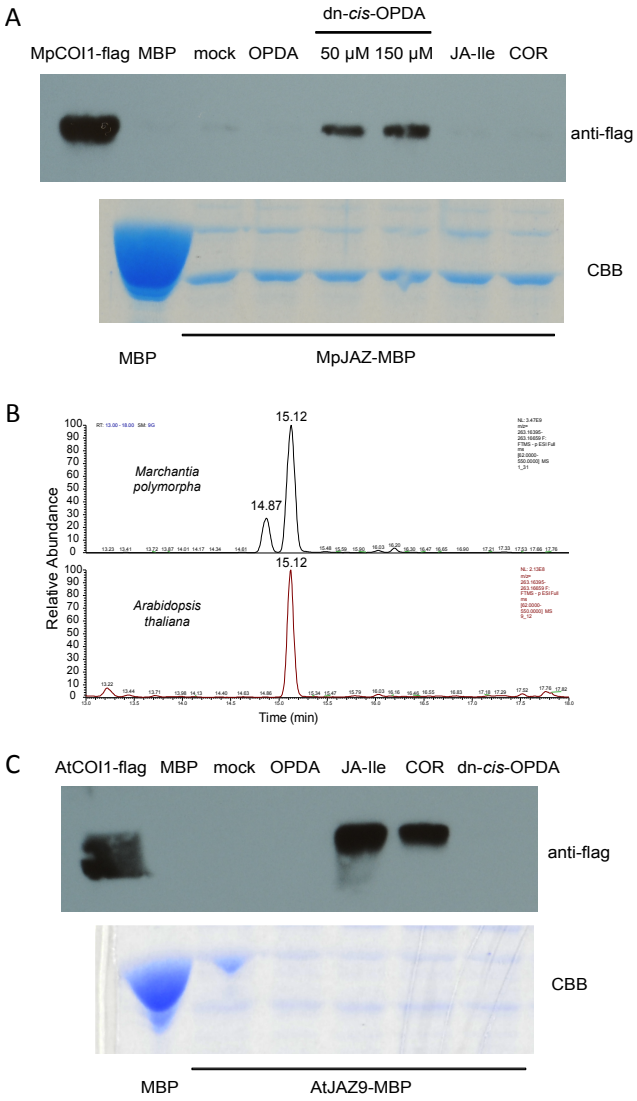

Supplementary Figure S9: The dinor-OPDA ligand binds to MpCOI1/MpJAZ but not to the AtCOI1/AtJAZ9 co-receptor. A) Immunoblot (anti-flag antibody) of recovered MpCOI1-flag (from 35S:Mp*COI1*-flag Arabidopsis extracts) after pull-down reactions using recombinant MpJAZ-MBP protein alone or with OPDA (50 µM), dinor-*cis*-OPDA (50 and 150 µM), JA-Ile (50 µM) and COR (0.5 µM). Coomassie blue staining of MpJAZ-MBP after Factor Xa cleavage (bottom). B) Chromatogram of dinor-OPDA (15.2) and dinor-*iso*-OPDA (14.87) in wounded *M. polymorpha* and *A. thaliana*. C) Immunoblot (anti-flag antibody) of recovered AtCOI1-flag (from 35S:At*COI1*-flag Arabidopsis extracts) after pull-down reactions using recombinant AtJAZ9-MBP protein alone or with OPDA (50 µM), JA-Ile (50 µM), COR (0.5 µM) and dinor-*cis*-OPDA (50 µM). Coomassie blue staining of AtJAZ9-MBP after Factor Xa cleavage (bottom).

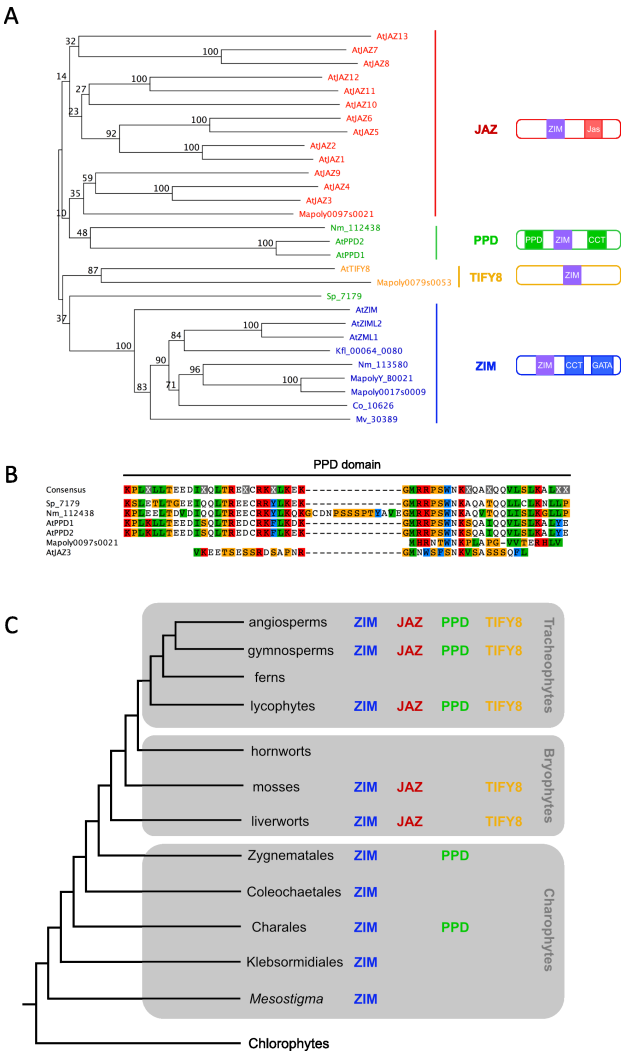

Supplementary Figure S10: TIFY superfamily conservation in the green lineage. A) TIFY superfamily phylogenetic tree of charophytes, *M. polymorpha* (Mapoly) and *A. thaliana* (At). Nm, *Nitella mirabilis*; Sp, *Spirogyra pratensis*; Kfl, *Klebsormidium flaccidum* (now reannotated as *K. nitens*); Co, *Coleochaete orbicularis*; Mv, *Mesostigma viridae*. Conserved domains of the JAZ, PPD, TIFY8 and ZIM families (right). Multiple sequence alignment was performed with DiAlign and tree was built with BioNJ. Numbers correspond to bootstraps values. B) Alignment of PPD domain in PPD sequences from *A. thaliana*, *S. pratensis* and *N. mirabilis*. Mapoly0097s0021 (MpJAZ) and AtJAZ3 were included due to partial conservation of PPD domain. Alignment was performed with DiAlign. C) TIFY superfamily evolution across the green lineage. Conservation of TIFY members in mosses (*Physcomitrella patens*), lycophytes (*Selaginella moellendorfii*) and angiosperms was already studied (Bai et al., 2011). Data from liverworts and charophytes are a summary of A. ZIM, JAZ, PPD and TIFY8 were identified in the gymnosperm *Picea abies*.

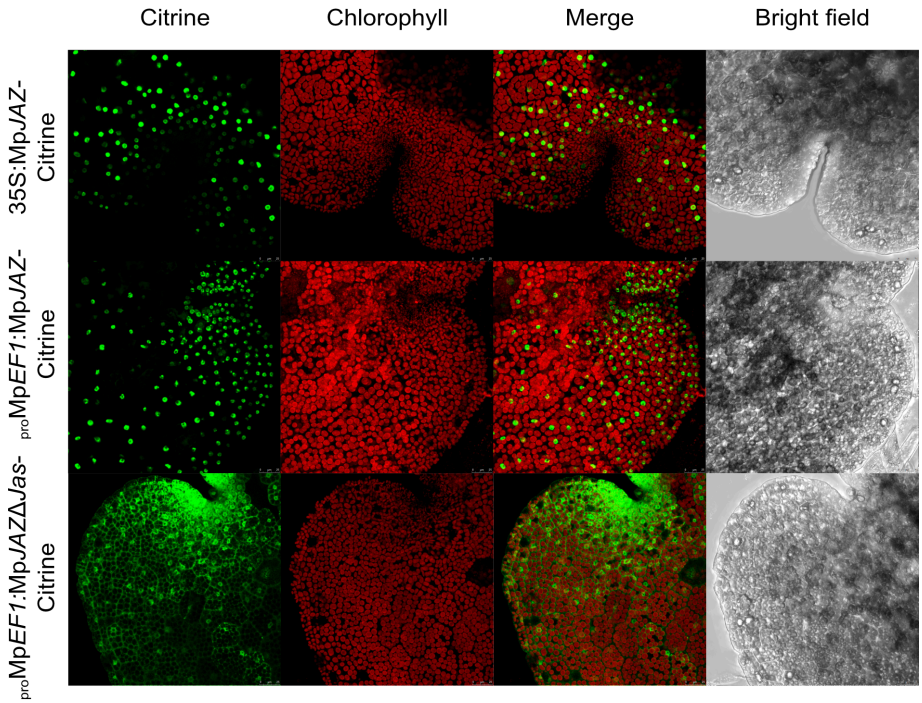

Supplementary Figure S11: MpJAZ and MpJAZΔJas subcellular localization in *M. polymorpha*. Close-up (3x) of the apical notch of gemmalings from Figure 11C. Confocal imaging of 2-day-old 35S:Mp*JAZ*-Citrine, $_{pro}$Mp*EF1*:Mp*JAZ*-Citrine and $_{pro}$Mp*EF1*: Mp*JAZ*Δ*Jas*-Citrine gemmalings.

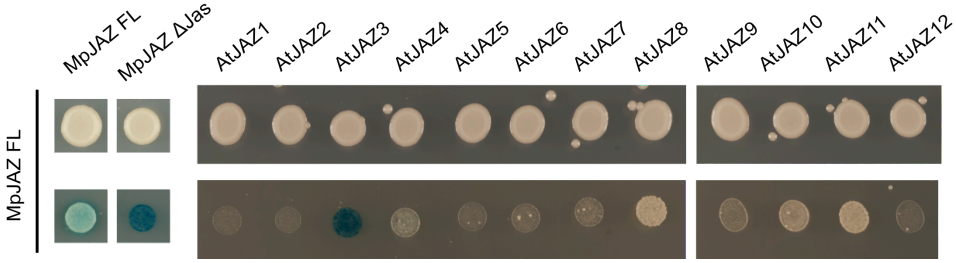

Supplementary Figure S12: Homo and hetero-dimerization of MpJAZ. Yeast two-hybrid assay between MpJAZ (fused to BD) and MpJAZ, MpJAZΔJas and the 12 canonical AtJAZ (fused to AD). Yeast growth on SD medium with glucose (top). Yeast growth on SD medium with galactose/ raffinose (bottom). Blue color means interaction.

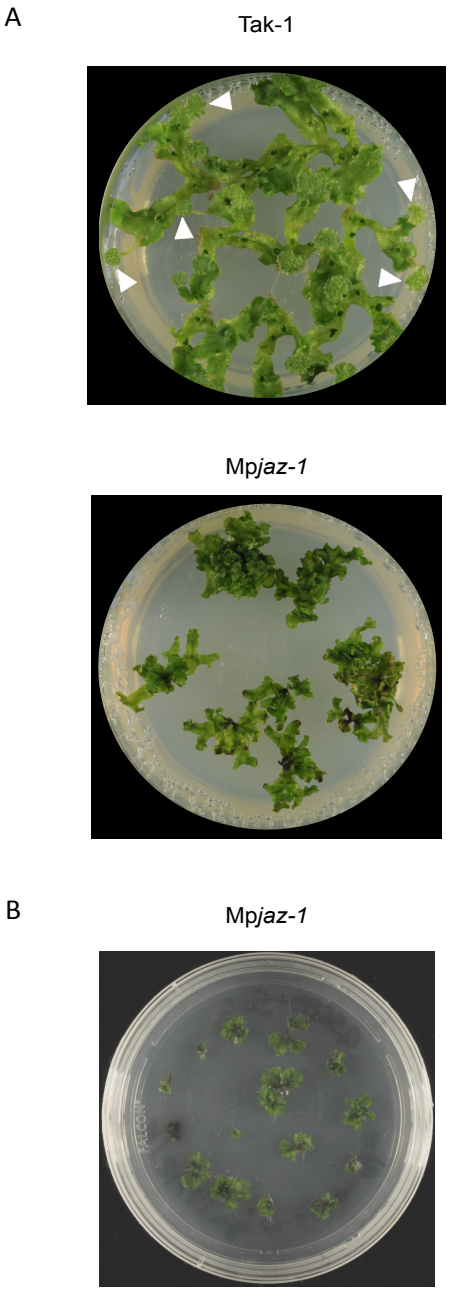

Supplementary Figure S13: Mp*jaz-1* is severely affected in antheridiophore and gemma cup development. A) Tak-1 and Mp*jaz-1* cut-thalli grown in 0.5 Gamborg's B5 jars with transparent lids and irradiated with FR lights for 23 days. White triangles, antheridiophores. B) Mp*jaz-1* cut-thalli grown on 0.5 Gamborg's B5 medium supplemented with sucrose for 3 weeks. Note the complete absence of gemma cups.

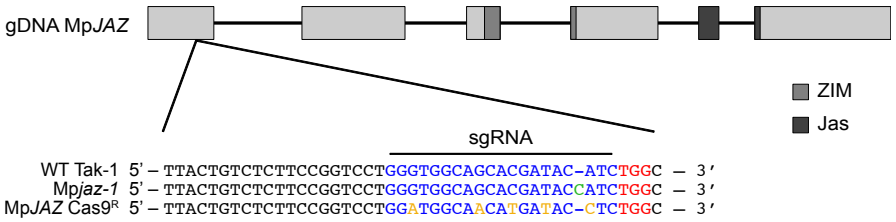

Supplementary Figure S14: Codon optimization to generate a Cas9-resistant version of Mp*JAZ*. Scheme of Mp*JAZ* locus. Light grey blocks, exons. ZIM and Jas domains are represented by two different shades of grey. Red, PAM sequence; blue color, sequence used as target for the sgRNA; green, insertion in Mp*jaz-1*; orange, synonymous mutations in Cas9-resistant Mp*JAZ* gene.

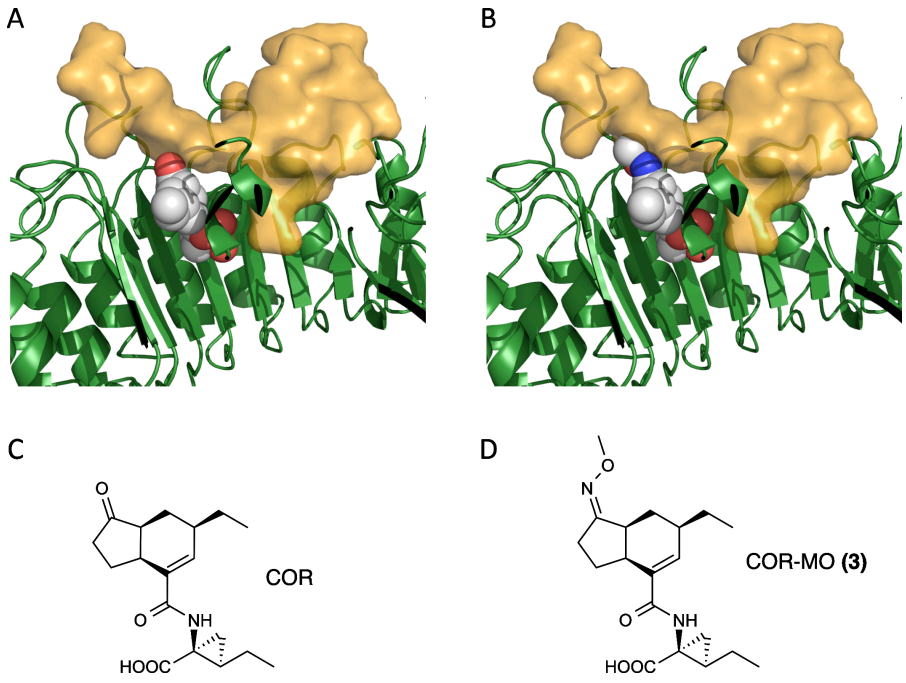

Supplementary Figure S15: A) Molecular model of the interaction of COR with the co-receptor AtCOI1 (green, ribbon representation) and AtJAZ1 degron (yellow, surface representation) based on crystal structure described by Sheard et al., 2010. B) The same complex as in A with COR-MO instead of COR, showing the sterical impediment of AtJAZ interaction. C) Structure of coronatine (COR). D) Structure of COR-MO.

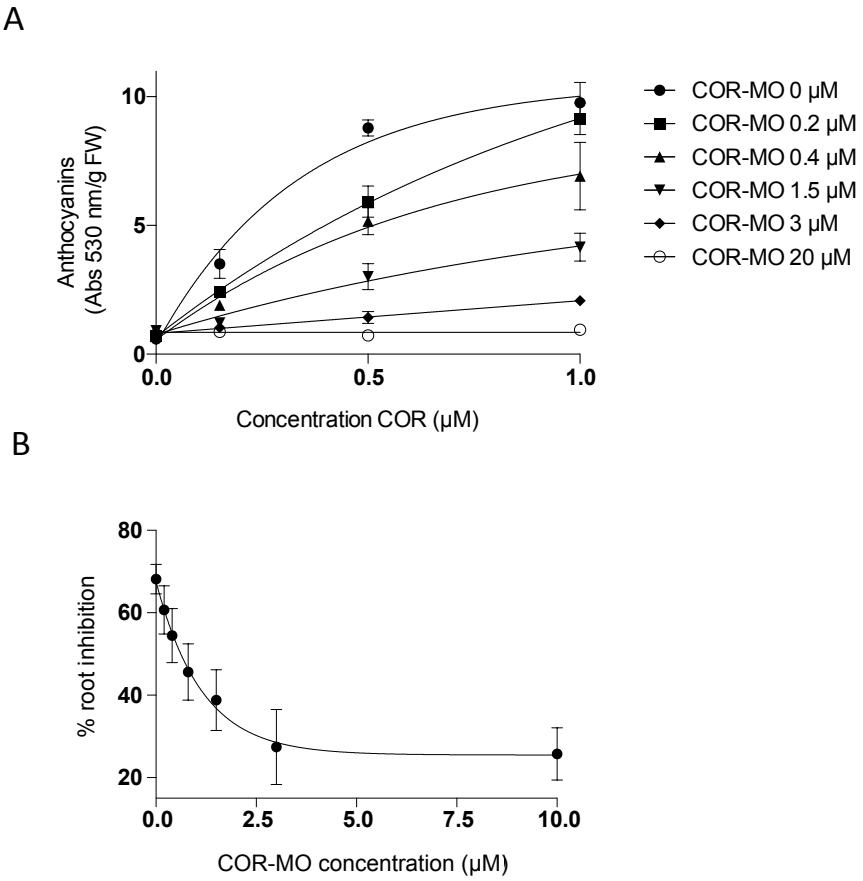

Supplementary Figure S16: A) Quantification of anthocyanin accumulation of 10-day-old *A. thaliana WT* seedlings grown in different concentrations of COR with or without COR-MO. B) Root growth inhibition of 10-day-old WT seedlings grown on COR 1 µM plus different concentrations of COR-MO, as in (Figure 19C). Data shown as mean ± S.D.

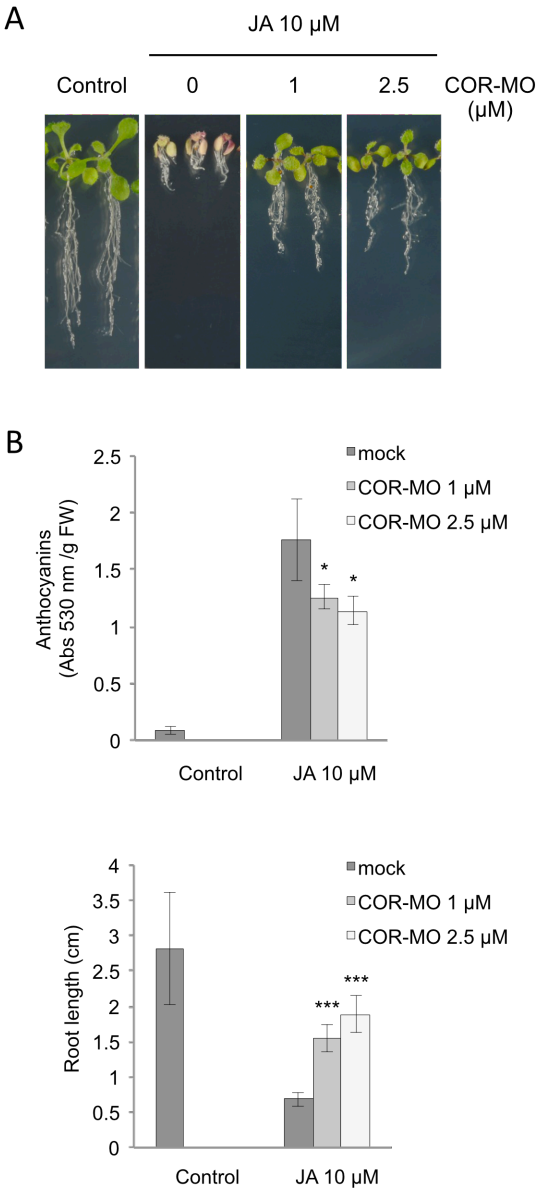

Supplementary Figure S17: Effect of COR-MO on JA-dependent root growth inhibition and anthocyanin accumulation. Phenotype; scale bar, 1 cm (A) and quantification (B) of root-growth inhibition and anthocyanin accumulation assays of 10-day-old *A. thaliana* WT seedlings grown in 10 µM JA with or without COR-MO (1 and 2.5 µM). Data shown as mean ± S.D. * $p < 0.05$; *** $p < 0.001$.

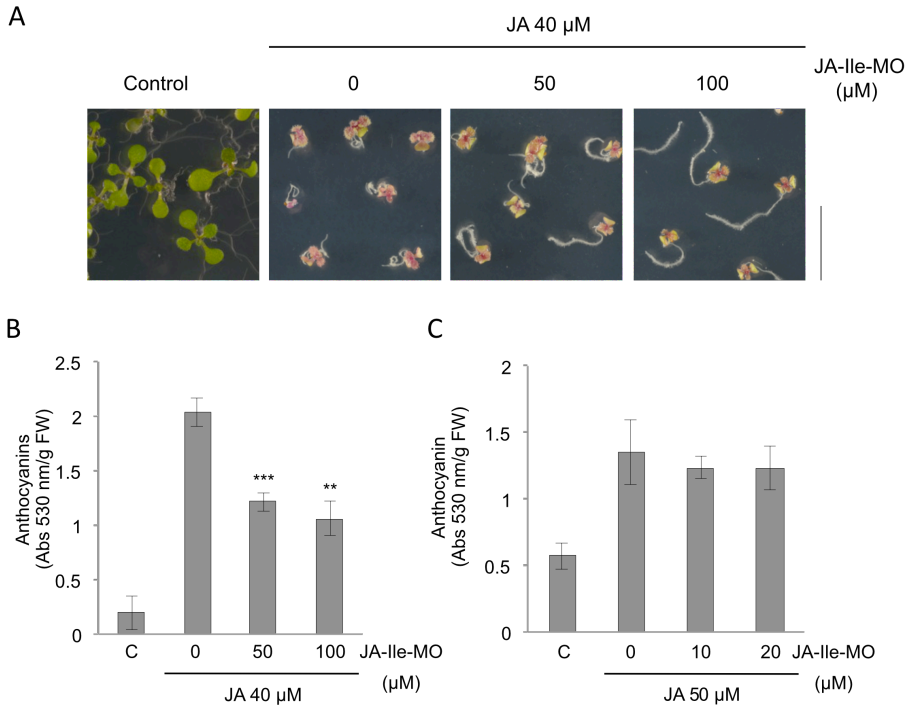

Supplementary Figure S18: Effect of JA-Ile-MO on JA-dependent root growth inhibition and anthocyanin accumulation. Phenotype of root-growth inhibition; scale bar, 1 cm (A) and quantification of anthocyanin accumulation (B,C). (B) 10-day-old *A. thaliana* WT seedlings grown in 40 µM JA with or without JA-Ile-MO (50 and 100 µM). ** $p < 0.01$; *** $p < 0.001$. C) Anthocyanin accumulation assays of 10-day-old *A. thaliana* WT seedlings grown in Johnson medium for 8 days and treated for 48 h with 50 µM JA with or without JA-Ile-MO (10 and 20 µM). Data shown as mean ± S.D.

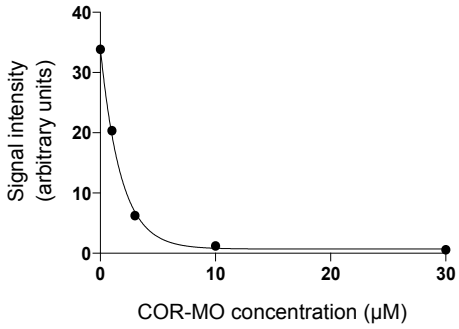

Supplementary Figure S19: Quantification of protein bands from Figure 19D using ImageJ. Data shown as mean ± S.D.

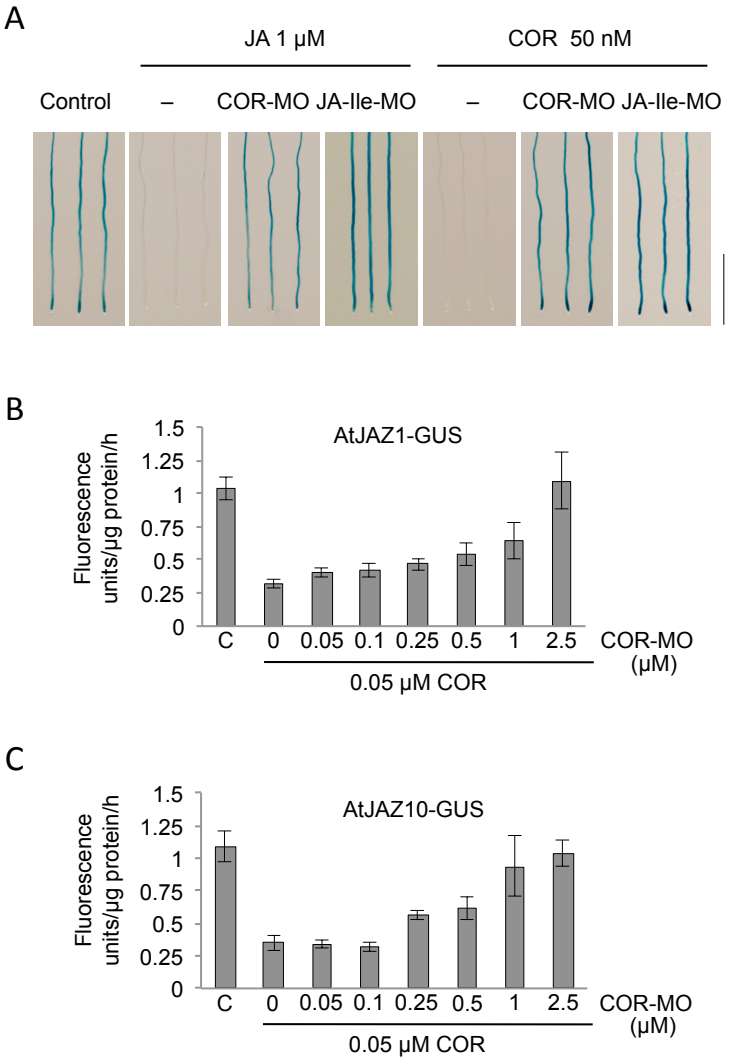

Supplementary Figure S20: COR-MO and JA-Ile-MO prevent AtJAZ degradation. A) Quantification of GUS activity in roots of 7-day-old transgenic *A. thaliana* 35S:At*JAZ1*-GUS and 35S:At*JAZ10*-GUS. Seedlings were pretreated with the indicated concentrations of COR-MO for 1 h and then treated with COR (50 nM) for another hour. B) 7-day-old 35S:At*JAZ1*-GUS seedlings were pretreated for 1 h with COR-MO (5 µM) or JA-Ile-MO (100 µM). Seedlings were then treated with JA (1 µM) or COR (50 nM) for 1 h. Scale bar, 0.25 cm. Data shown as mean ± S.D.

A

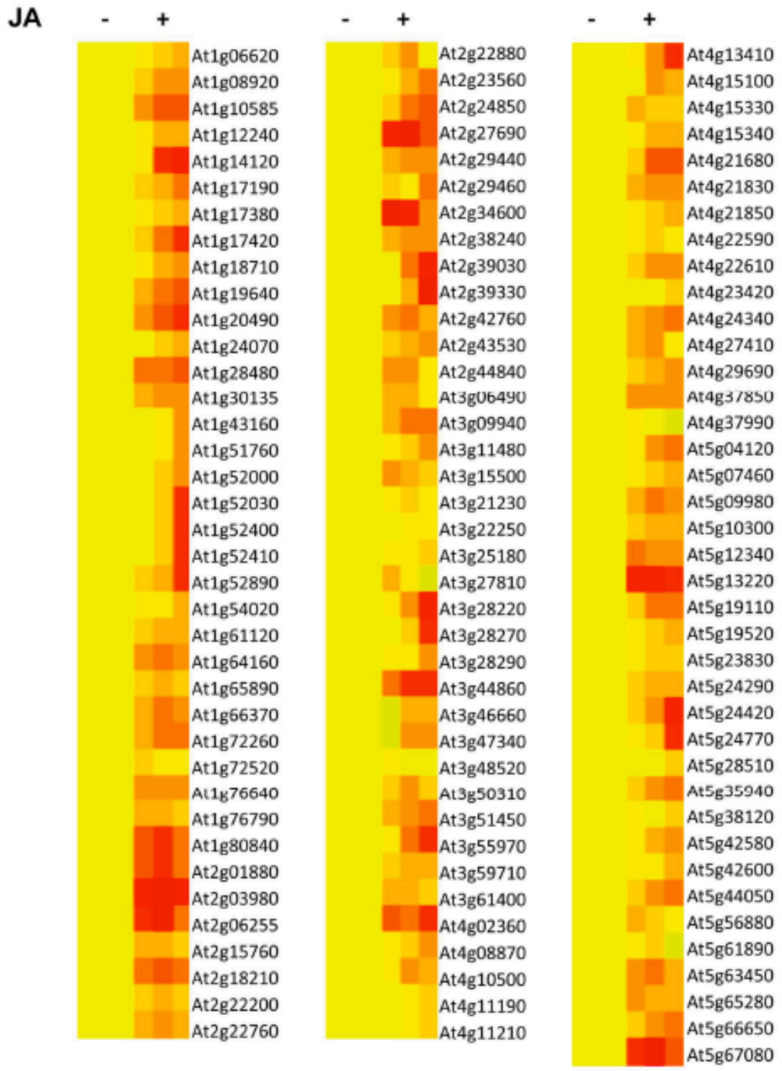

Supplementary Figure S21: COR-MO represses JA-mediated gene expression. A) Regulation by JA of genes downregulated by COR-MO in the transcriptomic profiling of *A.thaliana* seedlings treated with COR vs seedlings treated with COR+COR-MO. The panels show the JA induction (BAR data) of 115 genes downregulated by COR-MO using the criteria of FoldChange ≥3 or ≤-3 and FDR <0.05. B) Regulation by JA of genes upregulated by COR-MO in the transcriptomic profiling of *A.thaliana* seedlings treated with COR vs seedlings treated with COR+COR-MO. The panels show the JA downregulation (BAR data) of the 57 genes upregulated by COR-MO using the criteria of FoldChange ≥2 or ≤-2 and FDR<0.05. C) Percentage of JA-regulated genes (Induced or Repressed)

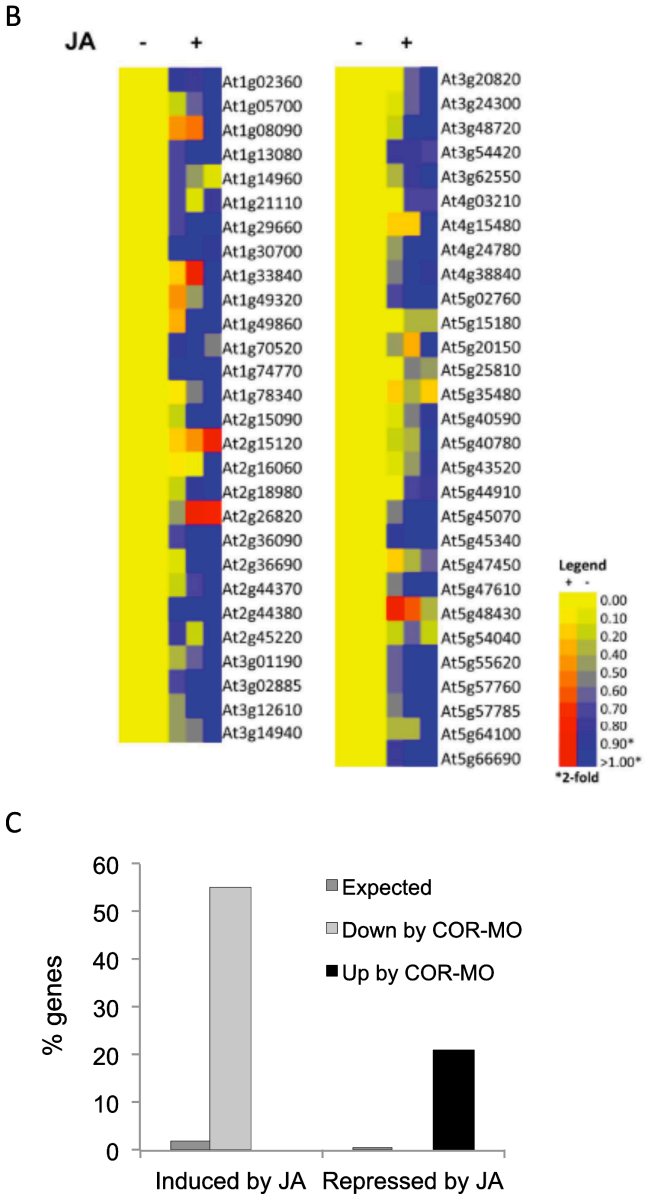

among those differentially expressed in the transcriptomic comparison of COR vs COR+COR-MO (GEO: GSE56027). Expected: genes expected to be induced or repressed by JA considering the whole genome data of JA treatments (0.5, 1 and 3h) in BAR (http://bar.utoronto.ca). Down by COR-MO: % of genes induced or repressed by JA within the list of genes downregulated by the COR-MO treatment (COR vs COR + COR-MO). Up by COR-MO: % of genes induced or repressed by JA within the list of genes upregulated by the COR-MO treatment (COR vs COR + COR-MO).

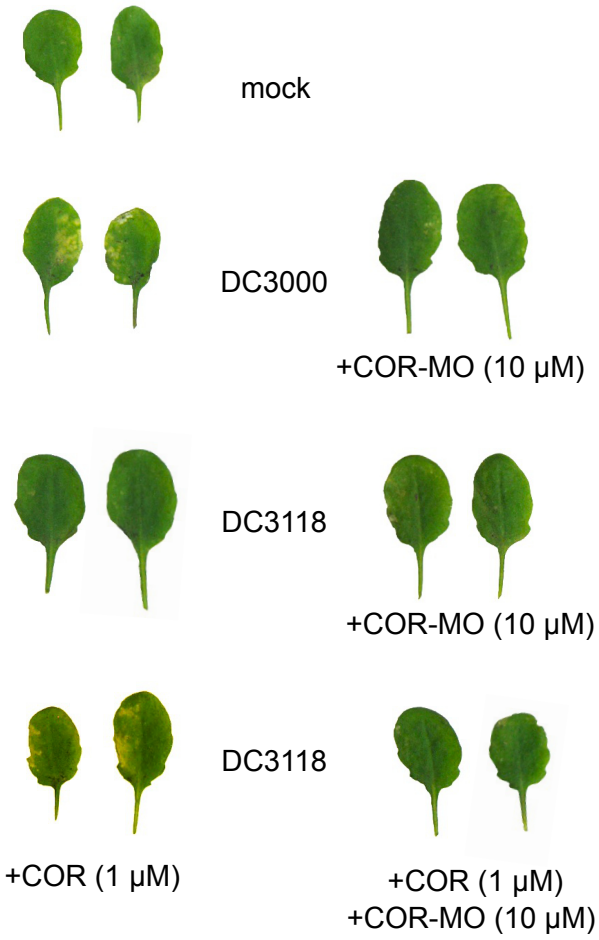

Supplementary Figure S22: Effect of COR-MO on the infection symptoms by the bacterial hemibiotrophic pathogen *Pst* DC3000 and DC3118 (COR⁻). Disease symptoms on *A. thaliana* Col-0 plants after infiltration of the indicated compounds together with *Pst* DC3000 and DC3118.

Supplementary Table S1: A) Cluster 1 (23 genes)

Term	%	p value	Benjamini
GO:0009611~response to wounding	17,4	0,001624	0,116199
GO:0010224~response to UV-B	13	0,002368	0,086149
GO:0009718~anthocyanin-containing compound biosynthetic process	8,7	0,022366	0,436195
GO:0031408~oxylipin biosynthetic process	8,7	0,028172	0,418974
GO:0009695~jasmonic acid biosynthetic process	8,7	0,02933	0,363951
GO:0006952~defense response	17,4	0,04173	0,417206
GO:0010252~auxin homeostasis	8,7	0,043114	0,380282
GO:0006635~fatty acid beta-oxidation	8,7	0,047668	0,371231

Supplementary Table S1: B) Cluster 2 (89 genes)

Term	%	p value	Benjamini
GO:0009611~response to wounding	11,7	3,61E-08	8,15E-06
GO:0008652~cellular amino acid biosynthetic process	7,45	9,19E-07	1,04E-04
GO:0009695~jasmonic acid biosynthetic process	5,32	5,60E-06	4,22E-04
GO:0051707~response to other organism	6,38	6,26E-06	3,54E-04
GO:0006979~response to oxidative stress	9,57	7,37E-05	0,0033236
GO:0031408~oxylipin biosynthetic process	4,26	1,96E-04	0,0073503
GO:0000162~tryptophan biosynthetic process	4,26	2,50E-04	0,0080352
GO:0080167~response to karrikin	6,38	3,63E-04	0,0102033
GO:0009699~phenylpropanoid biosynthetic process	4,26	6,10E-04	0,0152009
GO:0006559~L-phenylalanine catabolic process	3,19	6,15E-04	0,0138048
GO:0009423~chorismate biosynthetic process	3,19	7,88E-04	0,0160686
GO:0042744~hydrogen peroxide catabolic process	5,32	8,58E-04	0,0160329
GO:0009073~aromatic amino acid family biosynthetic process	3,19	0,002905	0,0493123
GO:0010224~response to UV-B	4,26	0,003068	0,0483879
GO:0055114~oxidation-reduction process	16	0,00392	0,0574597
GO:0040007~growth	3,19	0,006251	0,0847653
GO:0009753~response to jasmonic acid	5,32	0,006557	0,0837439
GO:0009664~plant-type cell wall organization	4,26	0,00935	0,1112562
GO:0006952~defense response	9,57	0,013012	0,1442573

Term	%	p value	Benjamini
GO:0009851~auxin biosynthetic process	3,19	0,013375	0,141148
GO:0009555~pollen development	5,32	0,013564	0,1366872
GO:0006635~fatty acid beta-oxidation	3,19	0,016267	0,1550544
GO:0010311~lateral root formation	3,19	0,019401	0,1751119
GO:0006633~fatty acid biosynthetic process	4,26	0,023185	0,1982031
GO:0010600~regulation of auxin biosynthetic process	2,13	0,023562	0,1939048
GO:0009800~cinnamic acid biosynthetic process	2,13	0,023562	0,1939048
GO:0034440~lipid oxidation	2,13	0,028209	0,2202035
GO:0009813~flavonoid biosynthetic process	4,26	0,031922	0,2378093
GO:0009737~response to abscisic acid	6,38	0,039827	0,2796616
GO:0009809~lignin biosynthetic process	3,19	0,041622	0,2820184
GO:0016042~lipid catabolic process	4,26	0,042795	0,2807116
GO:0009414~response to water deprivation	5,32	0,044136	0,2804162
GO:0009620~response to fungus	3,19	0,046139	0,2836715

Supplementary Table S1: C) Cluster 3 (41 genes)

Term	%	p value	Benjamini
GO:0009408~response to heat	20,75	1,20E-12	1,18E-10
GO:0009644~response to high light intensity	9,434	5,90E-06	2,92E-04
GO:0046686~response to cadmium ion	13,21	8,63E-05	0,002844
GO:0042542~response to hydrogen peroxide	7,547	2,15E-04	0,005313
GO:0055114~oxidation-reduction process	20,75	4,12E-04	0,008127
GO:0009414~response to water deprivation	9,434	0,0030196	0,048674
GO:0009407~toxin catabolic process	5,66	0,004443	0,061035
GO:0009636~response to toxic substance	5,66	0,007697	0,091189
GO:0006749~glutathione metabolic process	5,66	0,0079427	0,083982
GO:0042742~defense response to bacterium	7,547	0,0216199	0,194574
GO:0009723~response to ethylene	5,66	0,0294524	0,235898
GO:0006633~fatty acid biosynthetic process	5,66	0,0312225	0,230252
GO:0006915~apoptotic process	3,774	0,0444629	0,292742

Supplementary Table S2: Plants generated in this study

Mutant lines	Gene-targeting	Background	Transformation method
Mp*coi1-1* ♀	Homologous recombination	F1	Sporeling
Mp*coi1-2*	CRISPR/Cas9^{D10A}	Tak-1	Cut-thallus
Mp*coi1-3*	CRISPR/Cas9^{D10A}	F1	Sporeling
Mp*jaz-1*	CRISPR/Cas9	Tak-1	Cut-thallus

Transgenic lines	Vector	Background	Transformation Method
35S:Mp*COI1*-flag	pMpGWB111	BC4	Sporeling
35S:Mp*COI1*-flag	pMpGWB311	Mp*coi1-1*	Cut-thallus
35S:At*COI1*	pMpGWB311	Mp*coi1-1*	Cut-thallus
$_{pro}$Mp*EF1*:At*COI1*	pMpGWB310	Mp*coi1-1*	Cut-thallus
$_{pro}$Mp*EF1*:At*COI1*$^{1-188}$-Mp*COI1*$^{188-591}$-flag	pMpGWB310	Mp*coi1-1*	Cut-thallus
$_{pro}$Mp*EF1*:Mp*COI1*$^{1-187}$-At*COI1*$^{189-592}$-flag	pMpGWB310	Mp*coi1-1*	Cut-thallus
$_{pro}$Mp*EF1*:Mp*COI1*^{V377A}-flag	pMpGWB310	Mp*coi1-1*	Cut-thallus
35S:Mp*JAZ*-Citrine	pMpGWB106	BC4	Sporeling
$_{pro}$Mp*EF1*:Mp*JAZ*-Citrine	pMpGWB108	BC4	Sporeling
$_{pro}$Mp*EF1*:Mp*JAZΔJas*-Citrine	pMpGWB108	BC4	Sporeling
$_{pro}$Mp*EF1*:Mp*JAZ*^{Cas9R}-Citrine	pMpGWB308	Mp*jaz-1*	Cut-thallus
$_{pro}$Mp*EF1*:At*JAZ3*-Citrine	pMpGWB308	Mp*jaz-1*	Cut-thallus

Transgenic lines	Vector	Background	Transformation method
35S:Mp*COI1*-flag	pMpGWB111	coi1-30 het	Floral dipping
35S:Mp*JAZ*-GFP	pEG103	Col-0	Floral dipping
35S:Mp*JAZΔJas*-Citrine	pEG103	Col-0	Floral dipping
$_{pro}$At*JAZ2*:GUS	pGWB3	Col-0	Floral dipping
35S:At*JAZ9*-GUS	pMDC140	Col-0	Floral dipping
35S:At*JAZ10*-GUS	pMDC140	Col-0	Floral dipping

Supplementary Table S3: Primers

Name	Sequence
attB1 MpCOI1	GGGGACAAGTTTGTACAAAAAAGCAGGCTCCATGGAGGTGAGG GGTCCGGCCG
attB2 MpCOI1	GGGGACCACTTTGTACAAGAAAGCTGGGTTTCATAGTTCCCAATT TTCCCGCGCTGG
attB2 no stop MpCOI1	GGGGACCACTTTGTACAAGAAAGCTGGGTATAGTTCCCAATTTTC CCGCGCTGGTG
attB1 MpJAZ	GGGGACAAGTTTGTACAAAAAAGCAGGCTCCATGCATCGCAATA CTTGGAATAAGCC
attB2 MpJAZ	GGGGACCACTTTGTACAAGAAAGCTGGGTTCTAATGCCGTTGTG AGGGTGAAC
attB2 no stop MpJAZ	GGGGACCACTTTGTACAAGAAAGCTGGGTAATGCCGTTGTGAG GGTGAACCAG
attB2 MpJAZΔJas	GGGGACCACTTTGTACAAGAAAGCTGGGTTTTAGAGCATACCTT GATGAAGGATTG
attB2 nostop MpJAZΔJas	GGGGACCACTTTGTACAAGAAAGCTGGGTAGAGCATACCTTGAT GAAGGATTGC
AtCOI1 Rv MpCOI1 tail	TGTATTATTGAGAGCAAGCTCATGAAGCCACTTACCAT
MpCOI1 Fw AtCOI1 tail	GGTAAGTGGCTTCATGAGCTTGCTCTCAATAATACAACGTTG
MpCOI1 Rv AtCOI1 tail	TGTGTTGTGCTGAGCCAGCTCATGTAACCATTCACCGCC
AtCOI1 Fw MpCOI1 tail	GGTGAATGGTTACATGAGCTGGCTCAGCACAACACATC
MpCOI1 V377A Rv	ATGTCCACAACATACATCGCAAGAAACTCGAG
MpCOI1 V377A Fw	GCTCGAGTTTCTTGCGATGTATGTTGTGGAC
MpJAZ Cas9R Rv	GGTGTCATGTTGCCATCCAGGACCGGAAGAGACAGTAAG
MpJAZ Cas9R Fw	GGATGGCAACATGACACCTCTGGCCAATCTCACGCTTCA
MpCOI1 Fwd PacI HR	CTAAGGTAGCGATTATTTGAATTCCGTGCTCTCCA
MpCOI1 Rev PacI HR	GCCCGGGCAAGCTTAACCCGAGTGTCTCATCCG
MpCOI1 Fwd AscI HR	TAAACTAGTGGCGCGTGCATGTTACCGATGCT
MpCOI1 Rev AscI HR	TTATCCCTAGGCGCGTTAGTACCACAACCTATATA
gRNA1 MpCOI1 Fw	CTCGGCGACGATATGATGTGCTGC
gRNA1 MpCOI1 Rv	AAACGCAGCACATCATATCGTCGC
gRNA2 MpCOI1 Fw	CTCGGCCGAAGAAGTGACGACAGA
gRNA2 MpCOI1 Rv	AAACTCTGTCGTCACTTCTTCGGC
gRNA3 MpCOI1 Fw	CTCGTGTCAGTGTTGAAACTACAG
gRNA3 MpCOI1 Rv	AAACCTGTAGTTTCAACACTGACA
gRNA4 MpCOI1 Fw	CTCGGATTATGGTTCTTGTCATTC

Name	Sequence
gRNA4 MpCOI1 Rv	AAACGAATGACAAGAACCATAATC
gRNA MpJAZ Fw	CTCGGGGTGGCAGCACGATACATC
gRNA MpJAZ Rv	AAACGATGTATCGTGCTGCCACCC
MpCOI a	AGGACAGAAGGCACTGAAGTTC
MpCOI b	CTGCTTCTCAGAAACAGTCATGC
Primer X (MpEF)	GAAGGCTTCTGATTGAAGTTTCCTTTTCTG
Fw genotype Mpjaz	ATCGATCAATGGCTCTTTGG
Rv genotype Mpjaz	CCACATTGTACCGAGGAGGT
pJAZ2 Fwd	CACCGACTAAGAATTTGTTATGAAG
pJAZ2 Rev	CATCGTTGAAACCGAAATTGAAATCG
attB1_JAZ9	GGGGACAAGTTTGTACAAAAAAGCAGGCTTCATGGAAAGAGATT TTCTG
attB2stop_JAZ9	GGGACCACTTTGTACAAGAAAGCTGGGTCTTATGTAGGAGAAGT AGAAGA
attB1_JAZ10	GGGGACAAGTTTGTACAAAAAAGCAGGCTTCATGTCGAAAGCTA CCATA
attB2stop_JAZ10	GGGACCACTTTGTACAAGAAAGCTGGGTCTTATTAGGCCGATGT CGGATA
qPCR MpACT Fw	AGGCATCTGGTATCCACGAG
qPCR MpACT Rv	ACATGGTCGTTCCTCCAGAC
qPCR MpCOI1 1ex Fw	TCACTGAAGATTAAGGGCAAGCC
qPCR MpCOI1 1ex Rv	AACGAGCAGCTCATACTCGAAAG
qPCR MpJAZ Fw	ACAGAAGAATGGGTTGTCAGACG
qPCR MpJAZ Rv	GGACCGGAAGAGACAGTAAGAGTG
qPCR MpJAZ FL Fw	AGAGGAAAGACAGGGTTCGTG
qPCR MpJAZ FL Rv	CAGAAGTCGGTGCTACGTACG
qPCR MpJAZΔJas Fw	GAGCCACAAGAGGTGCCG
qPCR MpJAZΔJas Rv	GGCCTCAAATCATGTCACTAACTG
qPCR MpAOS2 Fw	CCGAAATTCTACGAGAACCGG
qPCR MpAOS2 Rv	CCGGTACACGGTGCTCTTATACT
qPCR MpAOC Fw	TCGTCAGCGCATCCTTCTTT
qPCR MpAOC Rv	TGTCACCCTCGTTGAACTCG
qPCR MpCHL Fw	TATGGATTACCTGGACGACGATCT
qPCR MpCHL Rv	CCGGACAGTAAGCCTATAATACCAC

Supplementary Table S4: Ionization source working parameters

Instrumental parameters	Value
Sheath gas flow rate	44 au
Auxiliary gas flow rate	11 au
Sweep gas flow rate	1 au
Spray voltage	3.5 kV
Capillary temperature	340 ºC
S-lens RF level	50
Auxiliary gas heater temperature	300 ºC

Supplementary Table S5: Masses of phytohormones, internal standards and their principal fragments.

Analyte	$[M-H]^{-1}$ Phytohormone	$[M-H]^{-1}$ Fragment
JA	209.11832	59.01297
JA-Ile	322.20238	130.08735
OPDA	291.19657	165.12843
dn-OPDA	263.16527	165.12843
4,5-ddh-JA	207.10267	163.11282
4,5-ddh-JA-Ile	320.18673	130.08735
OPC-4	237.14962	125.09715
OPC-6	265.18092	96.95968
$^{2}H_5$-JA	214.1497	61.02555
$^{2}H_5$-JA-Ile	327.23377	170.15994
$^{2}H_5$-OPDA	296.22795	170.15994
$^{2}H_5$-dn-OPDA	268.19665	61.02555
$^{2}H_5$-tn-OPDA	235.13397	131.0937
$^{2}H_5$-4,5-ddh-JA	212.13405	170.15994
$^{2}H_5$-ddh-JA-Ile	325.21812	170.15994
$^{2}H_5$-OPC-4	242.181	242.181
$^{2}H_5$-OPC-6	270.2123	270.2123
$^{2}H_5$-JA	214.1497	214.1497
$^{2}H_5$-JA-Ile	324.21494	324.21494
$^{2}H_5$-OPDA	296.22795	296.22795
$^{2}H_5$-dn-OPDA	268.19665	268.19665

Supplementary Table S6: ^{1}H and ^{13}C NMR data for COR-MO.

δ ^{13}C [ppm]	^{13}C mult.	δ ^{1}H [ppm] mult. (J [Hz])
174.9	s (br)	-
172.1	s	-
169.6	s	-
169.2	s	- {minor isomer}
138.4	d	6.414 br s
136.4	s	-
61.7	q	3.804 s
61.5	q	3.787 s {minor isomer}
42.4	t	2.65
39.2	s (br)	-
39.1	d	2.91
38.9	d	2.16
33.2	d	1.02
30.9	t	1.75; 0.85
30.1	t	2.44; 1.42
29.2	t	1.51; 1.40
27.5	t	2.63; 2.33
23.2	t	1.47; 1.12
21.6	t	1.62
13.7	q	1.017 t (7.5)
11.6	q	1.004 t (7.2)

Supplementary Table S7: ^{1}H and ^{13}C NMR data for (±)-JA-MO.

δ ^{13}C [ppm]	^{13}C mult.	δ ^{1}H [ppm] mult. (J [Hz])
174.9	s (br)	-
172.1	s	-
169.6	s	-
169.2	s	- {minor isomer}
138.4	d	6.414 br s
136.4	s	-
61.7	q	3.804 s
61.5	q	3.787 s {minor isomer}
42.4	t	2.65
39.2	s (br)	-
39.1	d	2.91
38.9	d	2.16
33.2	d	1.02
30.9	t	1.75; 0.85
30.1	t	2.44; 1.42

δ ^{13}C [ppm]	^{13}C mult.	δ ^{1}H [ppm] mult. (J [Hz])
29.2	t	1.51; 1.40
27.5	t	2.63; 2.33
23.2	t	1.47; 1.12
21.6	t	1.62
13.7	q	1.017 t (7.5)
11.6	q	1.004 t (7.2)

Supplementary Table S8: ^{1}H and ^{13}C NMR data for (-)-JA-Ile-MO.

δ ^{13}C [ppm]	^{13}C mult.	δ ^{1}H [ppm] mult. (J [Hz])
174.8	s	-
174.7	s	-
168.7	s	- {minor isomer}
168.3	s	-
134.3	d	5.42
126.9	d	5.39
61.7	q	3.792 s
61.7	q	3.788 s {minor isomer}
58.2	d	4.352 d (5.9)
49.4	d	2.27
41.4	d	2.21
40.8	t	2.46; 2.18
38.2	d	1.878 m
29.5	t	2.33
29.3	t	1.997 m; 1.418 m
27.2	t	2.555 ddd (19.2, 8.7, 4.6); 2.26
26.3	t	1.518 m; 1.254 m
21.6	t	2.077 dq (7.6, 7.6)
16.1	q	0.953 d (6.9)
14.6	q	0.961 t (7.6)
11.8	q	0.931 t (7.5)

^{1}H chemical shifts with 2 decimal places only are chemical shifts of HSQC correlation peaks

^{15}N chemical shifts (chemical shifts of ^{1}H,^{15}N HMBC correlation peaks):
360.4 ppm
355.5 ppm {minor isomer}
121.8 ppm
(Ref.: δ ^{15}N NH_3 (liq.) = 0 ppm)